Dartmouth Health

Department of Medicine
DARTMOUTH CANCER CENTER

Imaging in Radiation Oncology

Joseph Weygand, Ph.D.

February 15th, 2024

Simulation

Rationale

- Radiation therapy is a localized intervention!
- 3 rules in radiation oncology

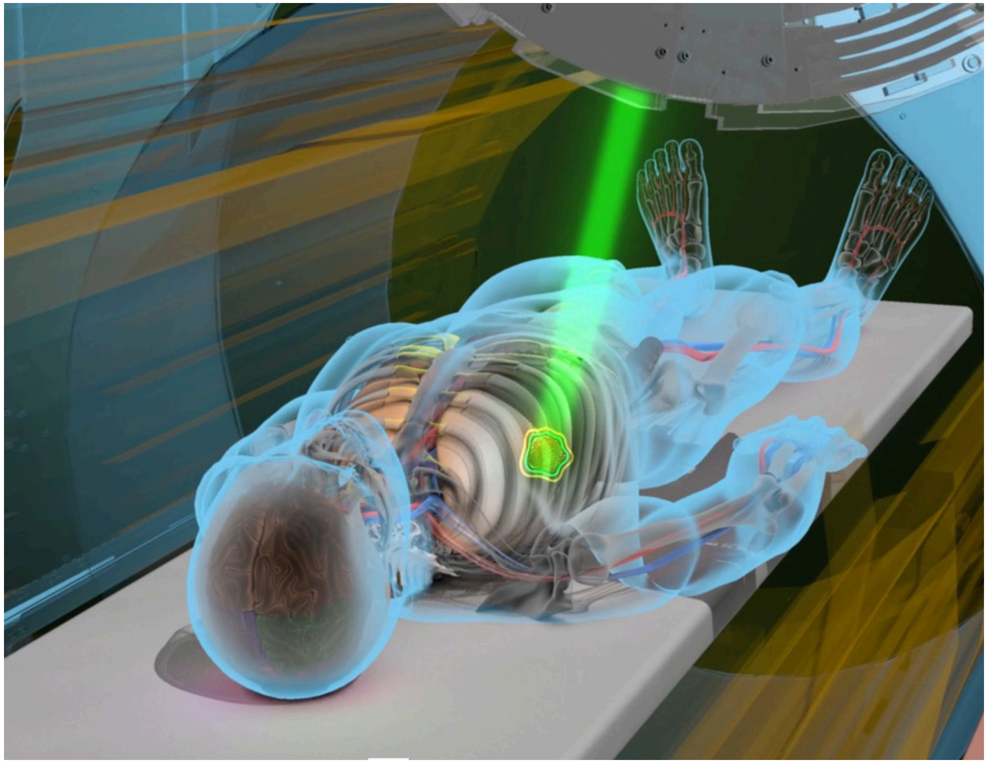

- Patient modeling / Dose calculation
- Target delineation
- Setup verification
- Procedure guidance
- Online adaptive radiotherapy
- Response assessment
- Personalized medicine one day?

Disclaimer

- Not meant to be exhaustive
- No endorsements implied

Simulation

Simulation

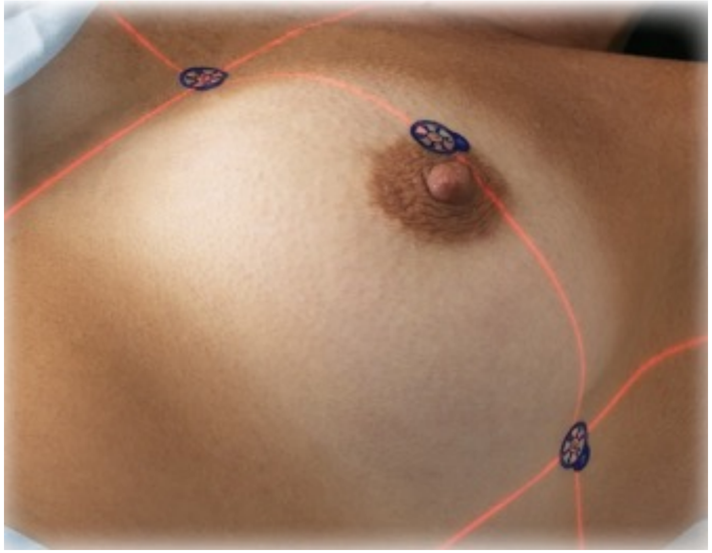

- A model of the patient's geometry
- Used for planning
- 2D
  - Conventional simulation
- 3D
  - CT simulation
- Markers allow for 'reproducible' set up

Conventional Simulation

- Two dimensional localization of the tumor
- Based on planar x-ray imaging
- kV energies
- Can locate the target and define field borders
- Going extinct in HIC’s
- Still quite common in LMIC’s

History of X-Rays

Wilhelm Röntgen (1895)

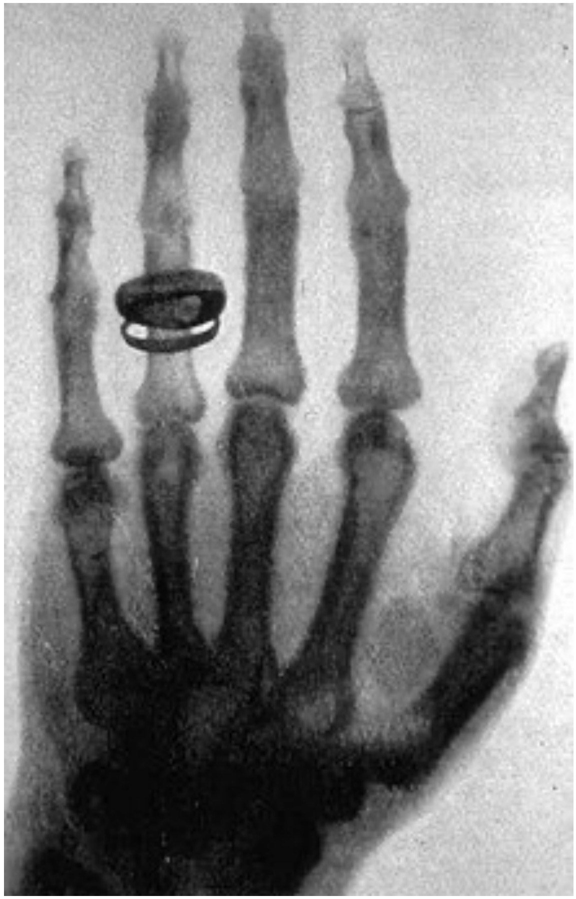

History of X-Rays

Frost Brothers (1896)

X-Ray Tube

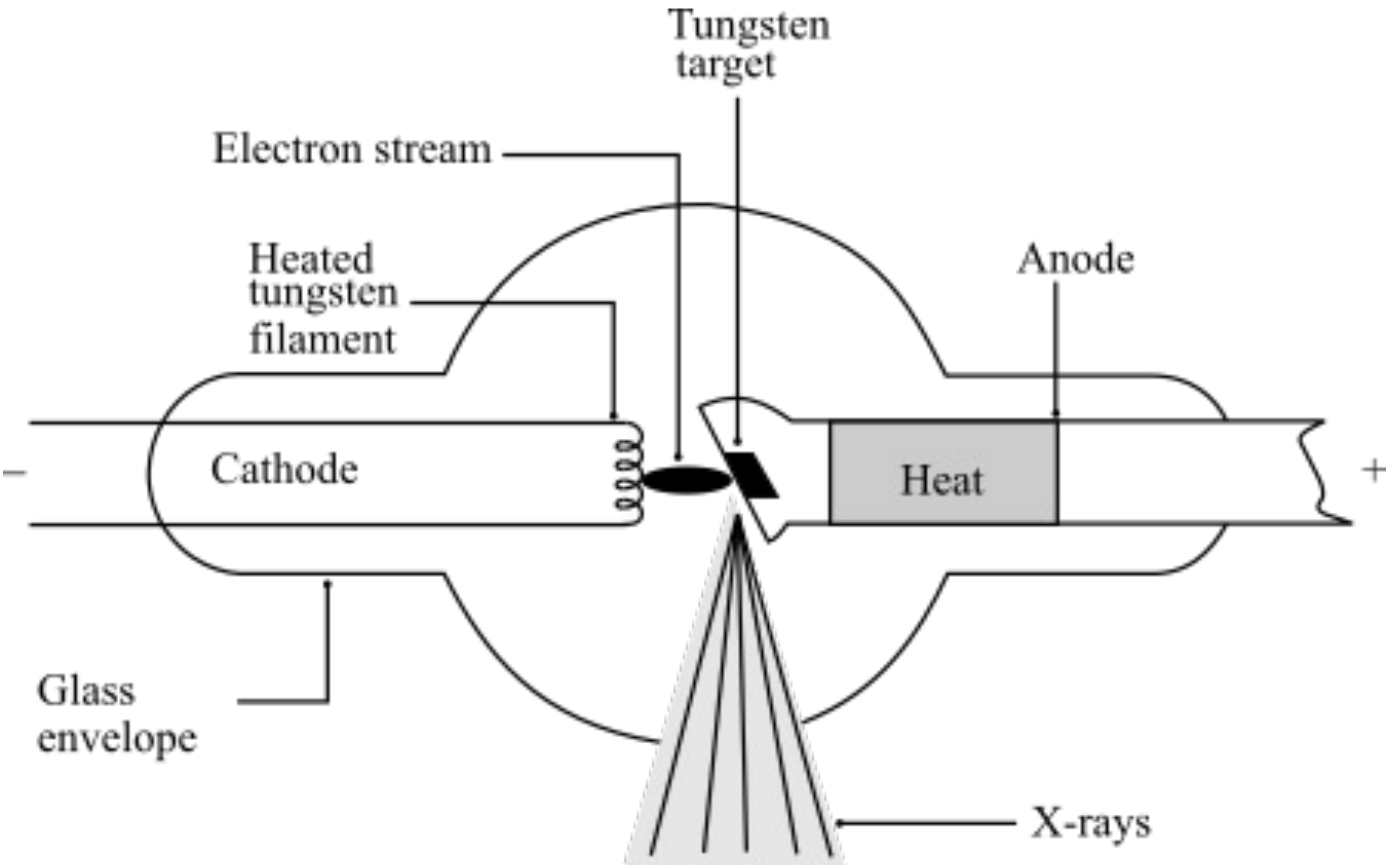
Tungsten target
Electron stream
Heated tungsten filament
Anode
Cathode
Heat
−
+
Glass envelope
X-rays

X-Ray Detection

- Silver halide grains
  - ➢Radiographic film
- Organic monomers
  - ➢Radiochromic film
- Photo-stimulated luminescence screens
  - ➢Computed Radiography
- Matrix of a-Si with photodiodes
  - ➢(Indirect) Digital Radiography
- Matrix of a-Se
  - ➢(Direct) Digital Radiography

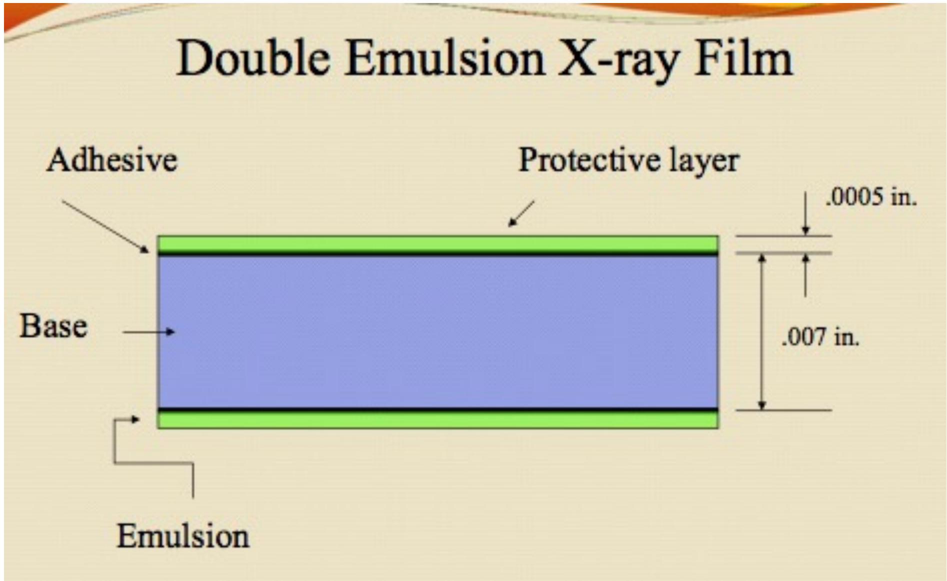

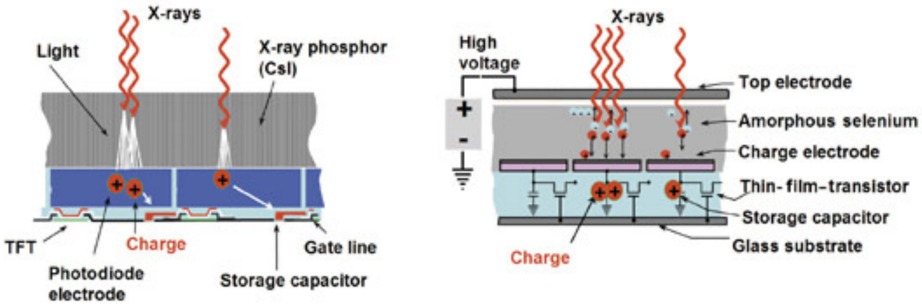

A. Indirect AMFPI: X-rays to light to charge

B. Direct AMFPI: X-rays to charge

X-Ray Imaging

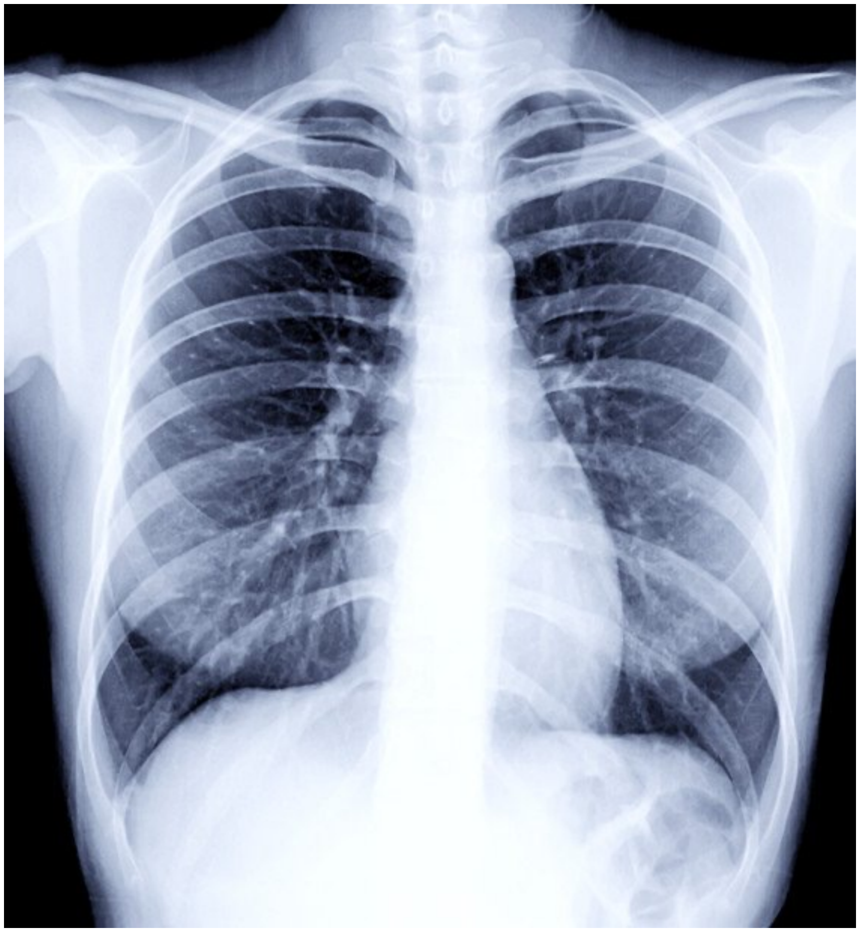

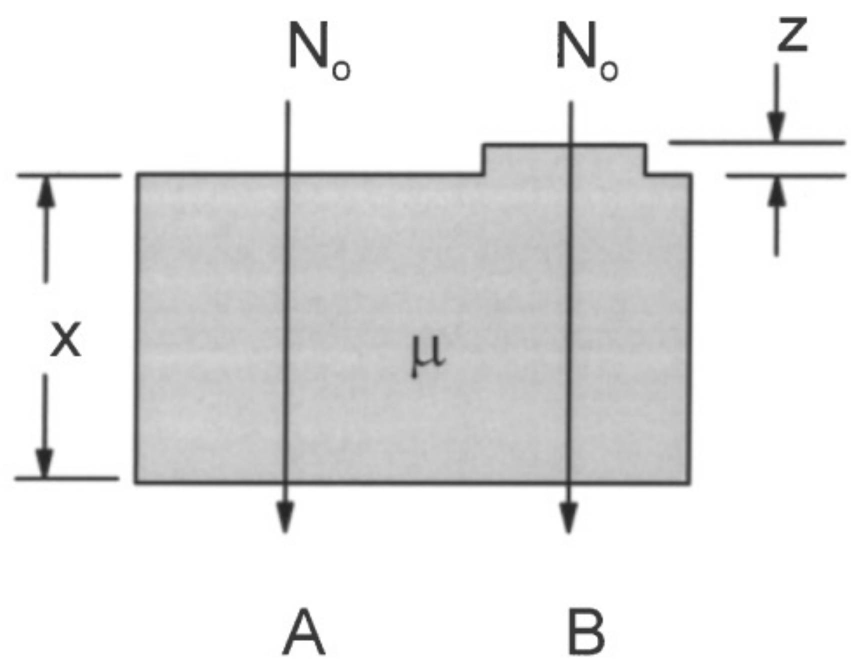

CT Simulation

- Three dimensional localization → 3D planning
- Additionally electron density information
- Also kV energies

$$\Sigma_{Compton} \sim n_e$$

$$HU \sim n_e$$

History of Computed Tomography

Godfrey Hounsfield (1972)

Principles of CT

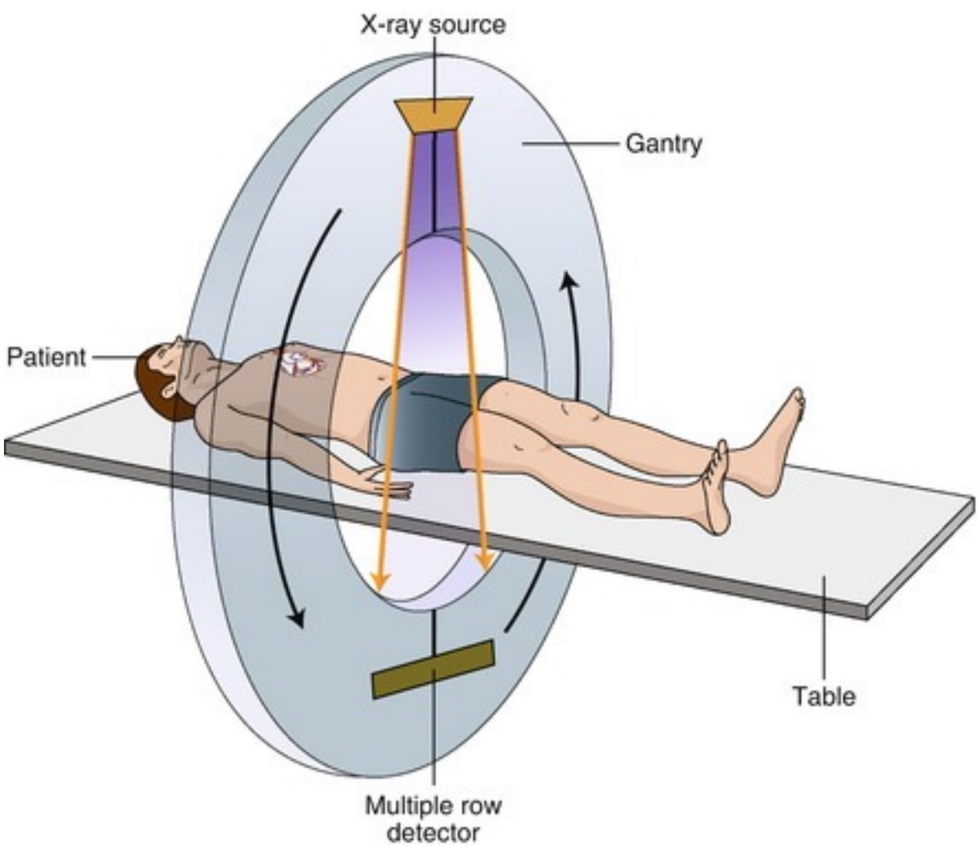

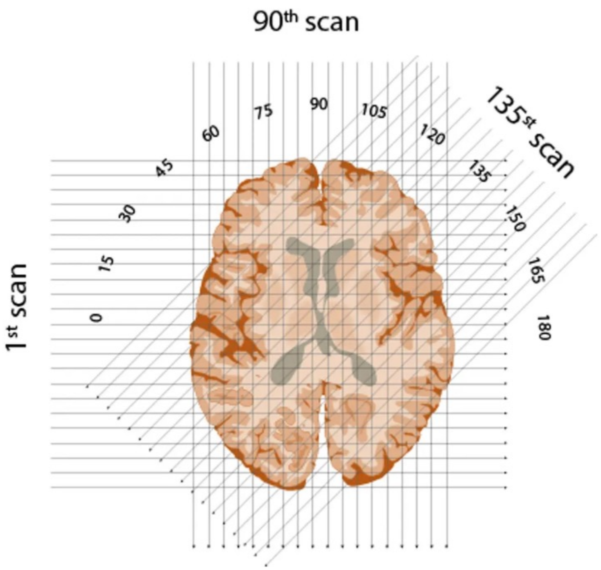

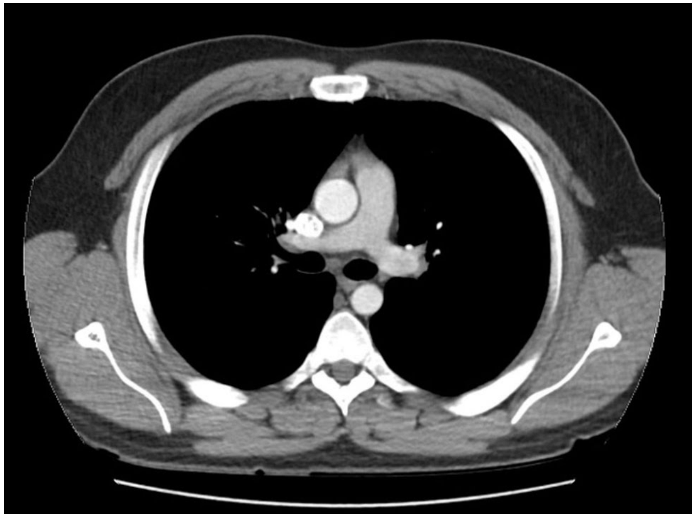

CT vs CT Sim

- CT sims must have flat table top (reproducibility)
- CT sims have a larger bore size
- CT sims rely on external lasers for positioning

AAPM TG 66

Quality assurance for computed-tomography simulators and the computed-tomography-simulation process: Report of the AAPM Radiation Therapy Committee Task Group No. 66

Sasa Mutic[a)]
Department of Radiation Oncology, Washington University School of Medicine, St. Louis, Missouri 63110

Jatinder R. Palta
Department of Radiation Oncology, University of Florida, Gainesville, Florida 32610

Elizabeth K. Butker
Department of Radiation Oncology, Emory University School of Medicine, Atlanta, Georgia

Indra J. Das
Department of Radiation Oncology, University of Pennsylvania, Philadelphia, Pennsylvania 19104

M. Saiful Huq
Department of Radiation Oncology, Thomas Jefferson University Hospital, Philadelphia, Pennsylvania 19107

Leh-Nien Dick Loo
Department of Medical Physics, Kaiser Permanente, Los Angeles, California 90039

Bill J. Salter
Department of Radiation Oncology, University of Texas Health Sciences Center, San Antonio, Texas 78229

Cynthia H. McCollough[b)]
Department of Radiology, Mayo Clinic, Rochester, Minnesota 55905

Jacob Van Dyk[b)]
Department of Clinical Physics, London Regional Cancer Center, London, Ontario N6A 4L6, Canada

(Received 21 April 2003; revised 1 July 2003; accepted for publication 25 July 2003; published 24 September 2003)

CT Simulator QA

Table II. Test specifications for electromechanical components.*

Performance parameter	Test objective	Frequency	Tolerance limits
Alignment of gantry lasers with the center of imaging plane	To verify proper identification of scan plane with gantry lasers	Daily	±2 mm
Orientation of gantry lasers with respect to the imaging plane	To verify that the gantry lasers are parallel and orthogonal with the imaging plane over the full length of laser projection	Monthly and after laser adjustments	±2 mm over the length of laser projection
Spacing of lateral wall lasers with respect to lateral gantry lasers and scan plane	To verify that lateral wall lasers are accurately spaced from the scan plane. This distance is used for patient localization marking	Monthly and after laser adjustments	±2 mm
Orientation of wall lasers with respect to the imaging plane	To verify that the wall lasers are parallel and orthogonal with the imaging plane over the full length of laser projection	Monthly and after laser adjustments	±2 mm over the length of laser projection
Orientation of the ceiling laser with respect to the imaging plane	To verify that the ceiling laser is orthogonal with the imaging plane	Monthly and after laser adjustments	±2 mm over the length of laser projection
Orientation of the CT-scanner tabletop with respect to the imaging plane	To verify that the CT-scanner tabletop is level and orthogonal with the imaging plane	Monthly or when daily laser QA tests reveal rotational problems	±2 mm over the length and width of the tabletop
Table vertical and longitudinal motion	To verify that the table longitudinal motion according to digital indicators is accurate and reproducible	Monthly	±1 mm over the range of table motion
Table indexing and position	To verify table indexing and position accuracy under scanner control	Annually	±1 mm over the scan range
Gantry tilt accuracy	To verify accuracy of gantry tilt indicators	Annually	±1° over the gantry tilt range
Gantry tilt position accuracy	To verify that the gantry accurately returns to nominal position after tilting	Annually	±1° or ±1 mm from nominal position
Scan localization	To verify accuracy of scan localization from pilot images	Annually	±1 mm over the scan range

Electromechanical Components Tests

- Lasers
- Couch
- Gantry

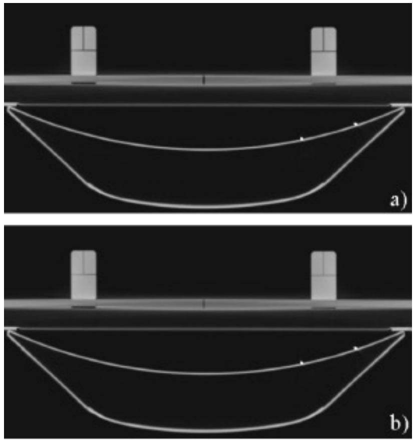

Table II. (*Continued.*)

Performance parameter	Test objective	Frequency	Tolerance limits
Radiation profile width	To verify that the radiation profile width meets manufacturer specification	Annually (This test is optional if the CTDI accuracy has been verified)	Manufacturer specifications
Sensitivity profile width	To verify that the sensitivity profile width meets manufacturer specification	Semiannually	±1 mm of nominal value
Generator tests	To verify proper operation of the x-ray generator	After replacement of major generator component	Manufacturer specifications or Report No. 39 recommendations

AAPM TG 66.

CT Simulator QA

Image Quality Tests

TABLE III. Test specifications for image performance evaluation.[a]

Performance parameter	Frequency	Tolerance limits
CT number accuracy	Daily—CT number for water Monthly—4 to 5 different materials Annually—Electron density phantom	For water, 0±5 HU
Image noise	Daily	Manufacturer specifications
In plane spatial integrity	Daily—*x* or *y* direction Monthly—both directions	±1 mm
Field uniformity	Monthly—most commonly used kVp Annually—other used kVp settings	within ±5 HU
Electron density to CT number conversion	Annually—or after scanner calibration	Consistent with commissioning results and test phantom manufacturer specifications
Spatial resolution	Annually	Manufacturer specifications
Contrast resolution	Annually	Manufacturer specifications

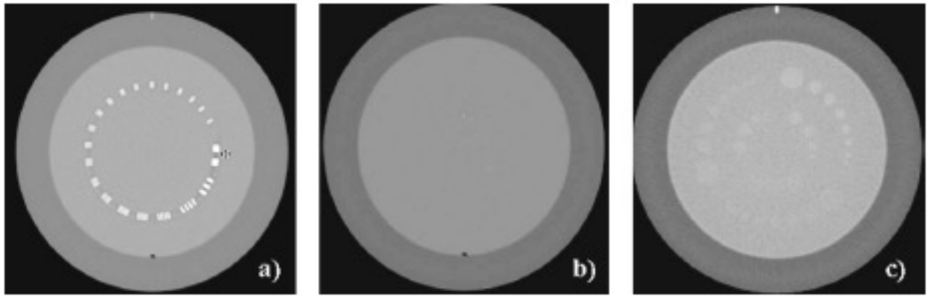

AAPM TG 66.

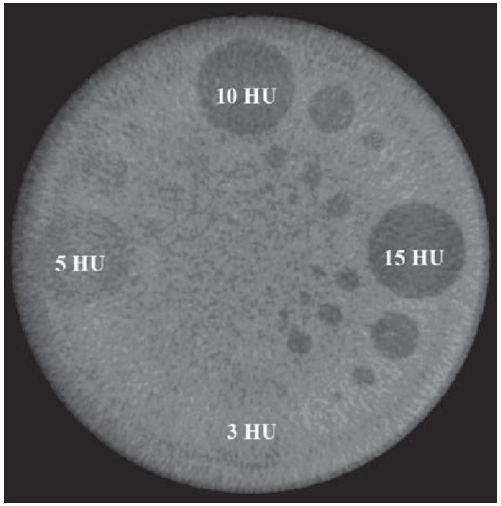

HU to Electron Density

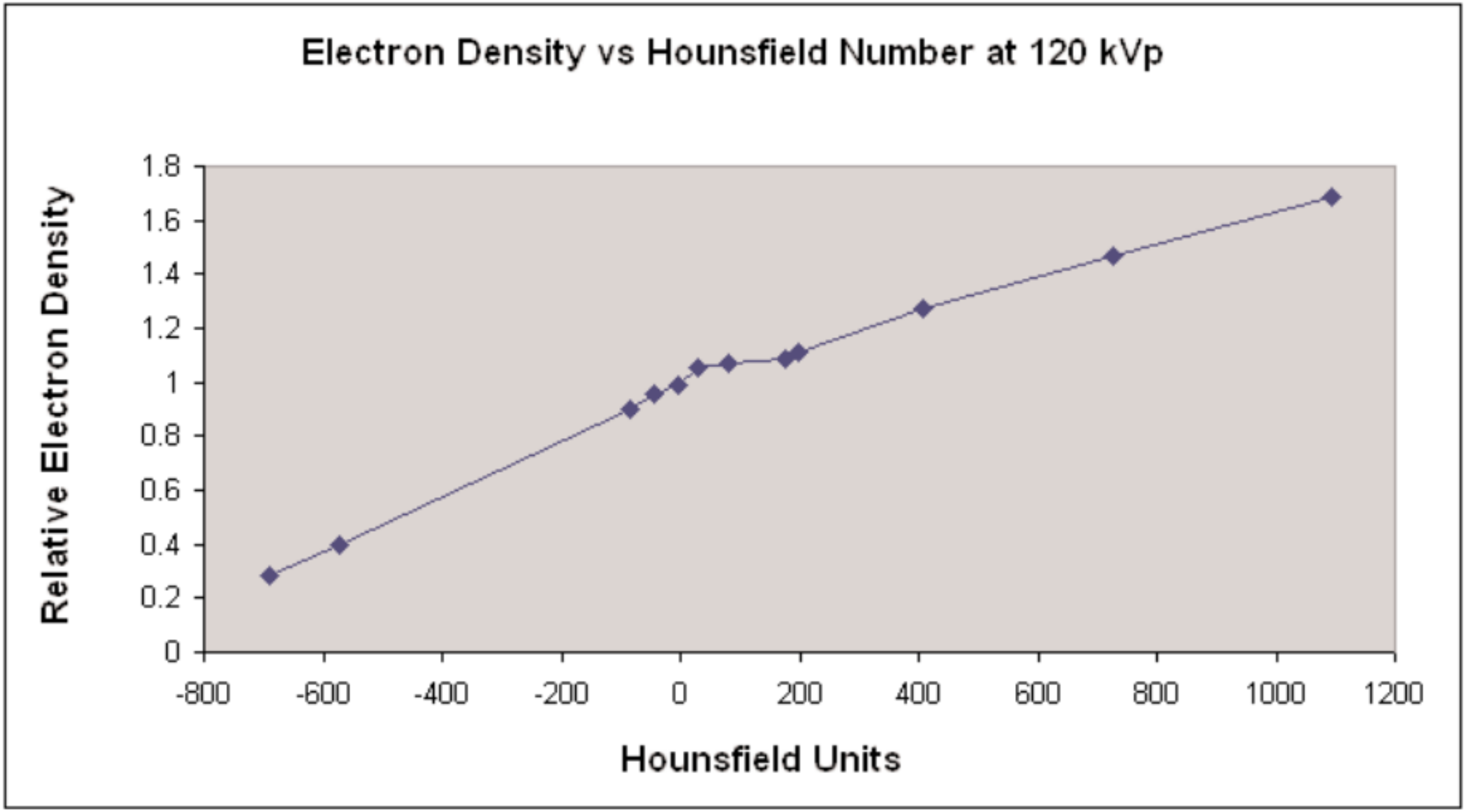

Digital Reconstructed Radiograph

- Retrospective reconstruction of volumetric CT data into a 2D projection

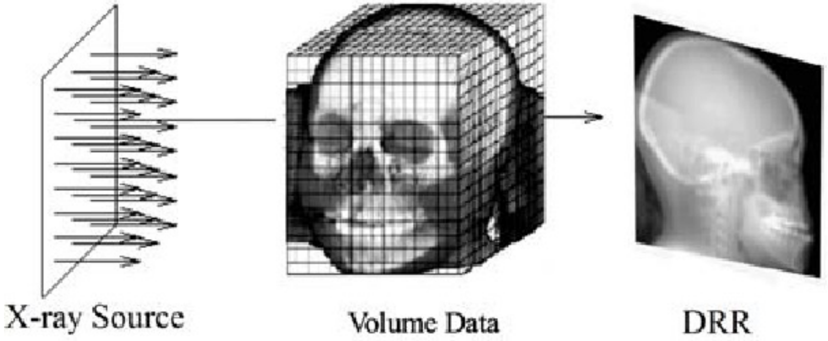

Montúfar et al. 2016.

4D CT

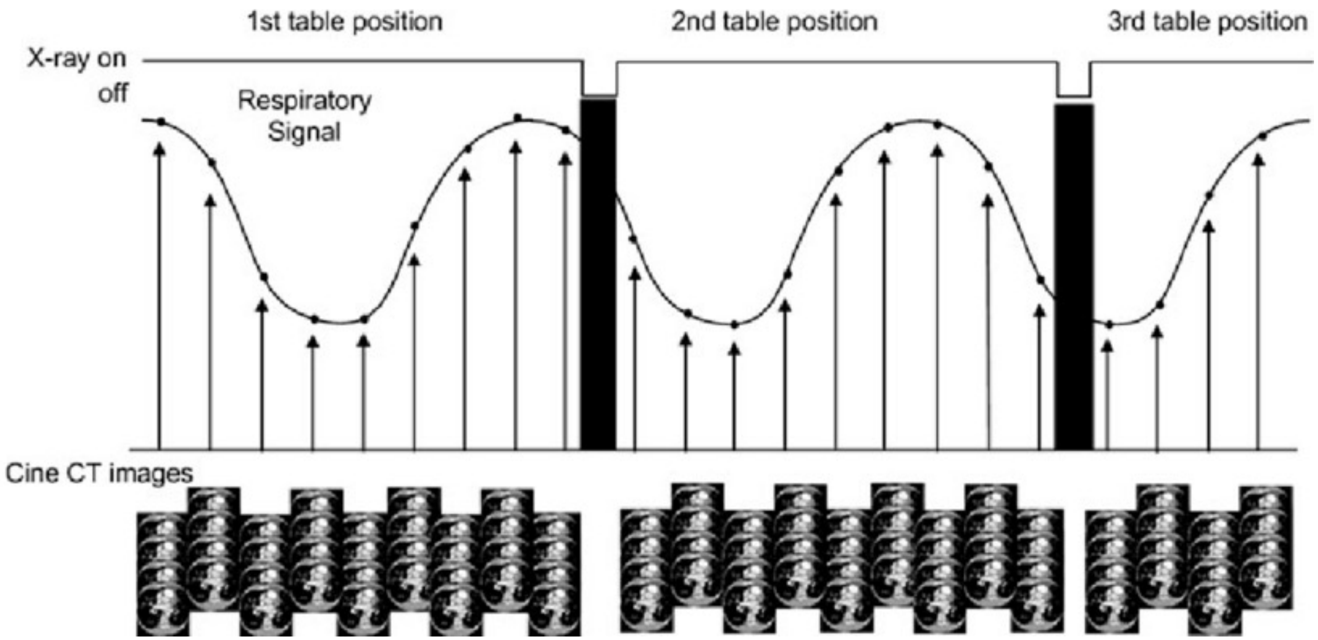

Pan et al. 2004.

Axial mode example above

- Very slow couch motion → low pitch
- Amplitude vs phase binning
- MIP/MinIP

MRI Simulation

- Superior soft tissue contrast → More accurate target/OAR delineation
- Functional capabilities
- No electron density information

History of NMR

Rabi - 1938

Bloch - 1946

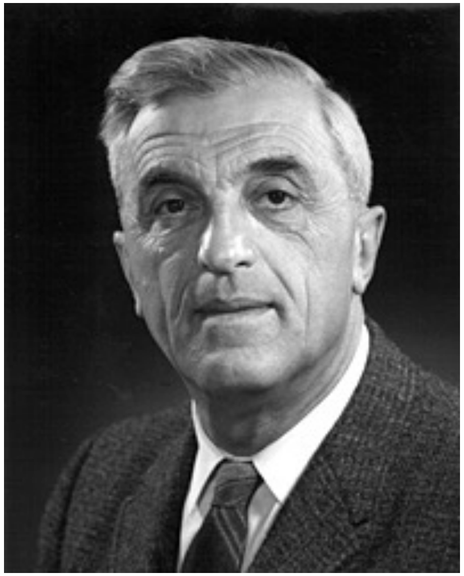

Purcell - 1946

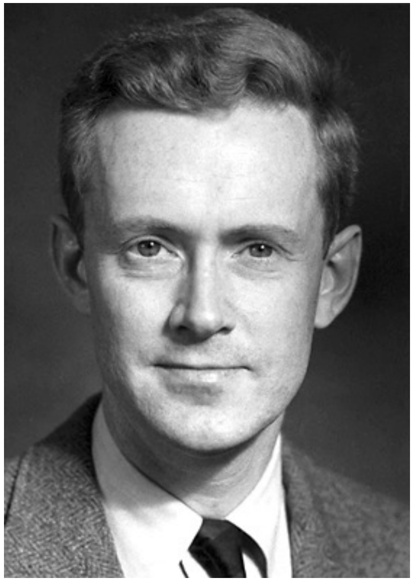

Ernst - 1964

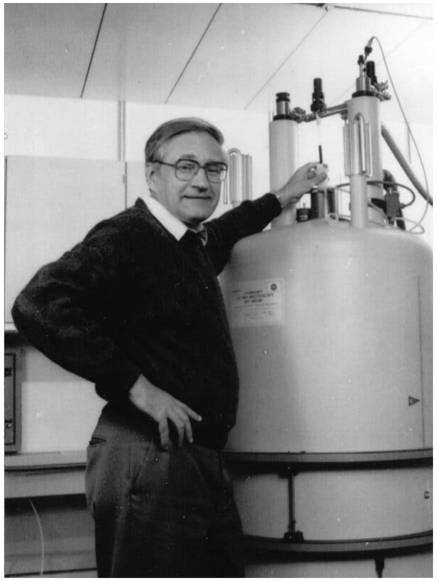

History of MRI

Lauterbur - 1973

Mansfield - 1977

Principles of MRI

Spins under normal conditions

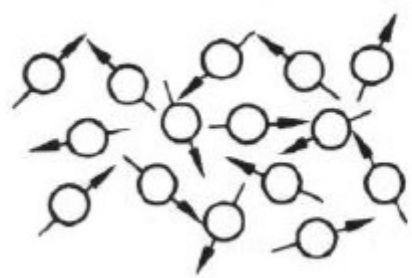

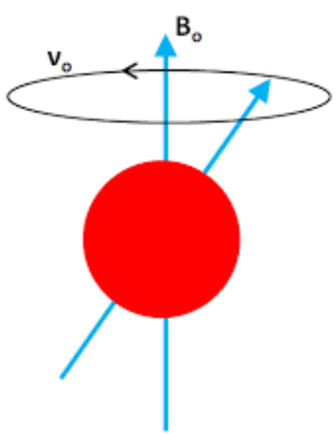

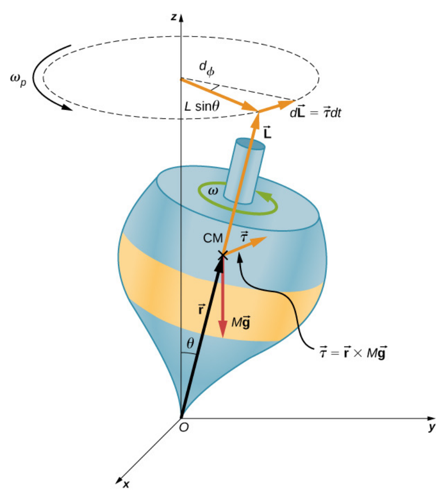

Spins in a magnetic field

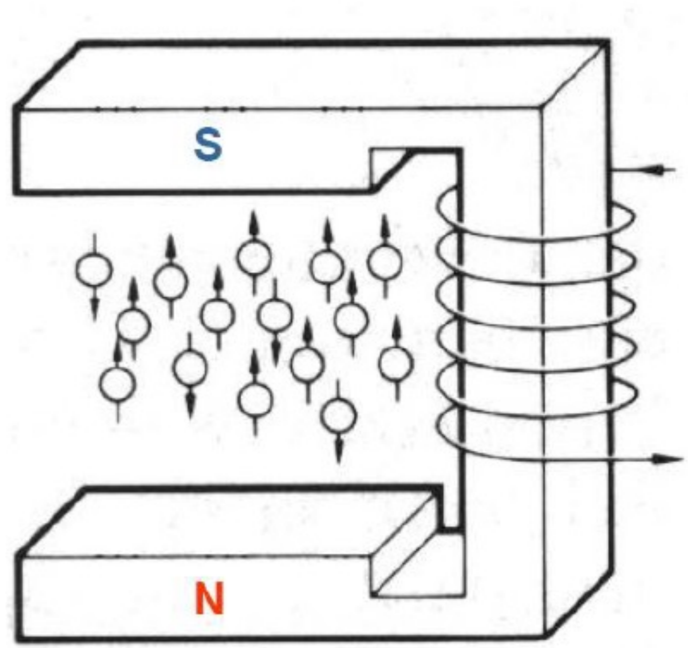

$$\omega_{Larmor} = \gamma B$$

Principles of MRI

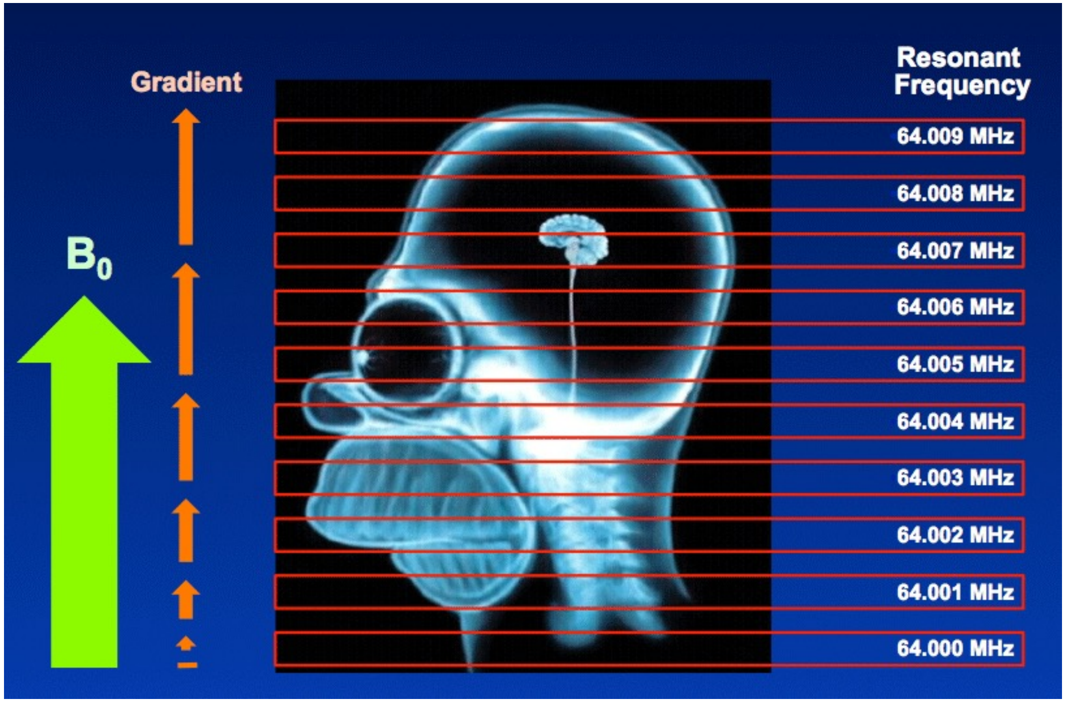

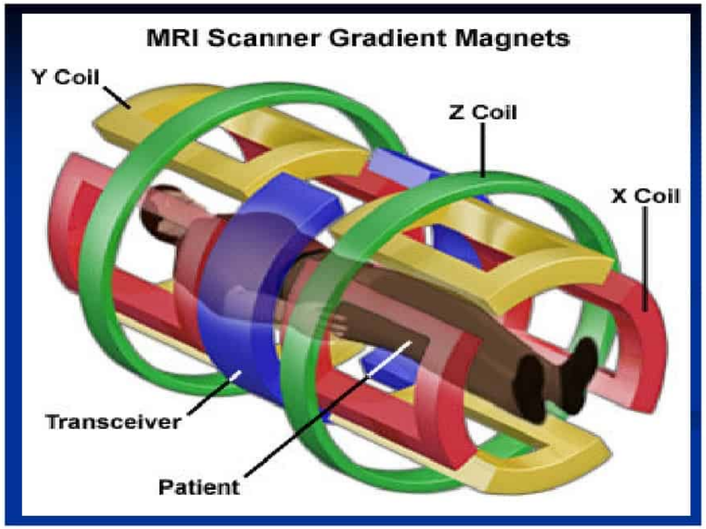

Principles of MRI

k-space

$s(k_x, k_y, k_z)$

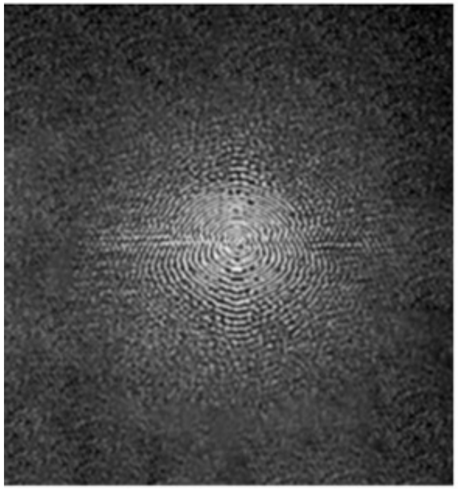

Image space

$\rho(x, y, z)$

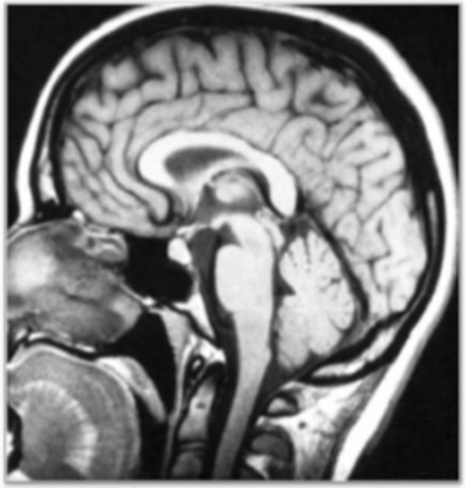

$$\rho(x,y,z) = \int_{-\infty}^{\infty}\int_{-\infty}^{\infty}\int_{-\infty}^{\infty} s(k_x,k_y,k_z)e^{2\pi i(k_x x + k_y y + k_z z)}\, dk_x dk_y dk_z$$

MR Simulator QA

Annual QA (subset)

Performance Parameter	Suggested Equipment	Suggested Method(s)	Tolerance/Reference	Recommended Frequency	Potential Clinical Impact
*Determine or verify external laser offset from MR isocenter	Phantom with scribes and internal landmarks for imaging	After verifying laser coincidence, level and align phantom to external lasers, translate couch known distance, acquire MRI, determine offset, iterate until tolerance is met.	≤ 1 mm	C, E, A	-Offset between patient and external lasers -Increased uncertainty in patient marking
*Table Alignment with B_0	Grid phantom	• Image with high-resolution spin echo sequence (0.5 mm in-plane resolution) at three couch positions along bore • Determine angle of grid phantom and vertical offset at each couch position	0 ± 0.3 degree between table and B_0 (cylindrical bore magnets) 90 ± 0.3 degree between table and B_0 (open bore magnets) <0.5 mm discrepancy in vertical offset	C, E	-Potential rotations or skewing of image volumes -Inaccurate laser marking
Informatics/ connectivity/ Data transfer	Phantom with landmarks noted for orientation	Ensure scanner is interfaced to required DICOM locations (e.g., Treatment Planning System, PACS and archive)	Site specific Per TG-248 guidelines[131]	C, E	-Workflow interruptions -Incorrect orientation
*Motion Verification	MR-compatible 4D motion platform	Play motion phantom with known waveform frequency and amplitude. Acquire dynamic images. Acquire respiratory triggered images using navigator or pneumatic bellows.	Amplitude based on prescribed motion waveform: • Preferred: 1 mm • Acceptable: 2 mm[78] Triggered acquisition window duration: • 30% of prescribed motion cycle Triggering delay: • Acquisition window centered over desired region of prescribed motion cycle	C, E	-Over/underestimate of target/OAR displacement -Inaccurate ITV estimation -Incorrect motion state of triggered images
*End-to-end Testing	Phantom with size, immobilization, and RF coil configuration per clinical use case (i.e., ACR MR quality control phantom for head)	• Complete for clinically applicable workflows (CT/MR-SIM, reverse workflow, MR-only) for common disease sites (head, abdomen/pelvis, extremities) • Image with optimized imaging protocols • Transfer/import data to TPS and verify:-Concordance of coordinate systems/orientation -Geometric integrity -Concordance of external laser system coordinates and spatial landmarks -Rigid co-registration accuracy between MR/CT	Data integrity verified via TG53[139] Verify image orientation Concordance of external laser system/landmarks: Preferred: 1 mm Acceptable: 2 mm Co-registration: Maximum cardinal direction error less than 0.5*voxel dimension size[140]	C, E	-Workflow interruptions -Localization inaccuracy -TPS incompatibility -Incorrect patient orientation

Monthly QA

Test	Suggested equipment	Protocol/parameter/tolerance
System		
Room temperature and humidity	Visual inspection of digital readout	Functional
Cold head operation	Audible pump sound	Functional
Cryogen level indicator	Digital readout from MRI console	Manufacturer specified (no change from baseline)
Mechanical		
Table movement smoothness and accuracy	Ruler	±1.0 mm from set distances
Laser alignment with imaging isocenter	Ruler and phantoms with internal landmarks	±2.0 mm from expected distance offsets
Laser movement smoothness and accuracy	Ruler	±2.0 mm from set distances
Patient marking		
Laser marking accuracy	Patient marking software	±2.0 mm
Image quality[a]		
Central frequency	Digital readout from MRI console after imaging reference phantom (i.e., ACR large MRI phantom or homogeneous phantom)	Manufacturer specified
Transmitter gain		± 5% from baseline
Flexible RF coil testing	Homogeneous phantom	Individual elements, exceeds minimum vendor-provided threshold
Geometric accuracy	Manufacturer supplied, in-house, or commercially available phantom > 30 cm in diameter/width	Verify ≤ 2 mm across 25 cm FOV
High contrast spatial resolution	ACR large MRI phantom with procedures/tolerances defined in Ref. 83	≤1.0 mm
Low contrast detectability		Total number of discernible spokes (for four slices) for fields < 3 T should range from 21 (0.3 T) to 36 (1.5 T), and 40 for 3 T.
Artifact evaluation		No obvious image artifacts
Percent image uniformity		Head coil: ≥ 87.5% for < 3 T ≥ 82.0% for 3 T
Percent signal ghosting		Ghosting Ratio ≤ 2.5%

AAPM TG 284.

MRI Safety

- Projectile effect
- RF heating
- Peripheral nerve stimulation
- Metal implants
- Pacemakers

Opoku et al. 2013.

Geometric Distortion

MRI is not geometrically precise!

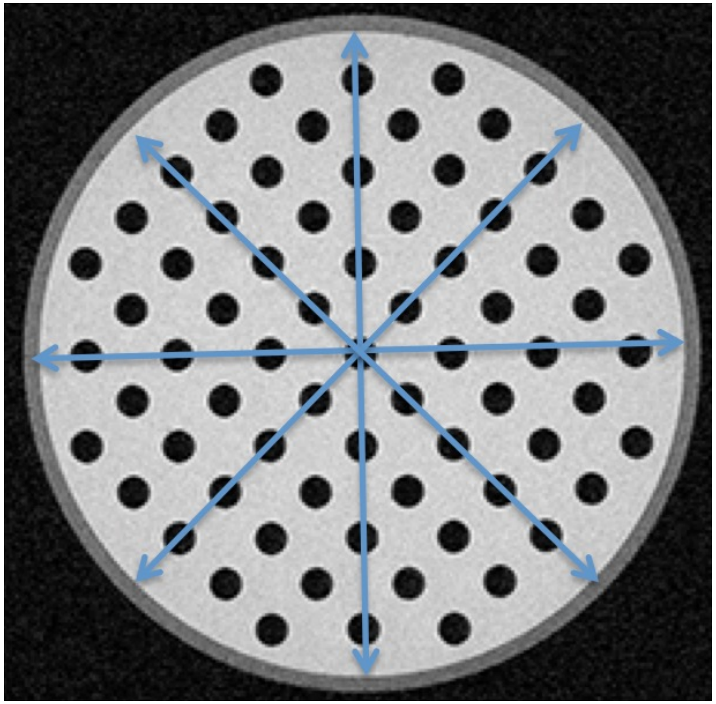

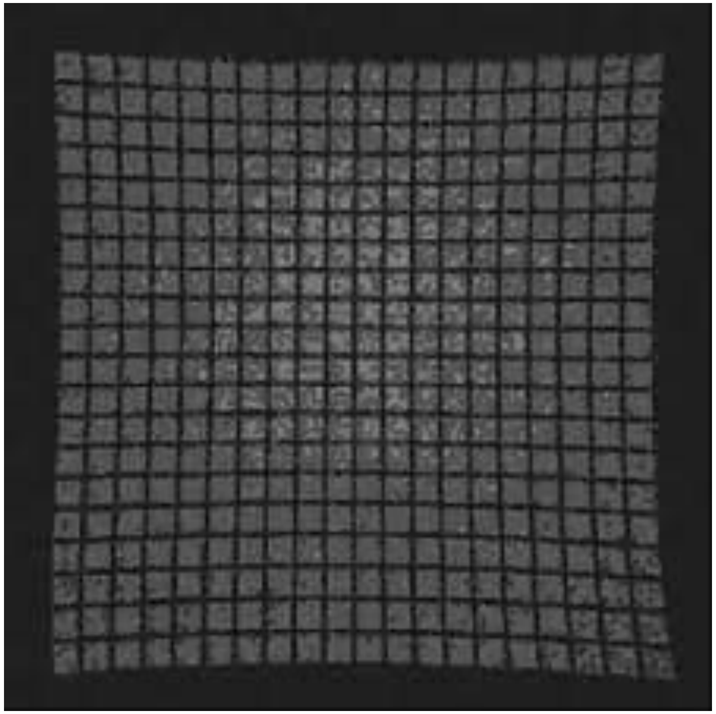

Wang et al. 2005.

Sources of Distortion

System Dependent

- Field inhomogeneities
- Gradient nonlinearities

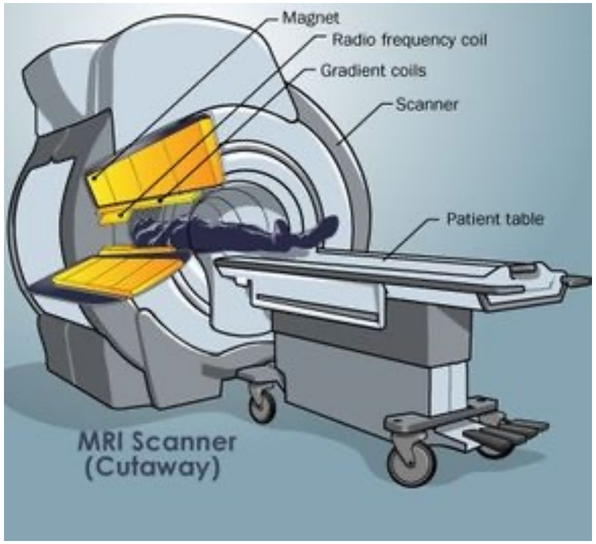

Patient Dependent

- Magnetic susceptibility
- Chemical shift

Worse at higher fields!

Static Field Inhomogeneities

- Field inhomogeneities on the order of ppm
- Causes geometric distortion since it alters Larmor frequency (figure to the right)
- Causes signal dropout due to magnetization dephasing
- Worse further off isocenter

$$\Delta x_{fi} = \frac{\Delta B_0(x, y, z)}{G_{read}}$$

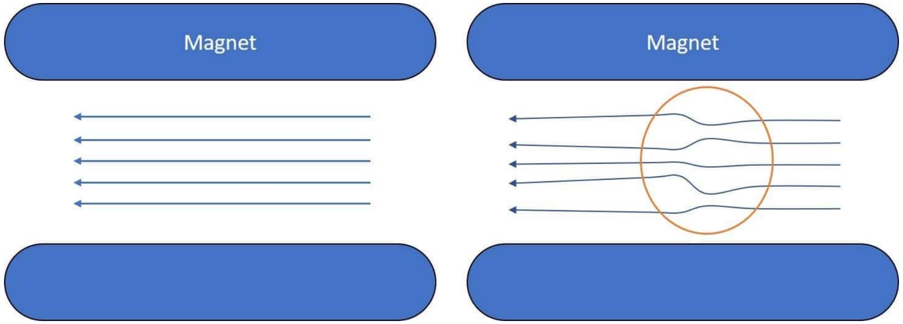

Shimming

- Shimming is the process that homogenizes the static magnetic field
- Passive shimming uses sheets of metal or ferromagnetic pellets
- Active shimming uses current
- Harmonic decomposition (Legendre polynomials)

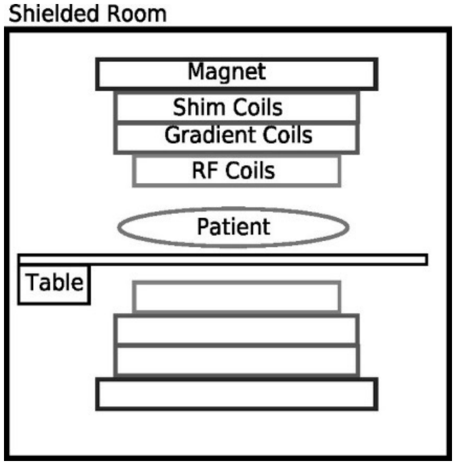

The first few associated Legendre functions $P_l^{|m|}(x)$

$$P_0^0(x) = 1$$

$$P_1^0(x) = x = \cos\theta$$

$$P_1^1(x) = (1 - x^2)^{1/2} = \sin\theta$$

$$P_2^0(x) = \tfrac{1}{2}(3x^2 - 1) = \tfrac{1}{2}(3\cos^2\theta - 1)$$

$$P_2^1(x) = 3x(1 - x^2)^{1/2} = 3\cos\theta\sin\theta$$

$$P_2^2(x) = 3(1 - x^2) = 3\sin^2\theta$$

$$P_3^0(x) = \tfrac{1}{2}(5x^3 - 3x) = \tfrac{1}{2}(5\cos^3\theta - 3\cos\theta)$$

$$P_3^1(x) = \tfrac{3}{2}(5x^2 - 1)(1 - x^2)^{1/2} = \tfrac{3}{2}(5\cos^2\theta - 1)\sin\theta$$

$$P_3^2(x) = 15x(1 - x^2) = 15\cos\theta\sin^2\theta$$

$$P_3^3(x) = 15(1 - x^2)^{3/2} = 15\sin^3\theta$$

Gradient Nonlinearities

$$\Delta x_{gn} = \frac{x \Delta G_{read}}{G_{read}}$$

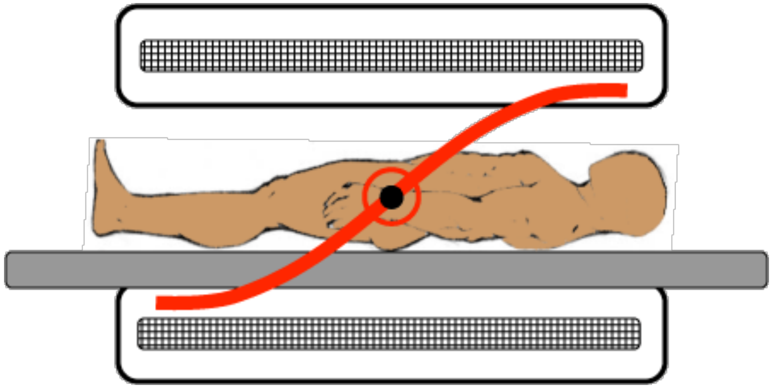

- We assume gradients are linear, but they are not so!
- Also, worse further off isocenter

Taylor expansion of the solution to the Biot–Savart law

$$B_z(z) = \frac{\mu_0 I a^2}{2}\left[\frac{1}{(a^2+s^2)^{\frac{3}{2}}} + \left(\frac{3s}{(a^2+s^2)^{\frac{5}{2}}}\right)z + \frac{1}{2}\left(\frac{12s^2-3a^2}{(a^2+s^2)^{\frac{7}{2}}}\right)z^2 + \frac{1}{6}\left(\frac{60s^3-45sa^2}{(a^2+s^2)^{\frac{9}{2}}}\right)z^3 + \cdots\right]$$

I = current a = coil radius s = axial position

Magnetic Susceptibility

- Bulk property of matter describing a medium's capacity to become polarized in a magnetic field
- Caused by the interaction between electrons and the magnetic field
- Inversely proportional to temperature
  - Curie's Law

$$\vec{M} = \chi\vec{B}$$

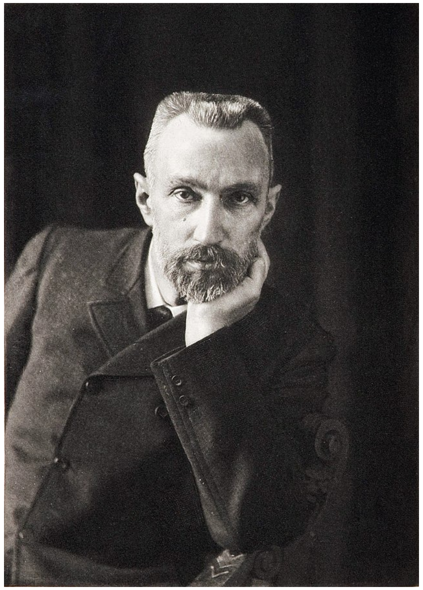

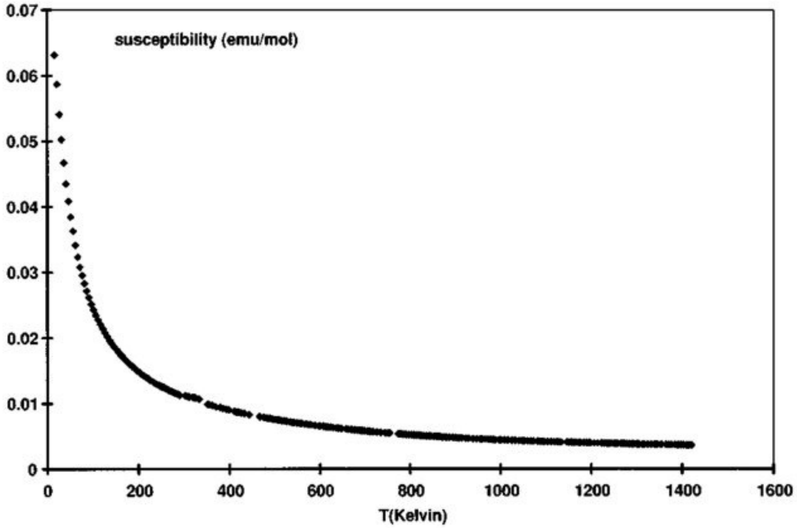

Susceptibility-Induced Distortion

Susceptibility artifact due to iron particles in mascara

$$B_0^{perturbed} = (1 + \chi)B_0$$

$$\Delta x_{ms} = \Delta\chi \frac{B_0}{G_{read}}$$

- Most prominent at interfaces with differing susceptibilities
  - Air – soft tissue
  - Bone – soft tissue

Chemical Shift Distortion

- Different chemical environments → different precessional frequencies
- Water protons precess 224 Hz more rapidly than fat protons at 1.5 T

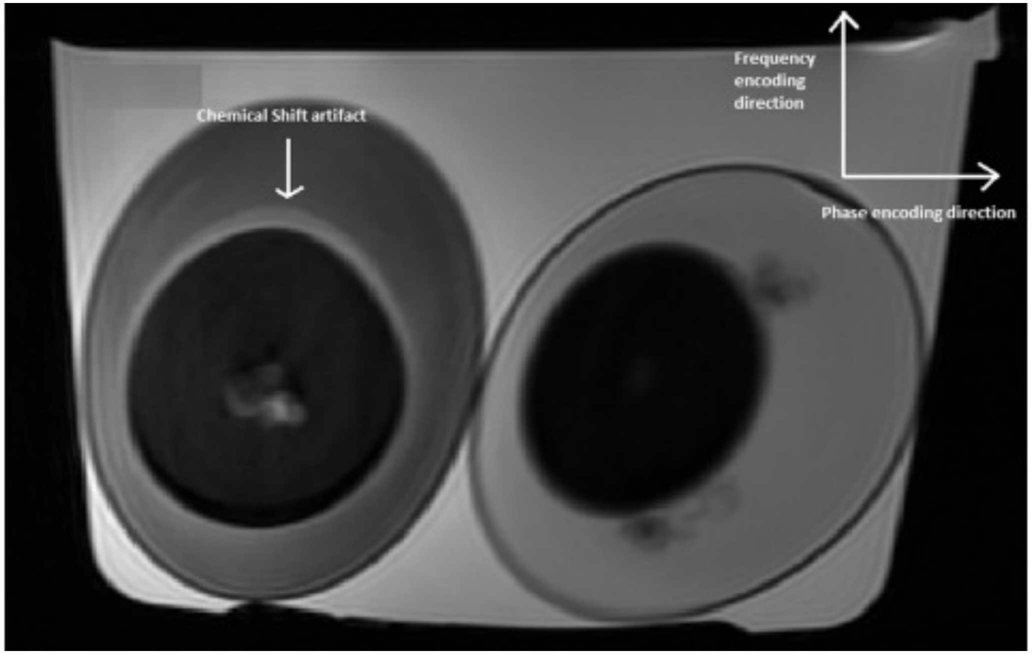

Magnitude of Geometric Distortion

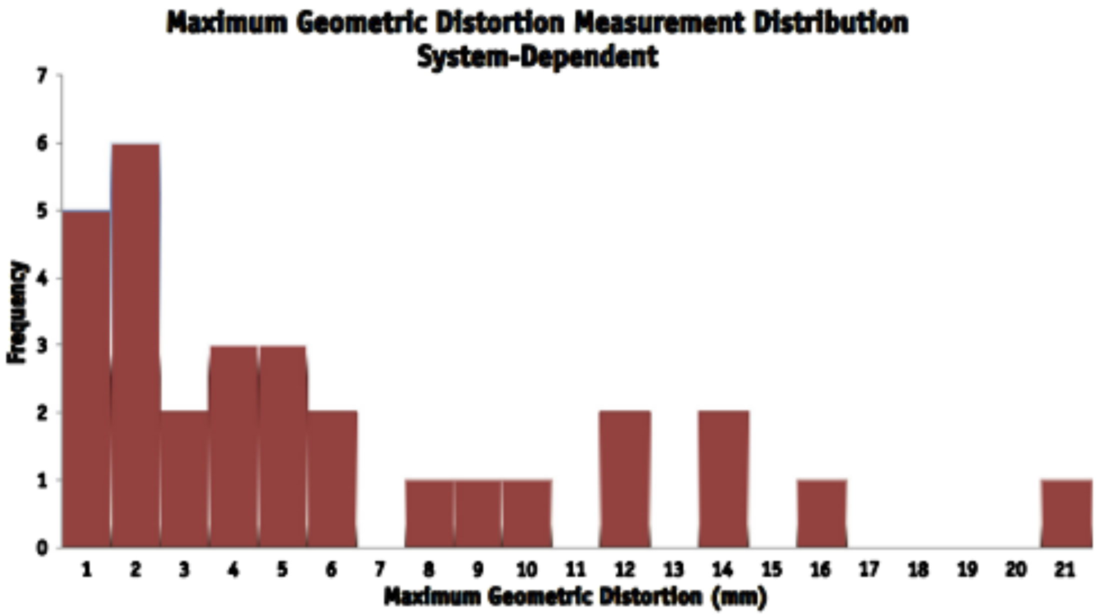

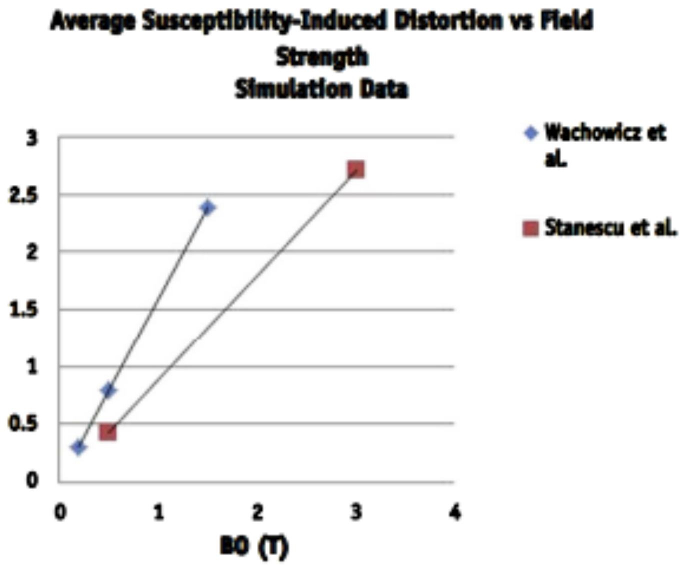

TG 117 under development!

Take Home Messages

- Magnitude of distortion on the order of 1 to 2 mm but can be greater at clinical field strengths
  - SRS?
- Scales with B_0
  - Less important at low field
- Air-soft tissue or bone-soft tissue interfaces
- Worse off isocenter
- Cautions against contouring directly off MRI at clinical field strengths

Segmentation

CT

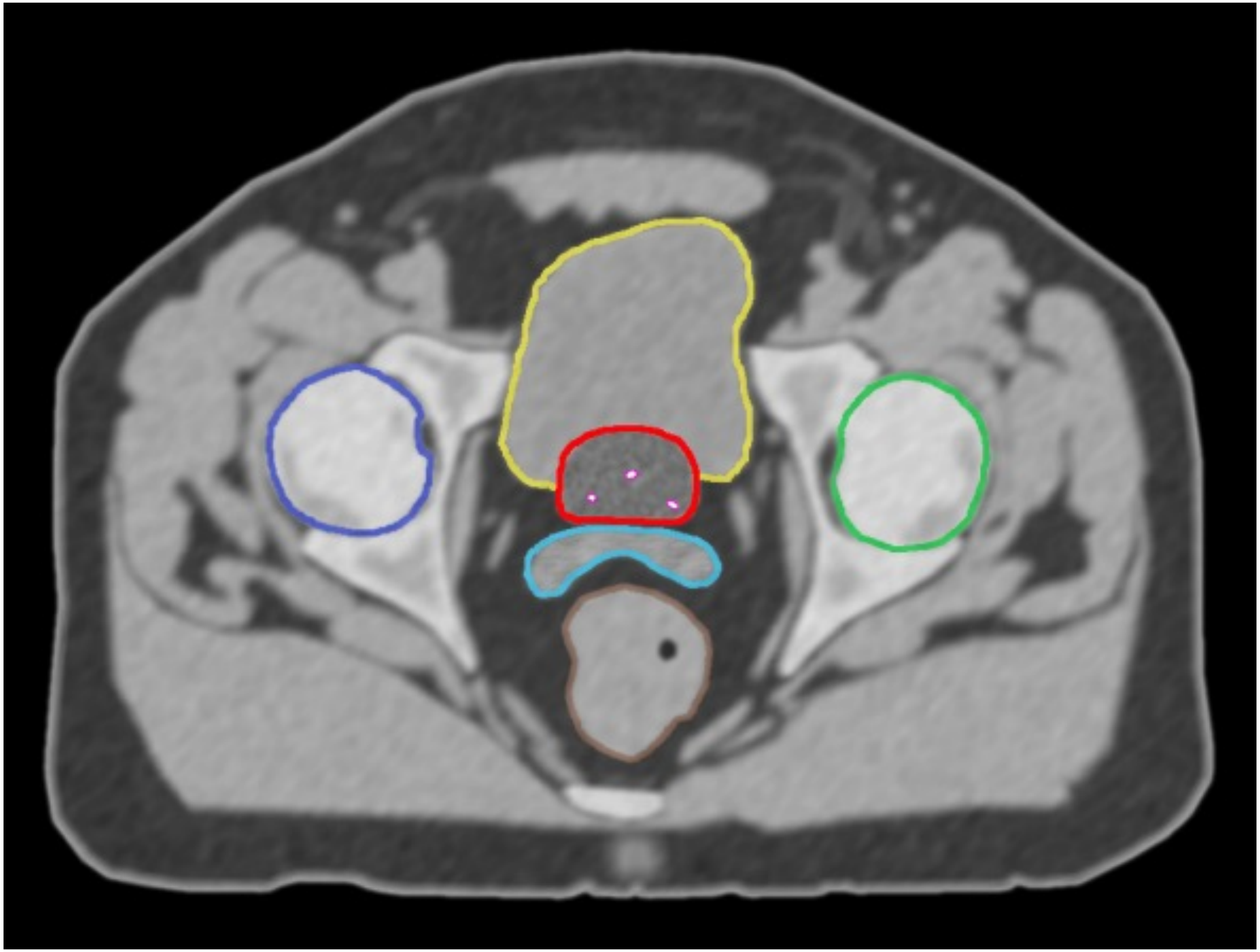

MRI

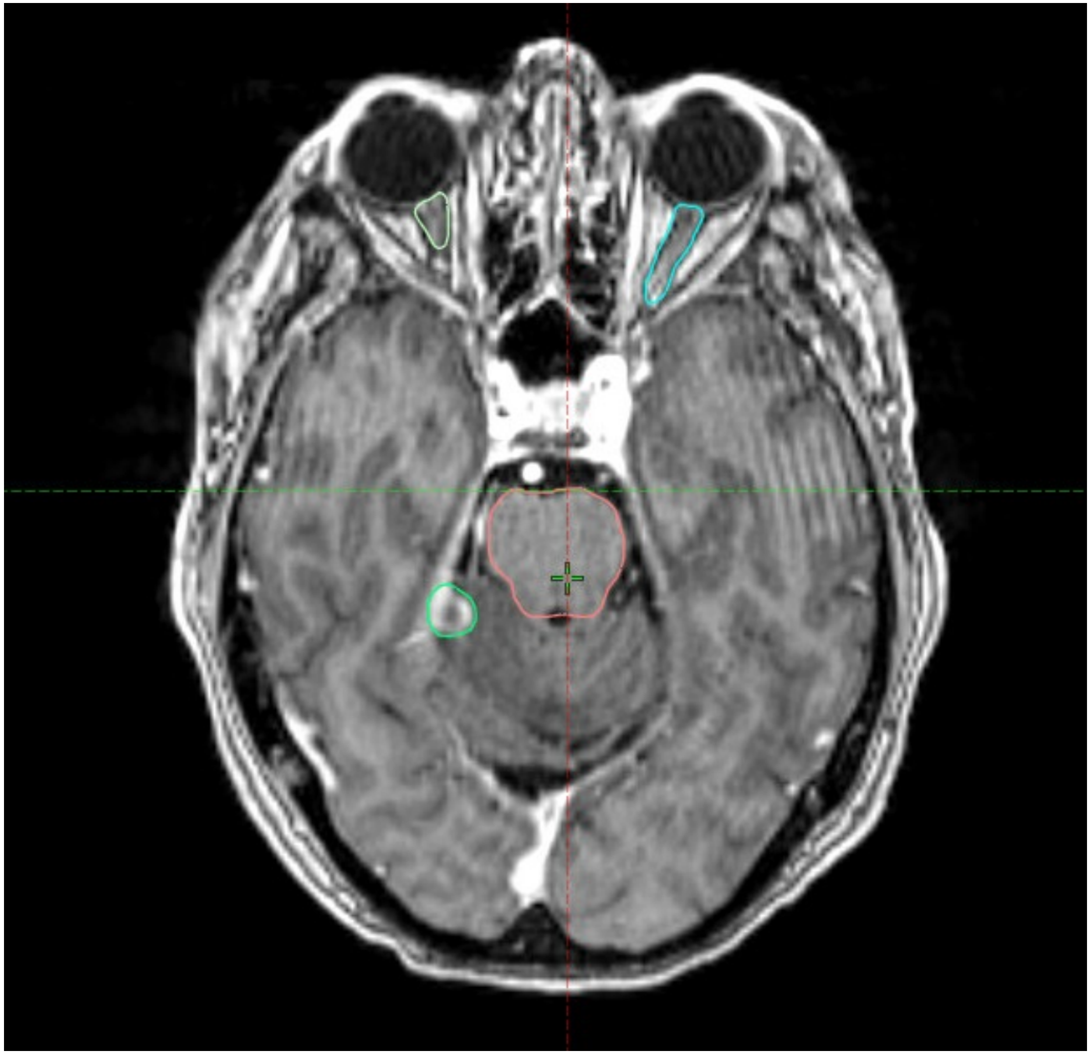

PET

PET = Positron emission tomography

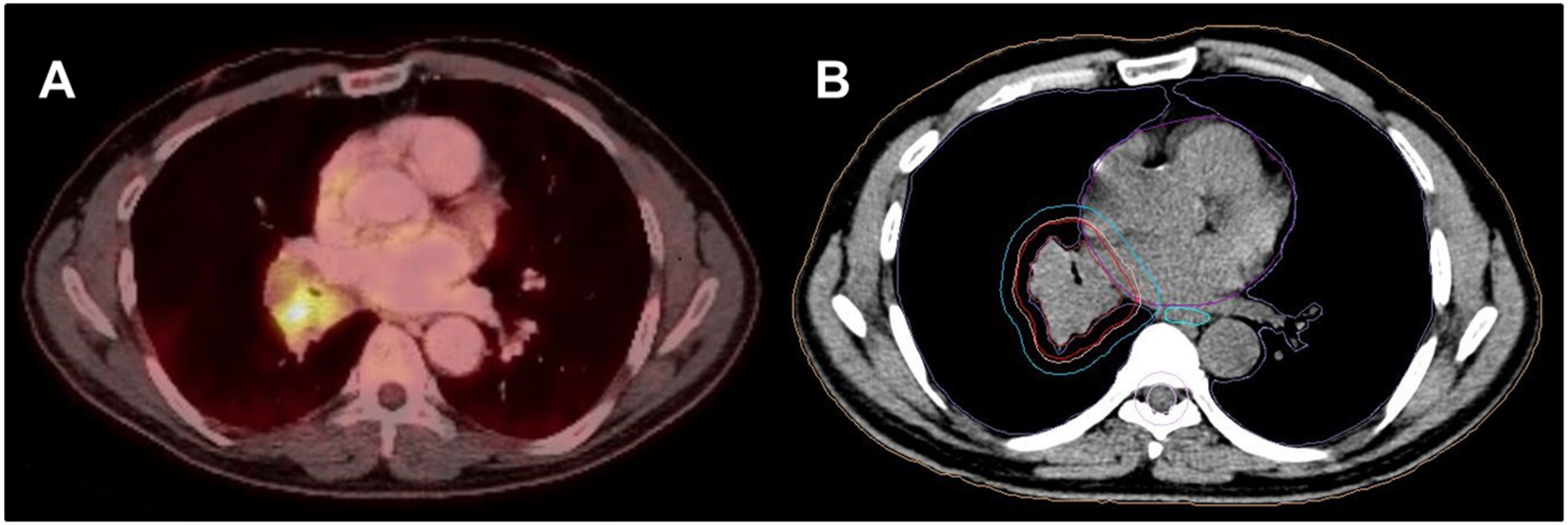

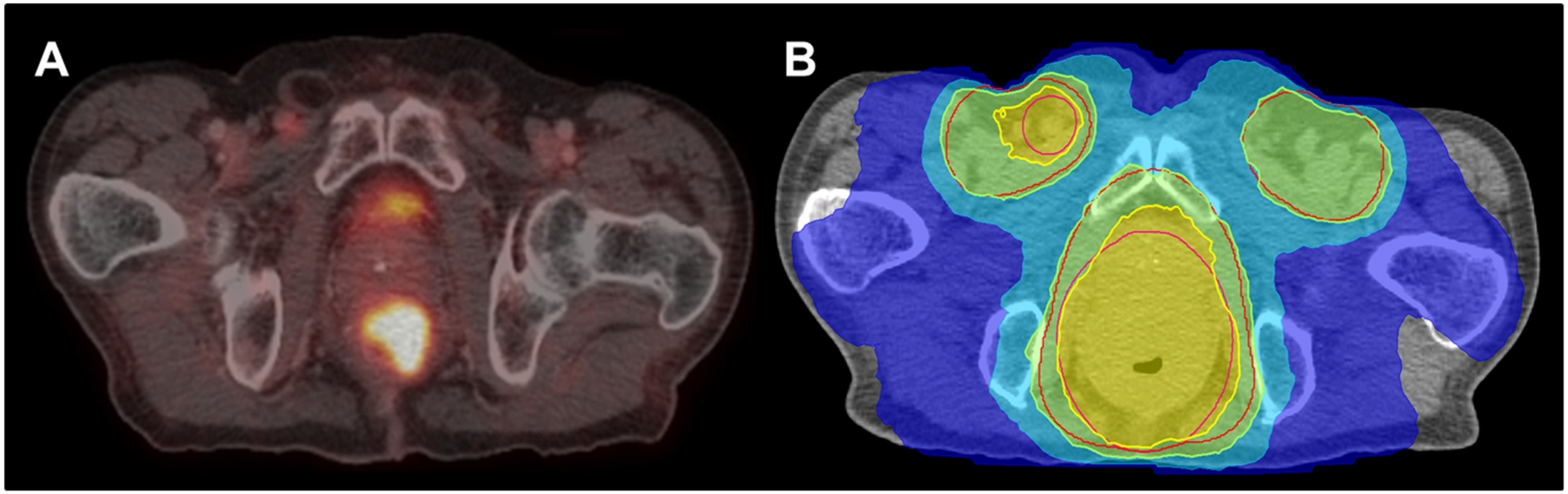

Unterrainer et al. 2020.

History of PET

Hoffman

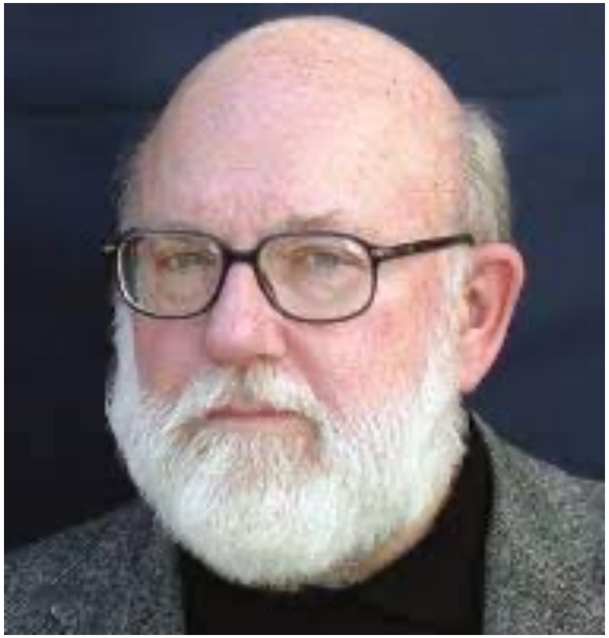

Phelps

Ter-Pogossian

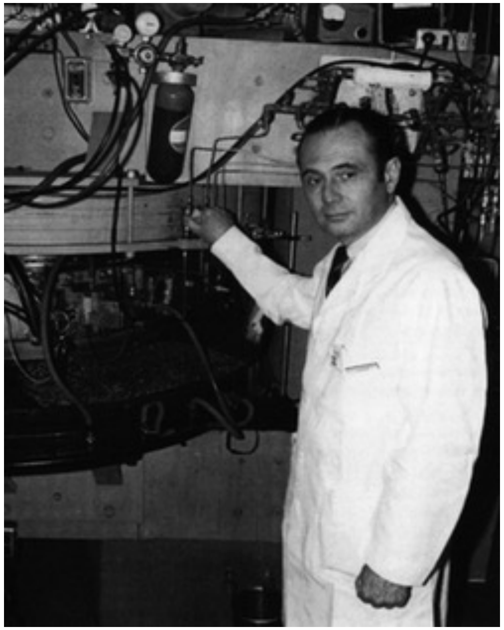

Principles of PET

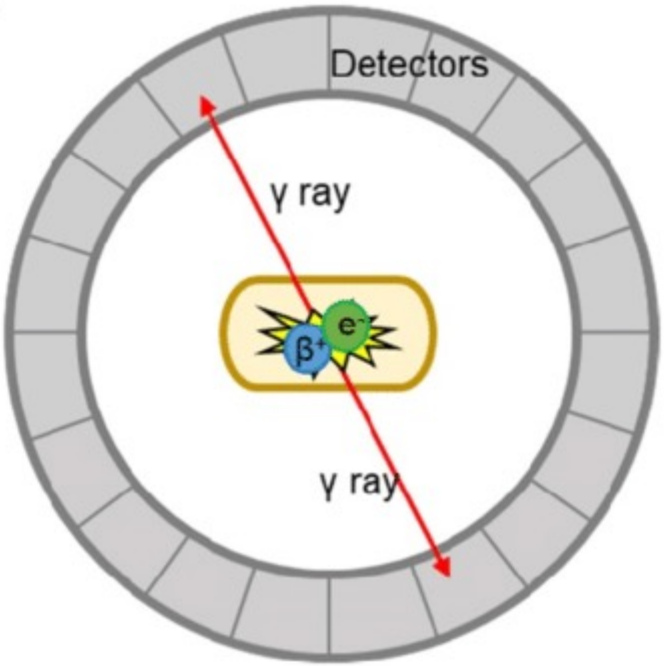

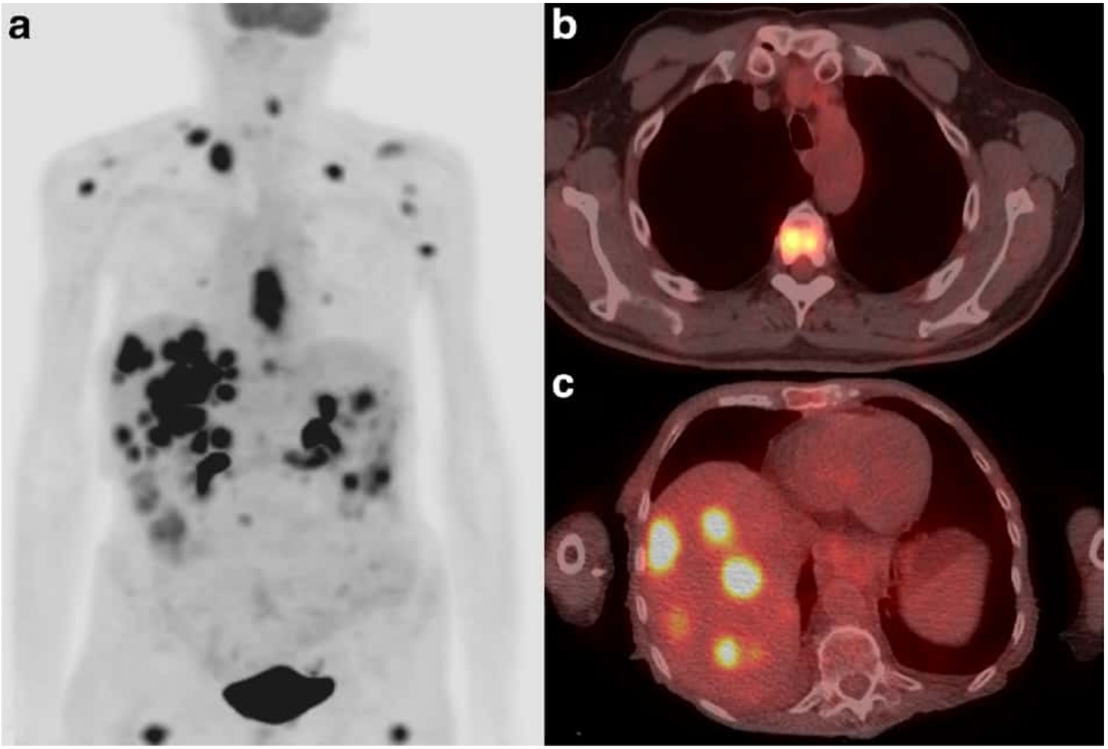

FDG

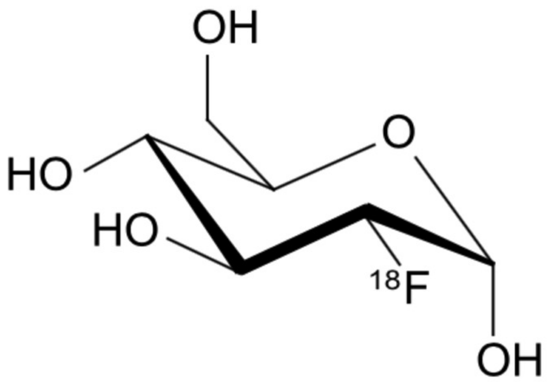

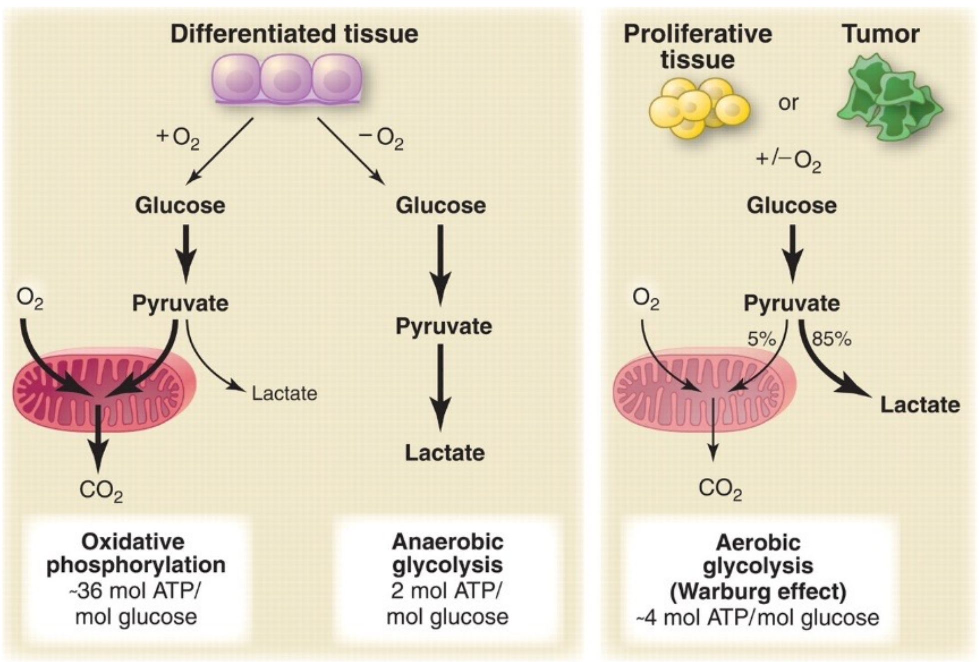

Vander Heiden et al. 2009

Warburg

FDG-PET in Radiation Oncology

Task Group 174 Report: Utilization of [^{18}F]Fluorodeoxyglucose Positron Emission Tomography ([^{18}F]FDG-PET) in Radiation Therapy

Shiva K. Das[a)], and Ross McGurk
Department of Radiation Oncology, University of North Carolina School of Medicine, Chapel Hill, NC, USA

Moyed Miften
Department of Radiation Oncology, University of Colorado School of Medicine, Aurora, CO, USA

Sasa Mutic
Department of Radiation Oncology, Washington University School of Medicine, St. Louis, MO, USA

James Bowsher
Department of Radiation Oncology, Duke University Medical Center, Durham, NC, USA

John Bayouth
Human Oncology, University of Wisconsin, Madison, WI, USA

Yusuf Erdi
Department of Medical Physics, Memorial Sloan-Kettering Cancer Center, New York, NY, USA

Osama Mawlawi
Department of Imaging Physics, University of Texas, M D Anderson Cancer Center, Houston, TX, USA

Ronald Boellaard
Department of Radiology and Nuclear Medicine, VU University Medical Center, Amsterdam, The Netherlands

Stephen R. Bowen
Department of Radiation Oncology, University of Washington, Seattle, WA, USA

Lei Xing
Department of Radiation Oncology, Stanford University School of Medicine, Stanford, CA, USA

Jeffrey Bradley
Department of Radiation Oncology, Washington University School of Medicine, St. Louis, MO, USA

Heiko Schoder
Molecular Imaging and Therapy Service, Memorial Sloan-Kettering Cancer Center, New York, NY, USA

Fang-Fang Yin
Department of Radiation Oncology, Duke University Medical Center, Durham, NC, USA

Daniel C. Sullivan
Department of Radiology, Duke University School of Medicine, Durham, NC, USA

Paul Kinahan
Department of Radiology, University of Washington, Seattle, WA, USA

(Received 6 April 2019; revised 30 April 2019; accepted for publication 6 June 2019; published 6 September 2019)

PSMA

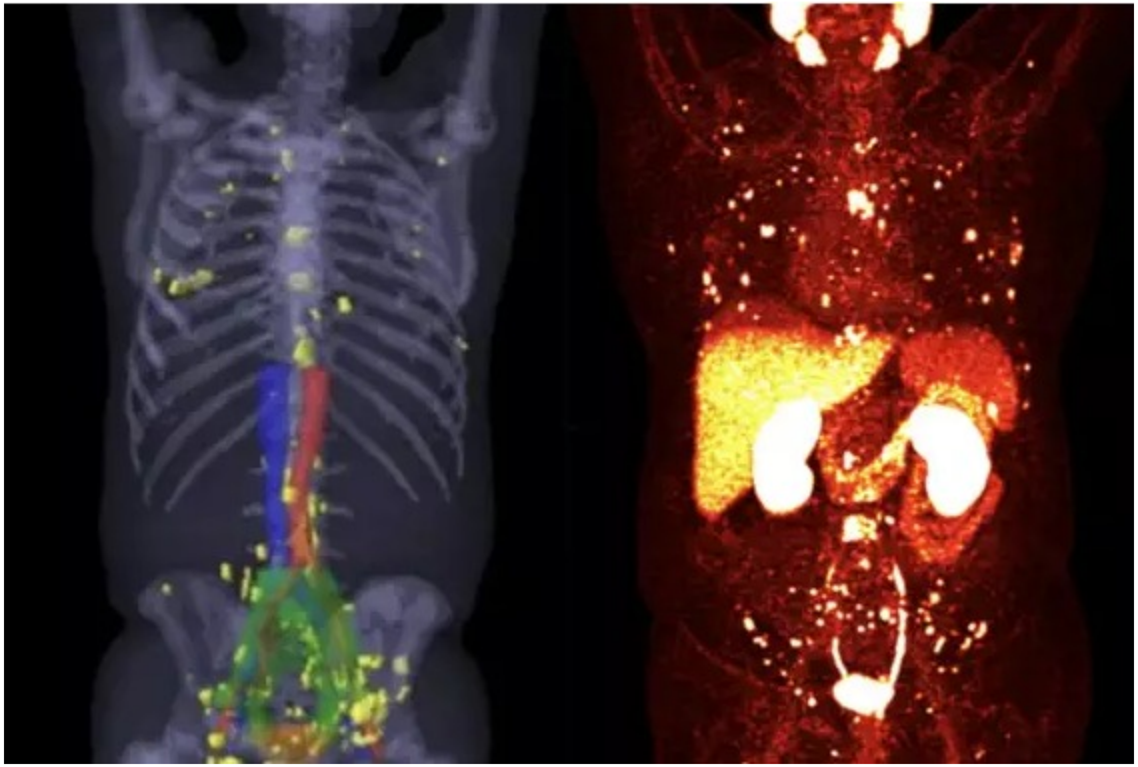

- Prostate specific membrane antigen
- Expressed on the surface of prostate cancer cells
- ^{68}Ga or ^{18}F
- Small molecule or peptide with affinity for PSMA is injected

Other PET Tracers

Molecular uptake mechanism	Tracer	Isotope	Organs of highest physiological uptake[a]	Availabiltiy
Amino acid transport and protein synthesis	Methionine	C-11	Liver, salivary glands, lachrymal glands, bone marrow, pancreas, bowels, renal cortical, urinary bladder	In-house production/cyclotron
	Fluoroethyltyrosine	F-18	Pancreas, kidneys, liver, heart, brain, colon, muscle	In-house production/cyclotron[b]
	FDOPA	F-18	Pancreas, liver, duodenum, kidneys, gallbladder, biliary duct	Commercially available
Glucose metabolism	FDG	F-18	Brain, myocardium, breast, liver, spleen stomach, intestine, kidney, urinary bladder, skeletal muscle, lymphatic tissue, bone marrow, salivary glands, thymus, uterus, ovaries, testicle, brown fat	Commercially available
Proliferation	FLT	F-18	Bone marrow, intestine, kidneys, urinary bladder, liver	In-house production/cyclotron[b]
Hypoxia	FMISO	F-18	Liver, urinary excretion	In-house production/cyclotron[b]
	FAZA	F-18	Kidneys, gallbladder, liver, colon	In-house production/cyclotron
	Cu-ATSM	Cu-64	Liver, kidneys, spleen, gallbladder[c]	In-house production/cyclotron[b]
Lipid metabolism	Choline	C-11	Liver, pancreas, spleen, salivary glands, lachrymal glands, renal excretion, bone marrow, intestine	In-house production/cyclotron
	Fluoroethylcholine	F-18	Liver, kidneys, salivary glands, urinary bladder, bone marrow, spleen	In-house production/cyclotron[b]
	Acetate	C-11	Gastrointestinal tract, prostate, bone marrow, kidneys, liver, spleen, pancreas	In-house production/cyclotron
Angiogenesis/integrin binding	Galacto-RGD	F-18	Bladder, kidneys, spleen, liver	In-house production/cyclotron
	AH111585	F-18	Bladder, liver, intestine, kidneys	In-house production/cyclotron
SSTR binding	DOTATOC	Ga-68	Pituitary and adrenal glands, pancreas, spleen, urinary bladder, liver, thyroid	In-house production/generator
	DOTATATE	Ga-68	Spleen, urinary bladder, liver	In-house production/generator

[a] Uptake ranking is from higher to lower organ activity concentration.
[b] In some countries commercially available but yet without marketing authorization.
[c] Estimated from calculations using ^{60}Cu-ATSM-PET.

Spatial Resolution in PET

Limited By:

- Positrons have nonzero energy
- Annihilation photons are not emitted at exactly 180°
- Intrinsic resolution of the detectors

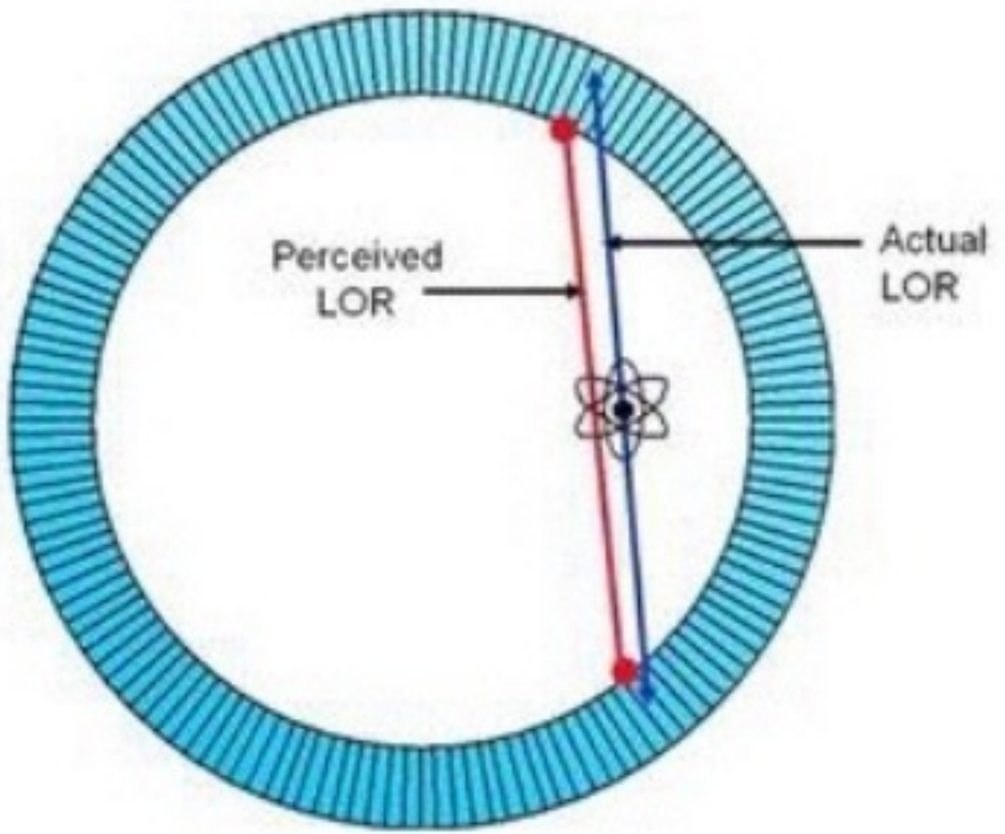

Image Registration

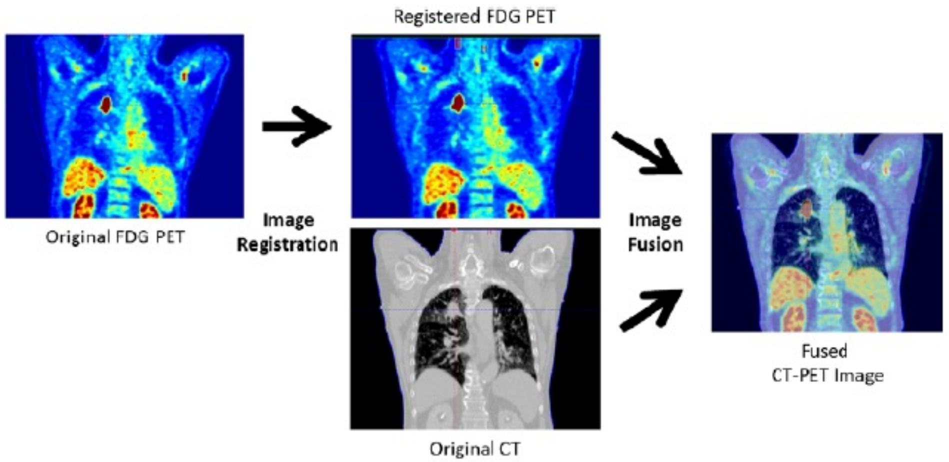

Use of image registration and fusion algorithms and techniques in radiotherapy: Report of the AAPM Radiation Therapy Committee Task Group No. 132

Kristy K. Brock[a)]
Department of Imaging Physics, The University of Texas MD Anderson Cancer Center, 1400 Pressler St, FCT 14.6048, Houston, TX 77030, USA

Sasa Mutic
Department of Radiation Oncology, Washington University School of Medicine, St. Louis, MO, USA

Todd R. McNutt
Department of Radiation Oncology, Johns Hopkins Medical Institute, Baltimore, MD, USA

Hua Li
Department of Radiation Oncology, Washington University School of Medicine, St. Louis, MO, USA

Marc L. Kessler
Department of Radiation Oncology, University of Michigan, Ann Arbor, MI, USA

- Manual vs automatic
- 3 components:
  - Transformation model
  - Metric
  - Optimization scheme
- Rigid vs affine vs deformable
- Sum-of-squares vs cross correlation vs mutual information
- Registration vs fusion

Setup Verification

In-Room kV Imaging Systems

- Rail-track mounted
- Ceiling-floor mounted
- Gantry mounted

Rail-Track Mounted Systems

- Imaging gantry travels on rails
- Two rails vs three rails
- Rails provide motion guidance and stability

AAPM TG 104.

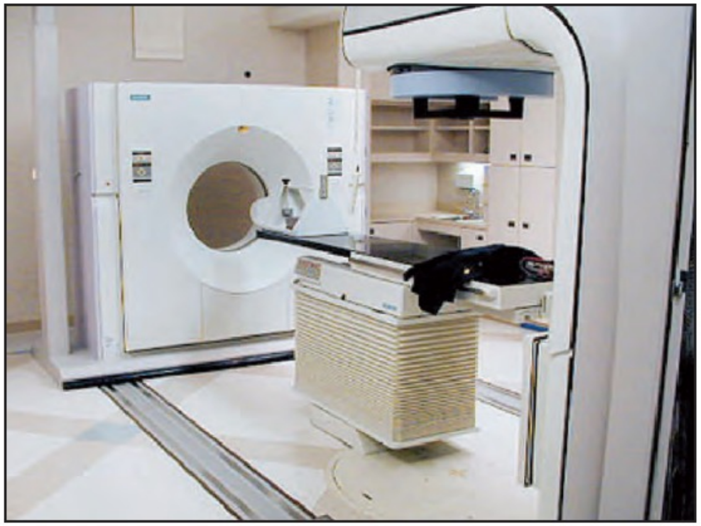

The Rails

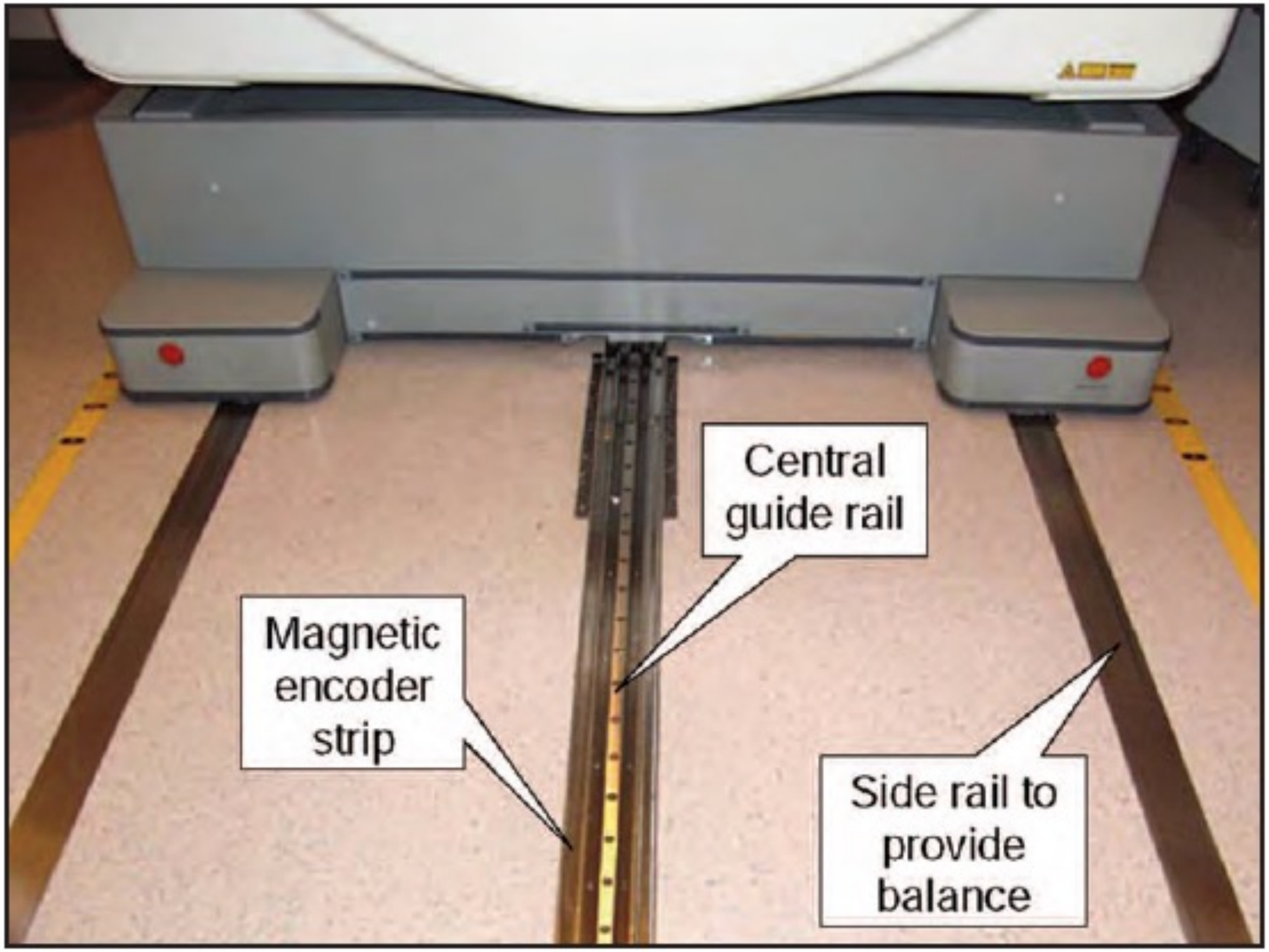

AAPM TG 104.

MRI-on-Rails

Ceiling-Floor Mounted Systems

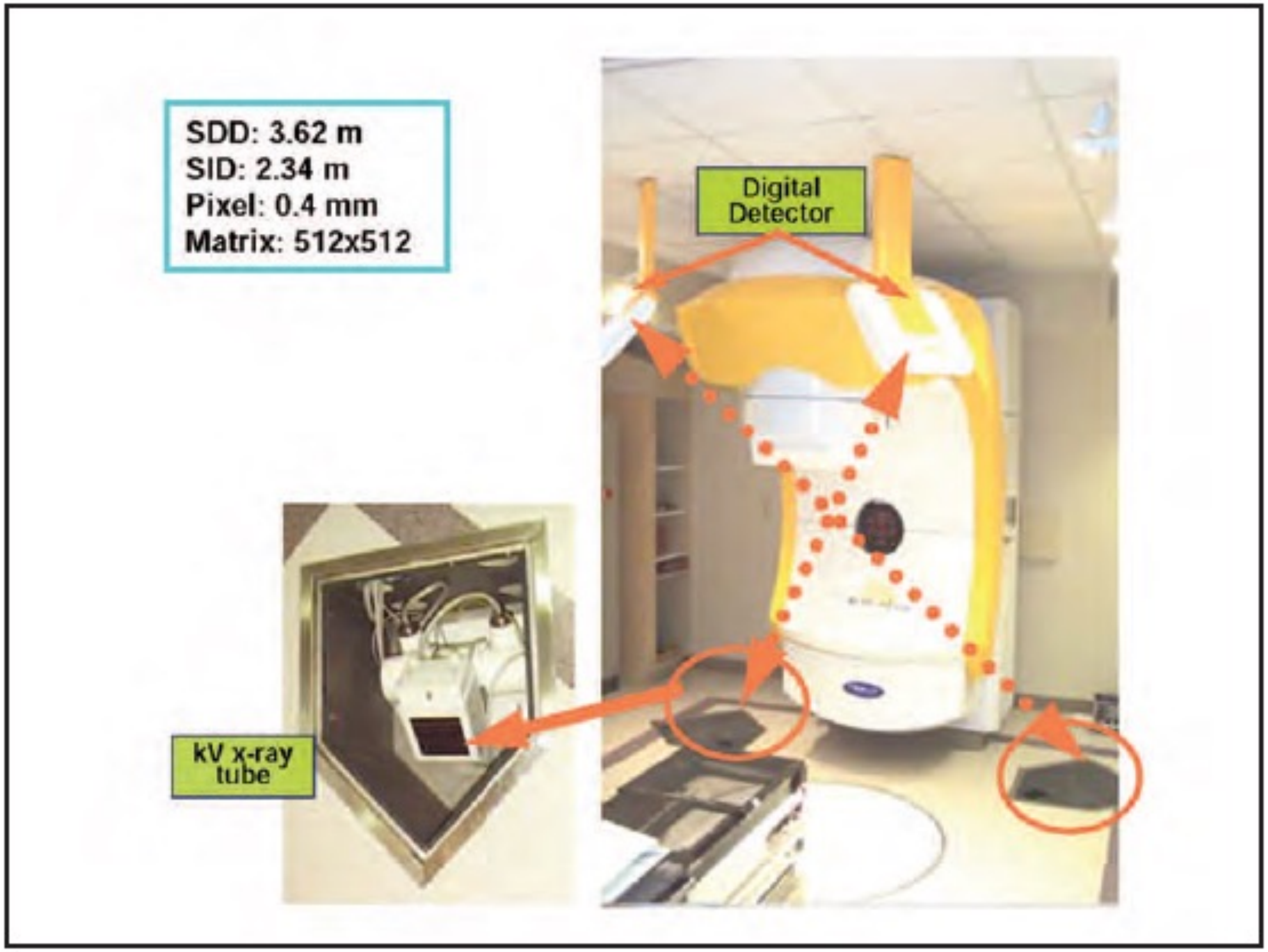

AAPM TG 104.

Dartmouth Health

ExacTrac System

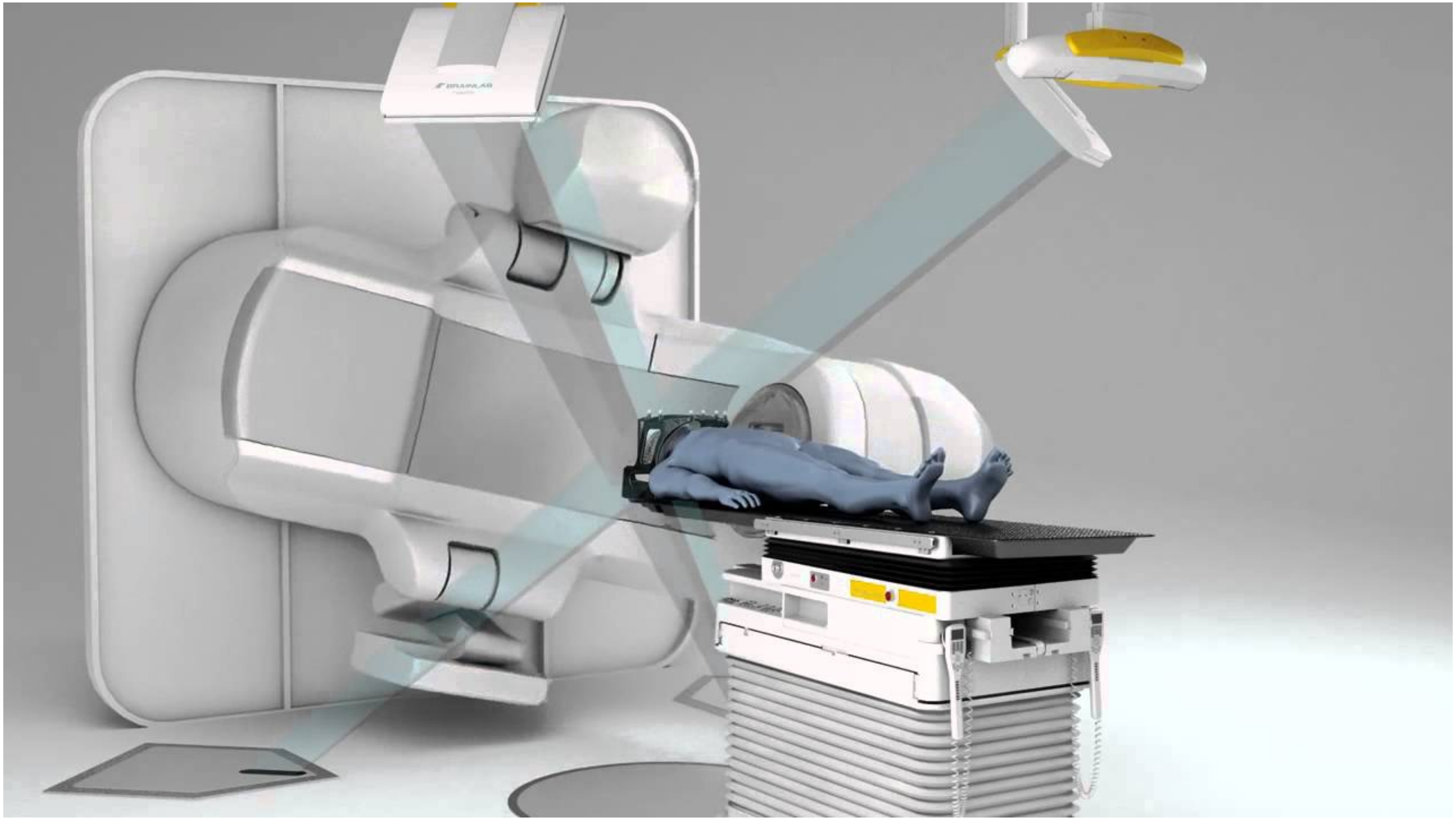

ExacTrac IR Subsystem

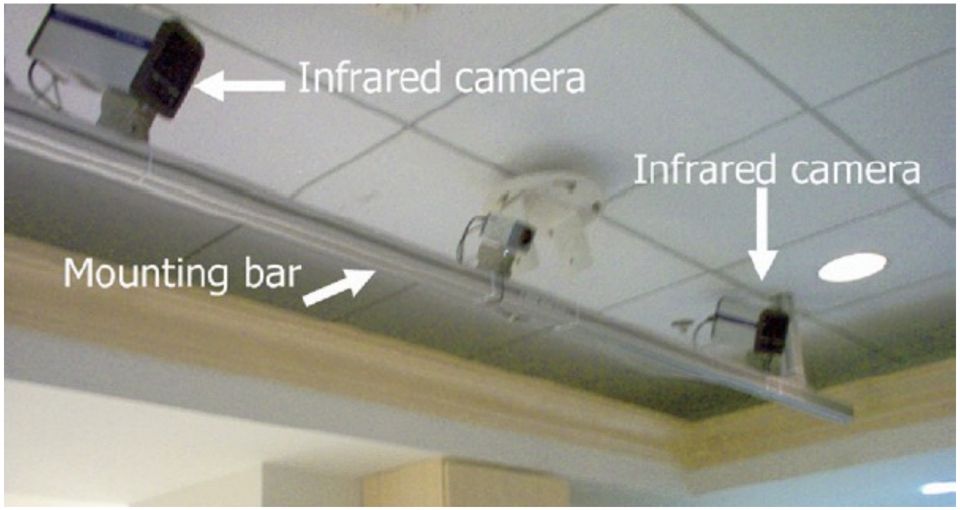

Wagner et al. 2007.

CyberKnife System

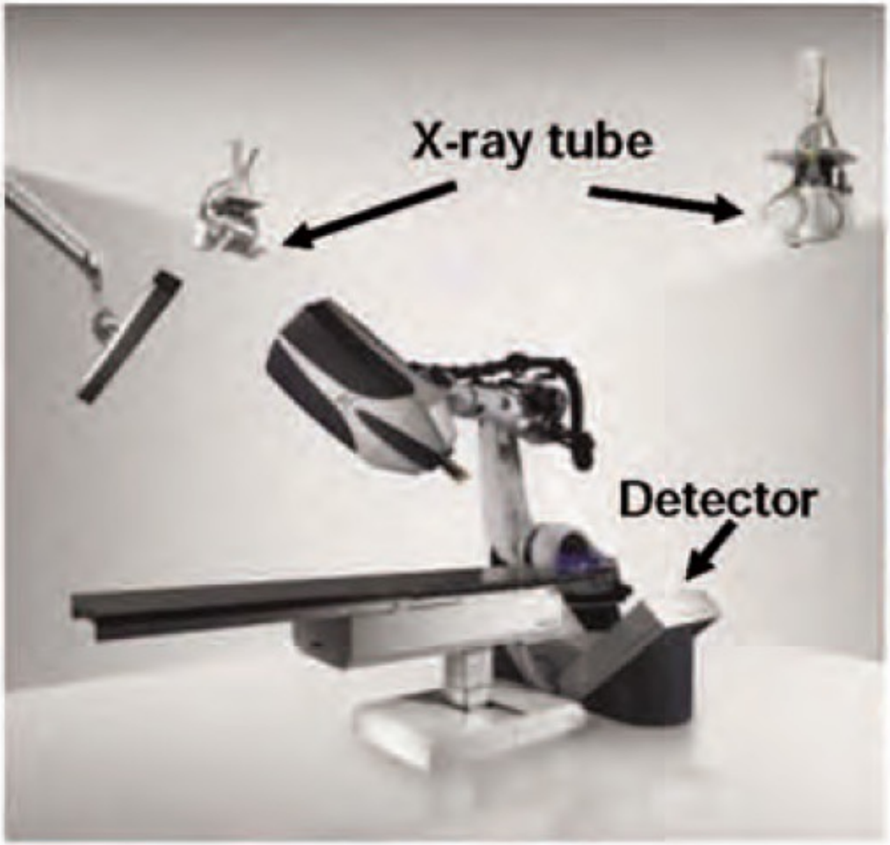

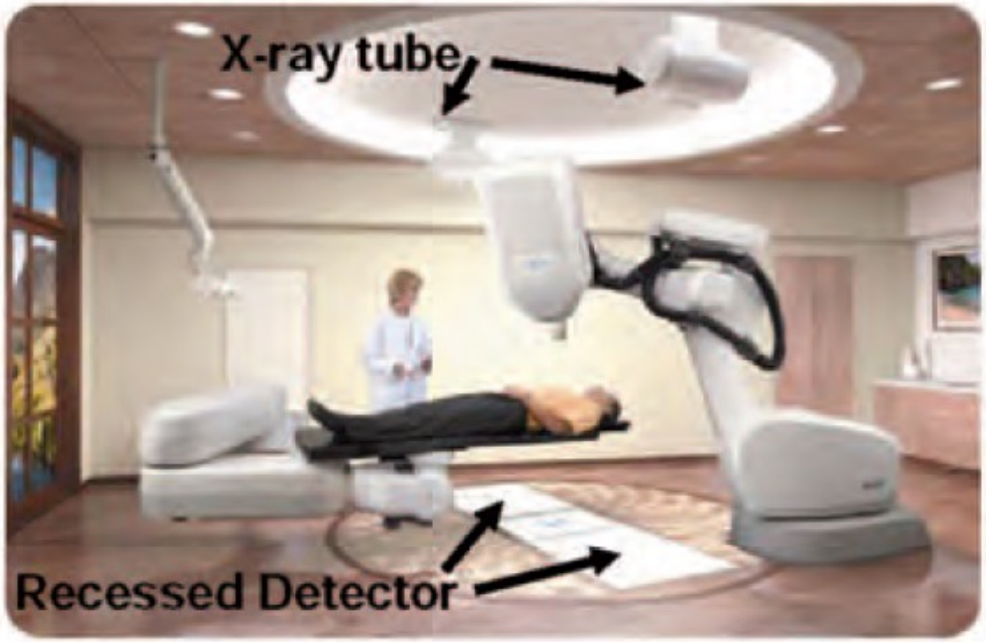

AAPM TG 104.

CyberKnife Imaging System

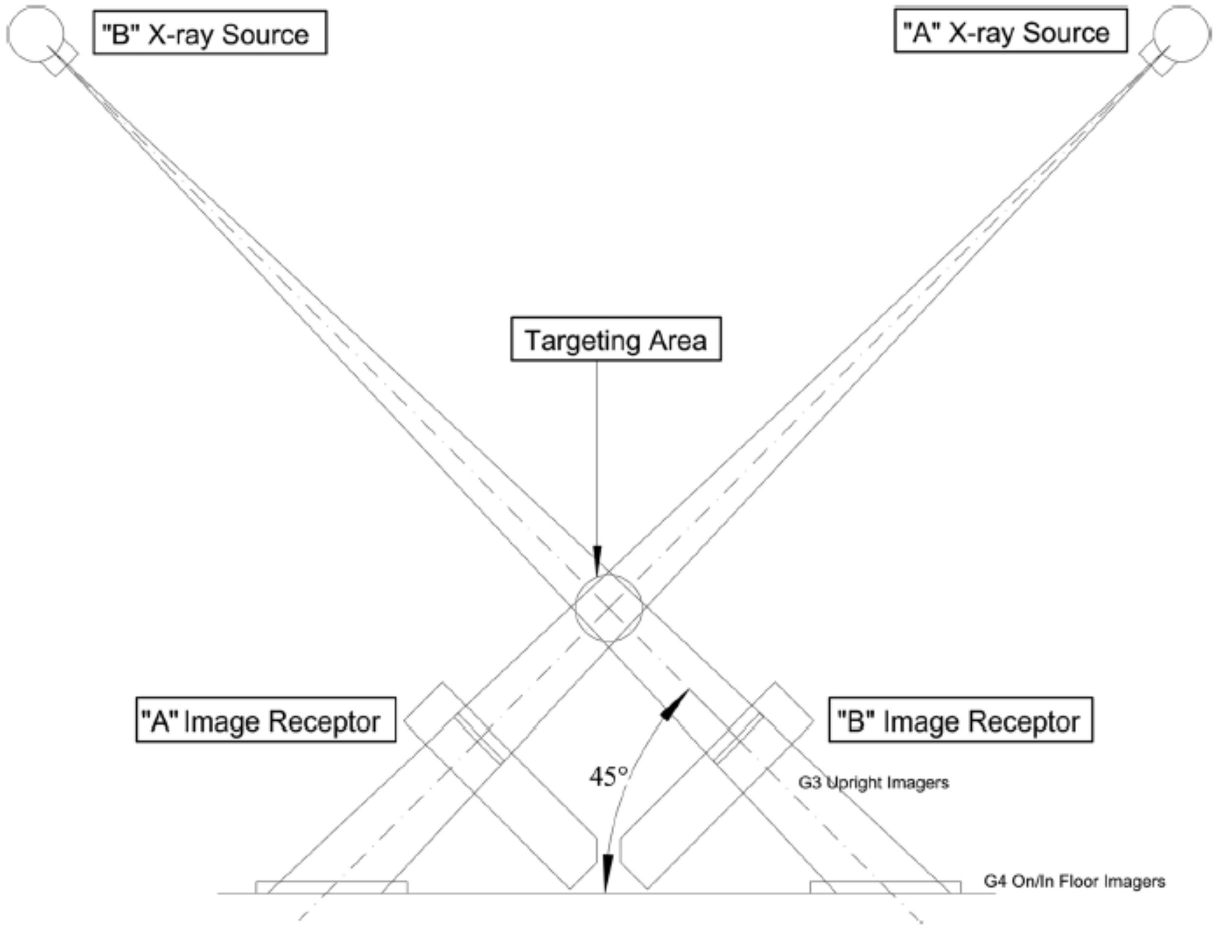

AAPM TG 135.

CyberKnife Principles

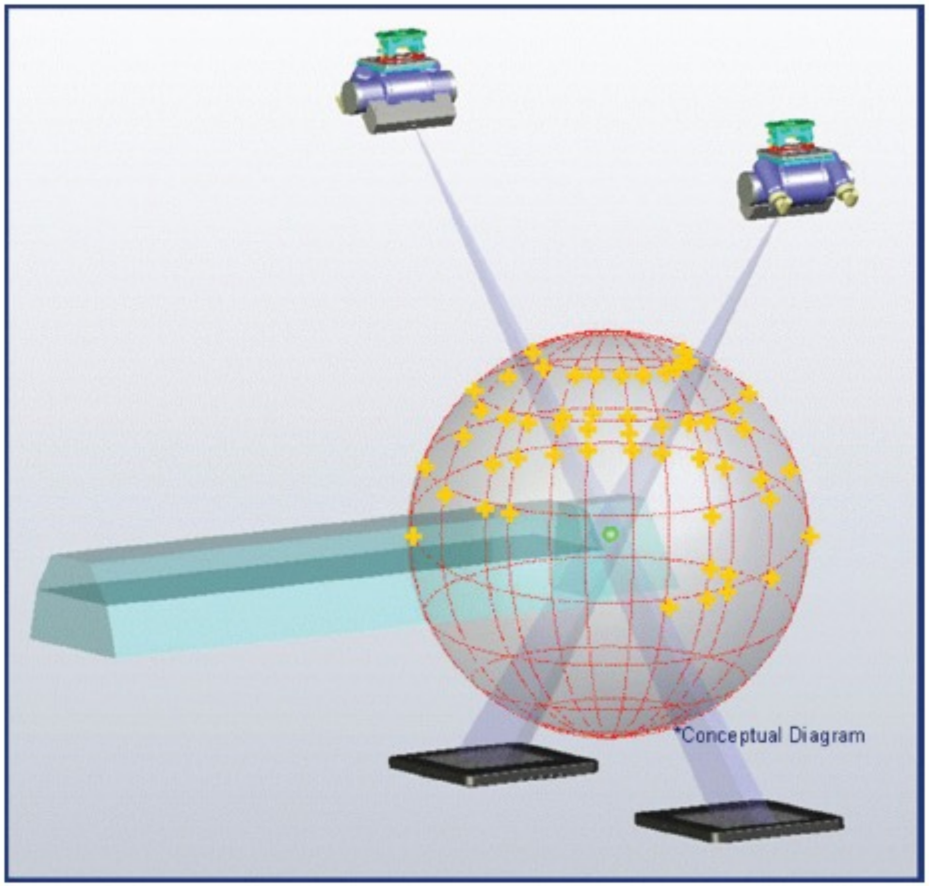

AAPM TG 135.

- Noncoplanar treatment
  - ➢ Head can both move around the patient and rotate
  - ➢ Nodes (see to the left)
- AI modeling
  - ➢ External surrogates vs internal kV imaging
- Tracking

Gantry Mounted Systems

- kV planar
- MV planar
- kV CBCT

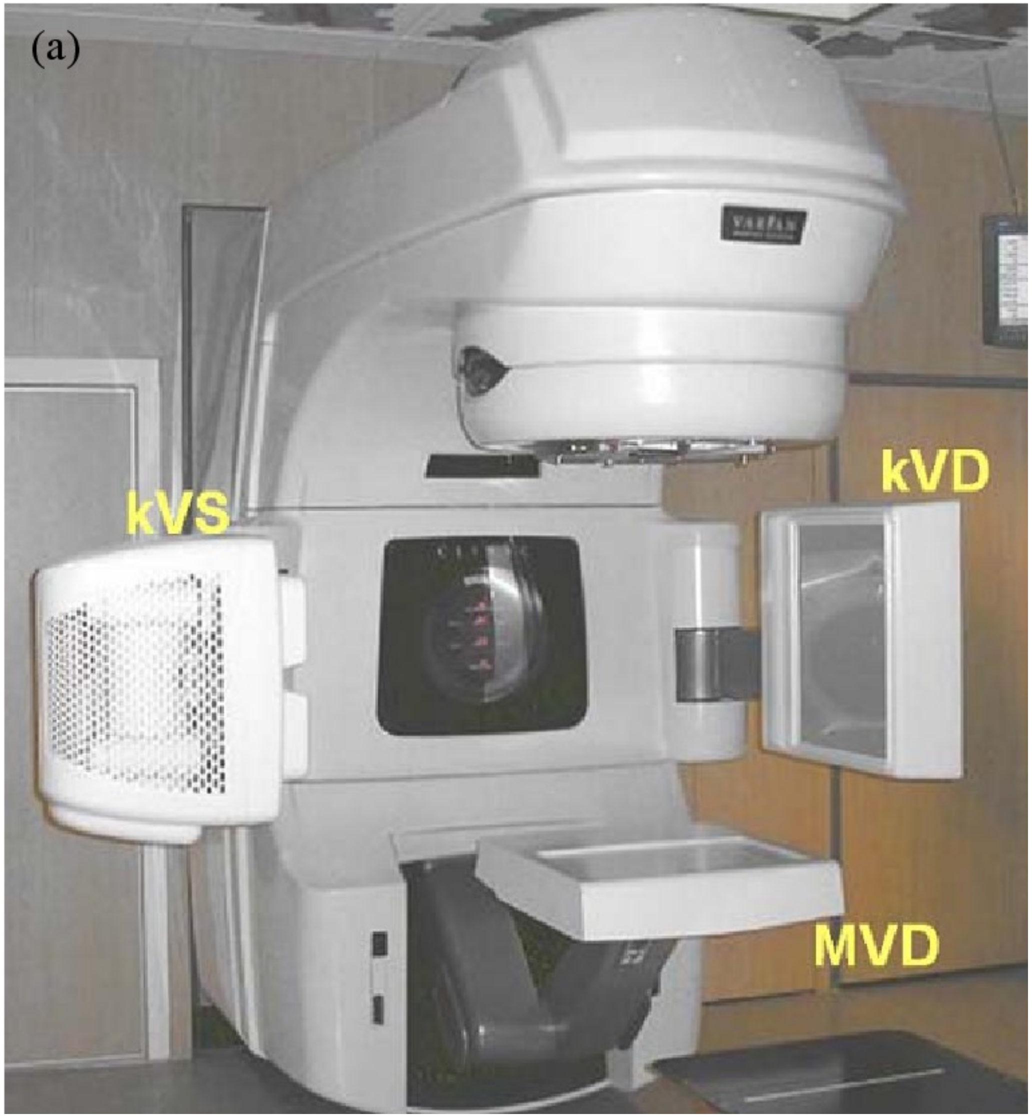

On-board imaging
vs
integrated imaging

Djordevic. 2007.

kV Planar Imaging

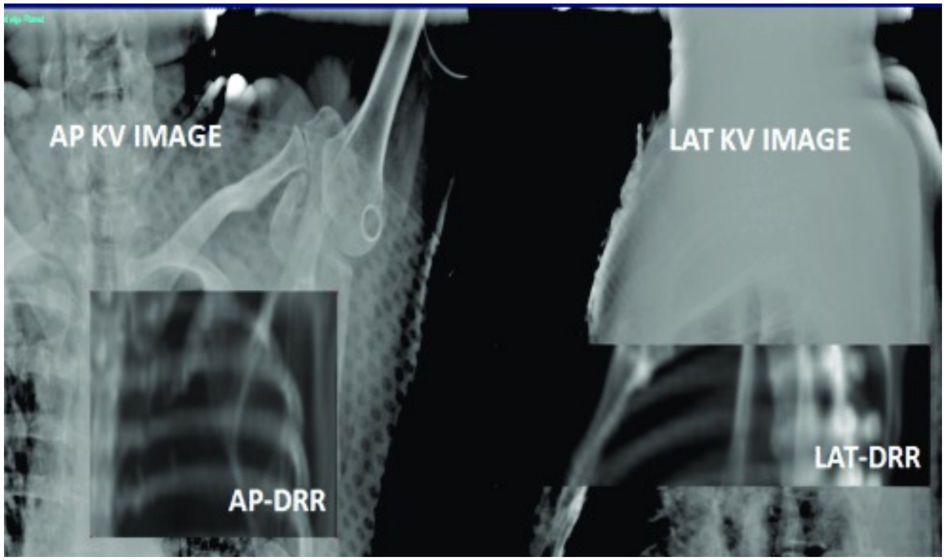

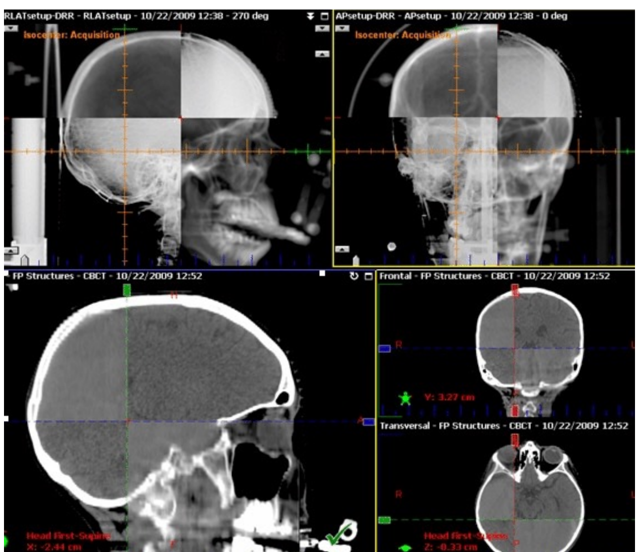

- Similar to diagnostic x-ray scanner
- Mounted to gantry
- Offset 90° from gantry head
- kV-kV matching
  - ➢ Often AP and LAT
  - ➢ Compared to DRR’s

Sanmugam et al. 2014.

Wang et al. 2010.

Portal Imaging (MV)

- Uses the treatment beam
- Historically uses film
- EPID = electronic portal imaging device
- Poor contrast
- Treatment beam verification
- Cine imaging

Pop Quiz

Why do you have worse contrast at MV than at kV?

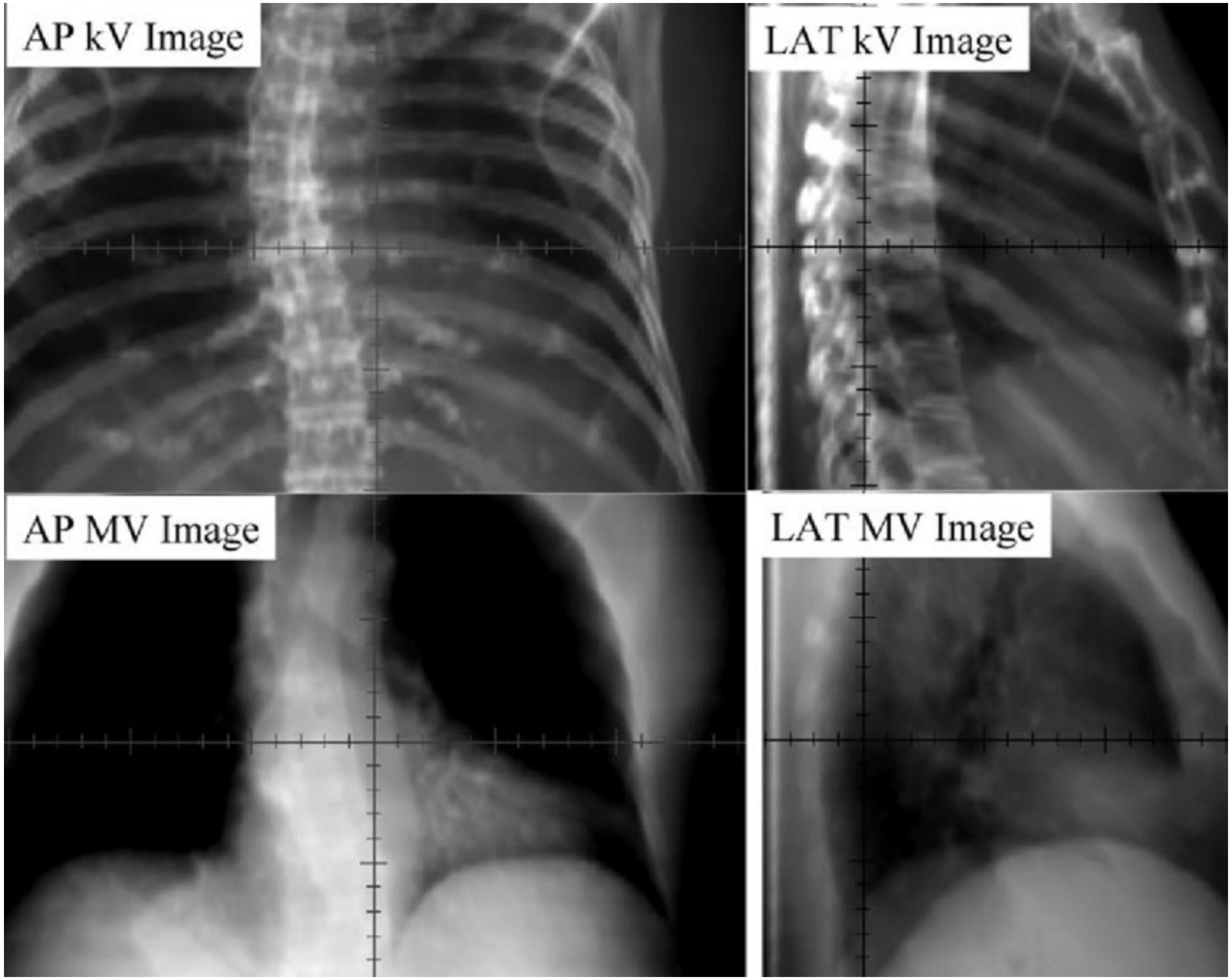

Li et al. 2012.

Pop Quiz

Why do you have worse contrast at MV than at kV?

Increased importance of Compton scattering at higher energy

$$C = \frac{P}{P + S}$$

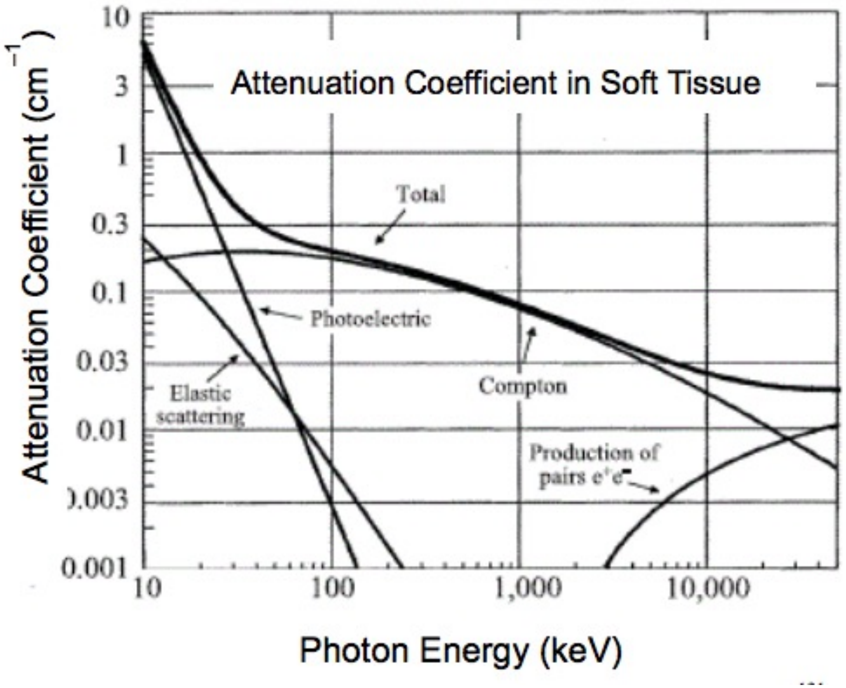

Photoelectric effect vs Compton scattering

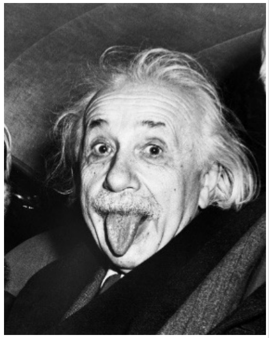

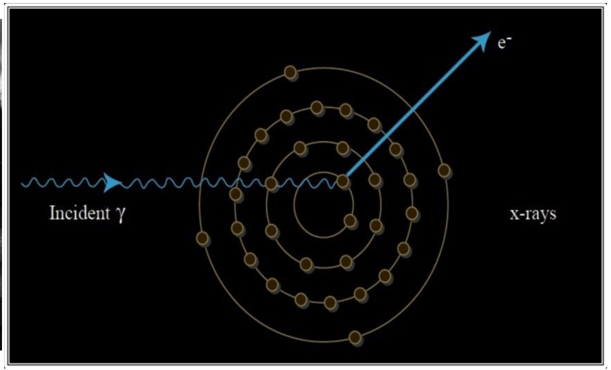

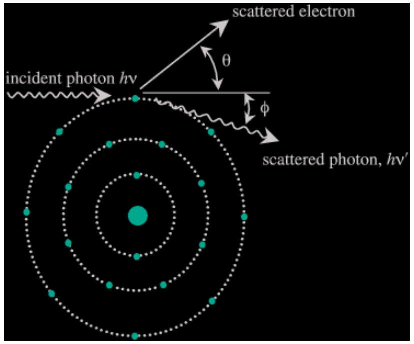

Cone Beam CT

- Cone-like geometry
- Opposed to fan-beam
  - ➢ Table does not move in CBCT
- Poorer image quality
- Importance in RT

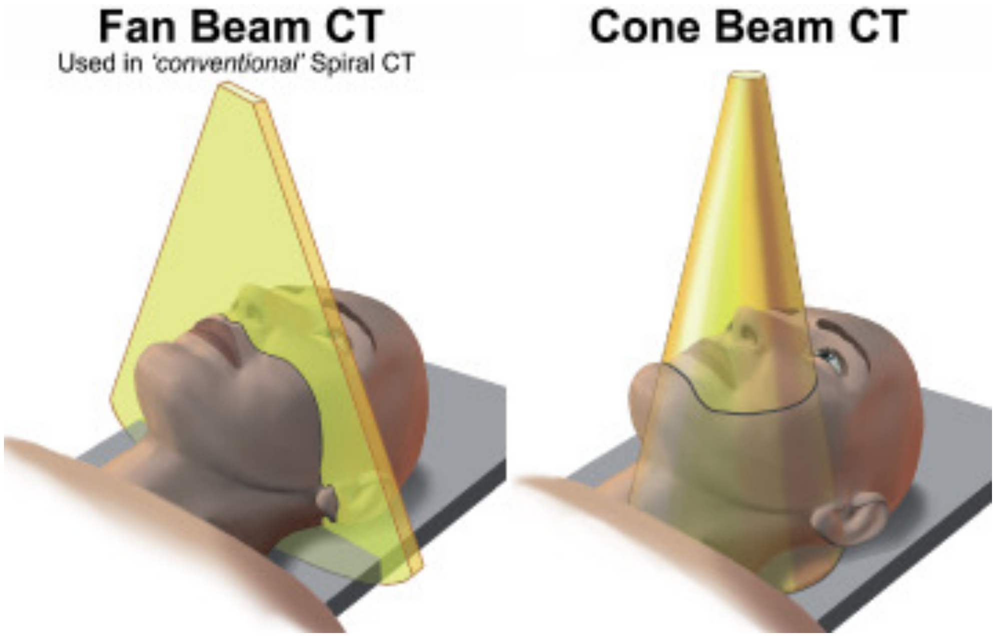

Jaffray

ELSEVIER
International Journal of Radiation Oncology*Biology*Physics
Volume 53, Issue 5, 1 August 2002, Pages 1337-1349

Physics contribution

Flat-panel cone-beam computed tomography for image-guided radiation therapy ☆

David A Jaffray Ph.D. [a], Jeffrey H Siewerdsen Ph.D. [a], John W Wong Ph.D. [a], Alvaro A Martinez M.D. [a]

CBCT in RT

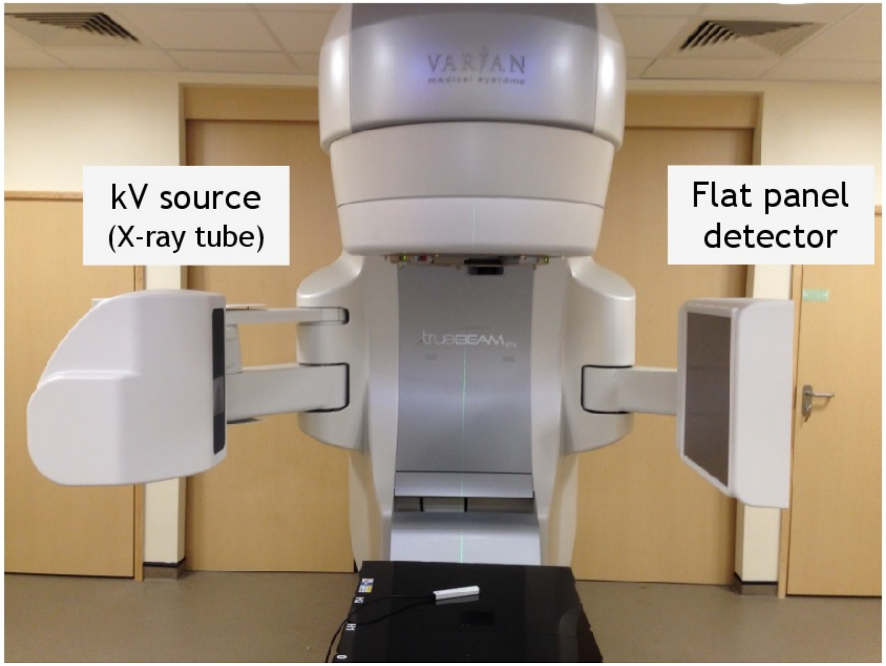

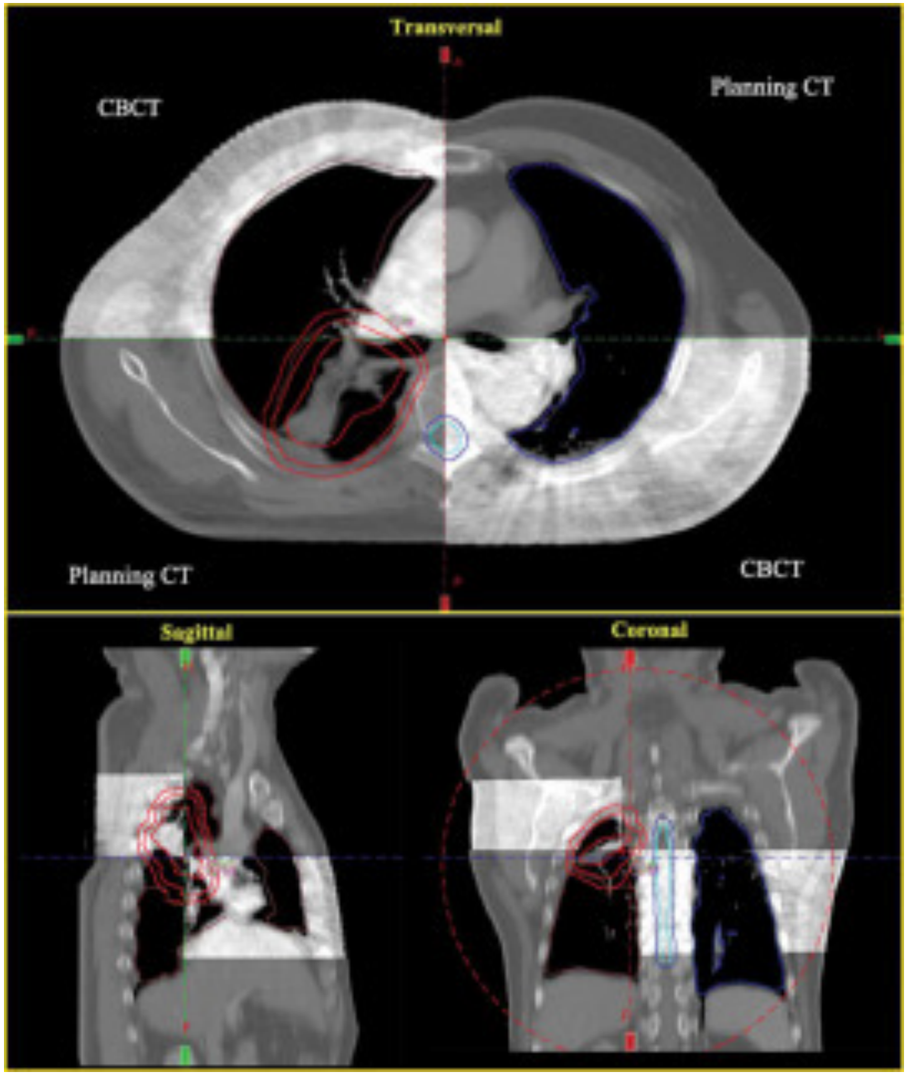

Abuhaimed. 2015.

Gui et al. 2021.

Brachytherapy Setup

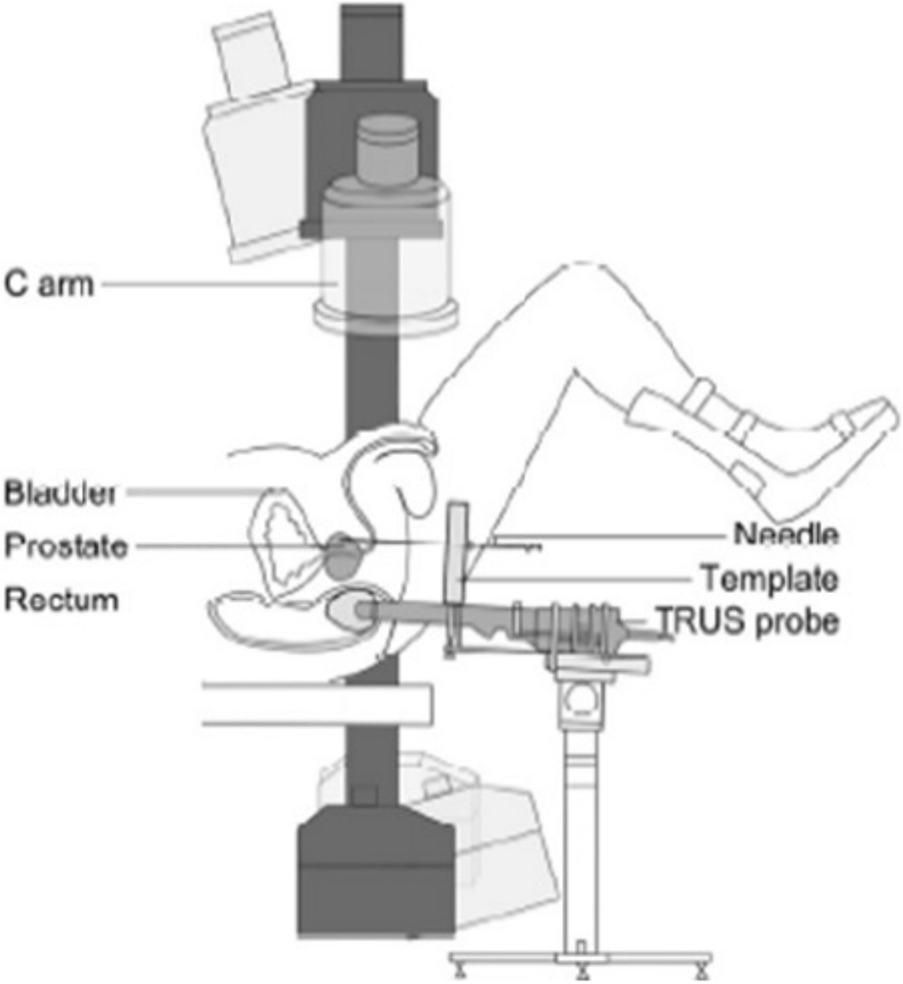

Fallavollita et al. 2010.

Surface-Guided Radiotherapy

Utilization of optical surface scanning to reconstruct and register in real-time (>1 fps) the patient surface (from the SGRT system) to the reference surface (from CT sim)

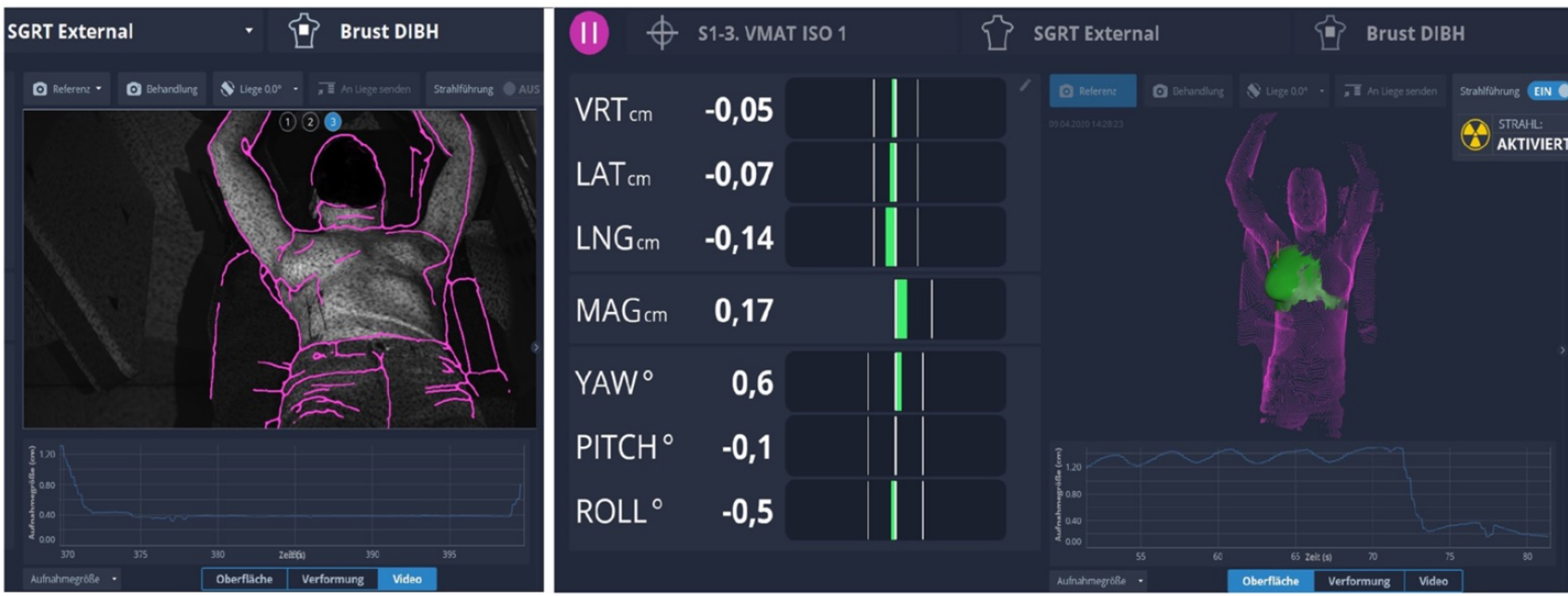

Freislederer et al. 2020.

Cherenkov Imaging

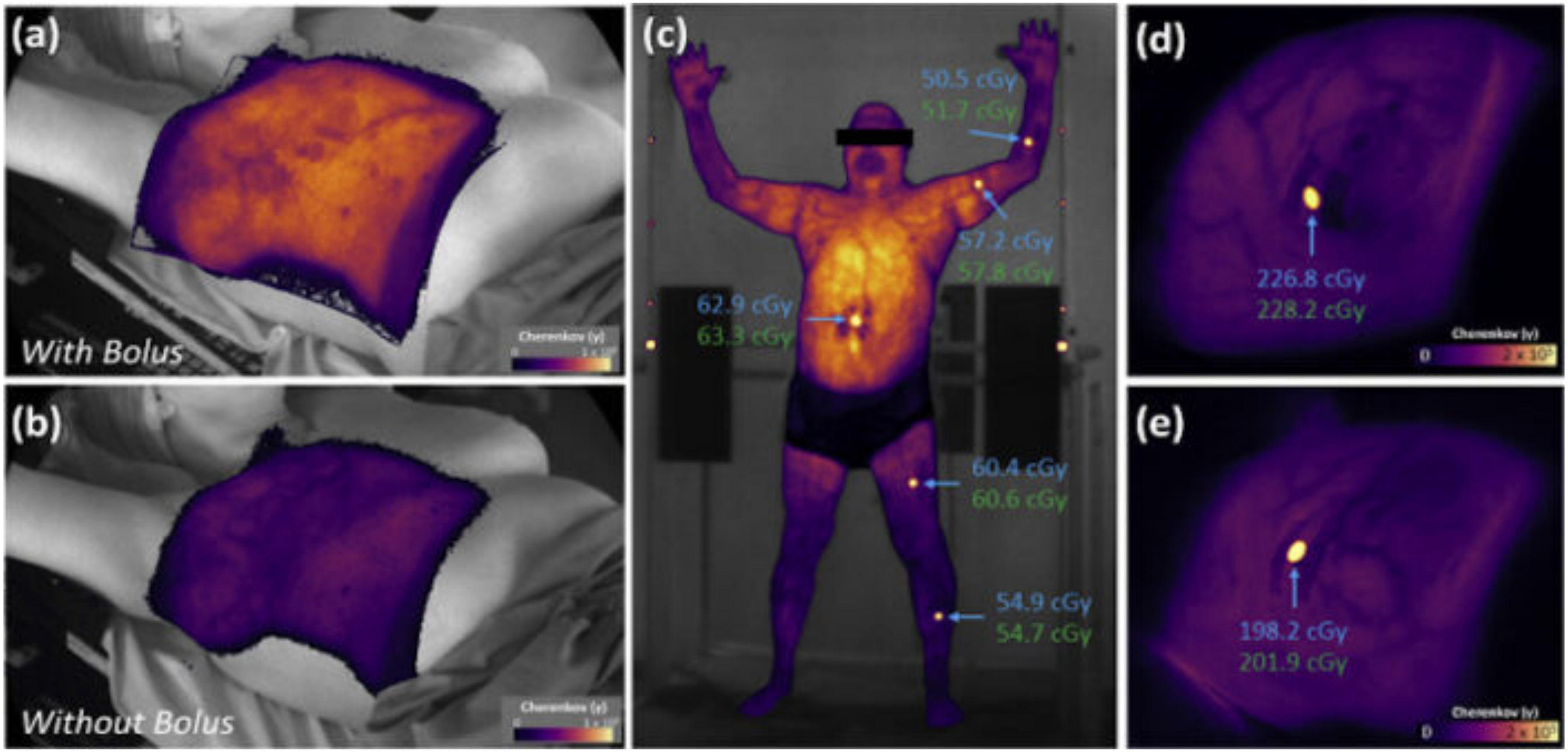

Procedure Guidance

TRUS Guidance

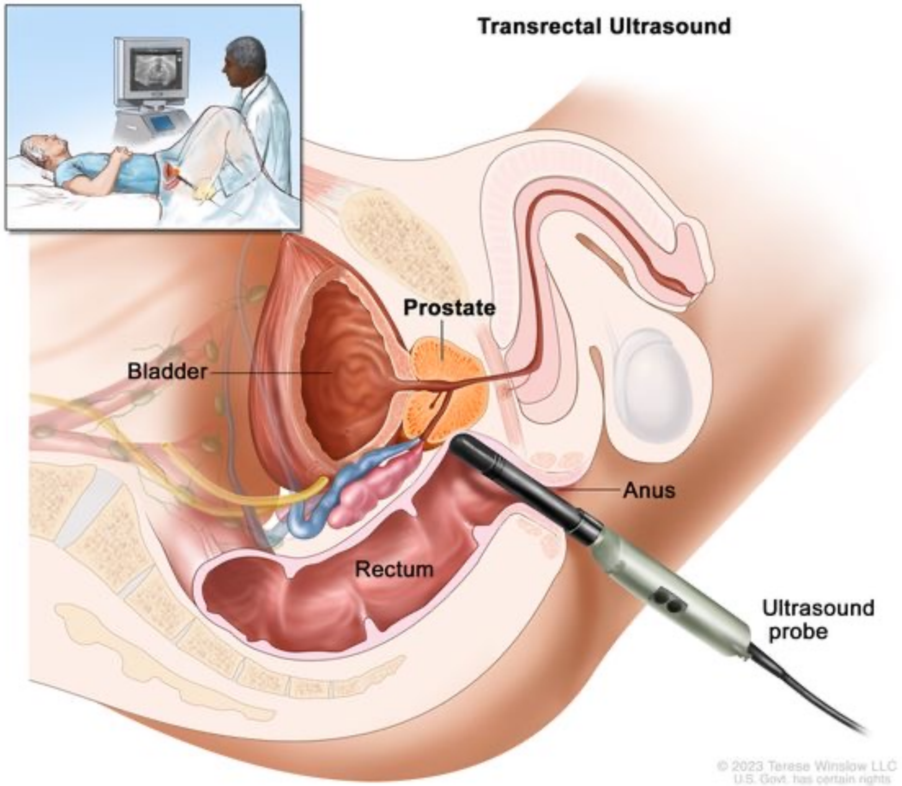

- Transrectal ultrasound
  - TRUS
- RT Applications
  - LDR Seed Placement and planning
  - HDR applicator placement
  - Prostate gold coils

LDR Seed Placement

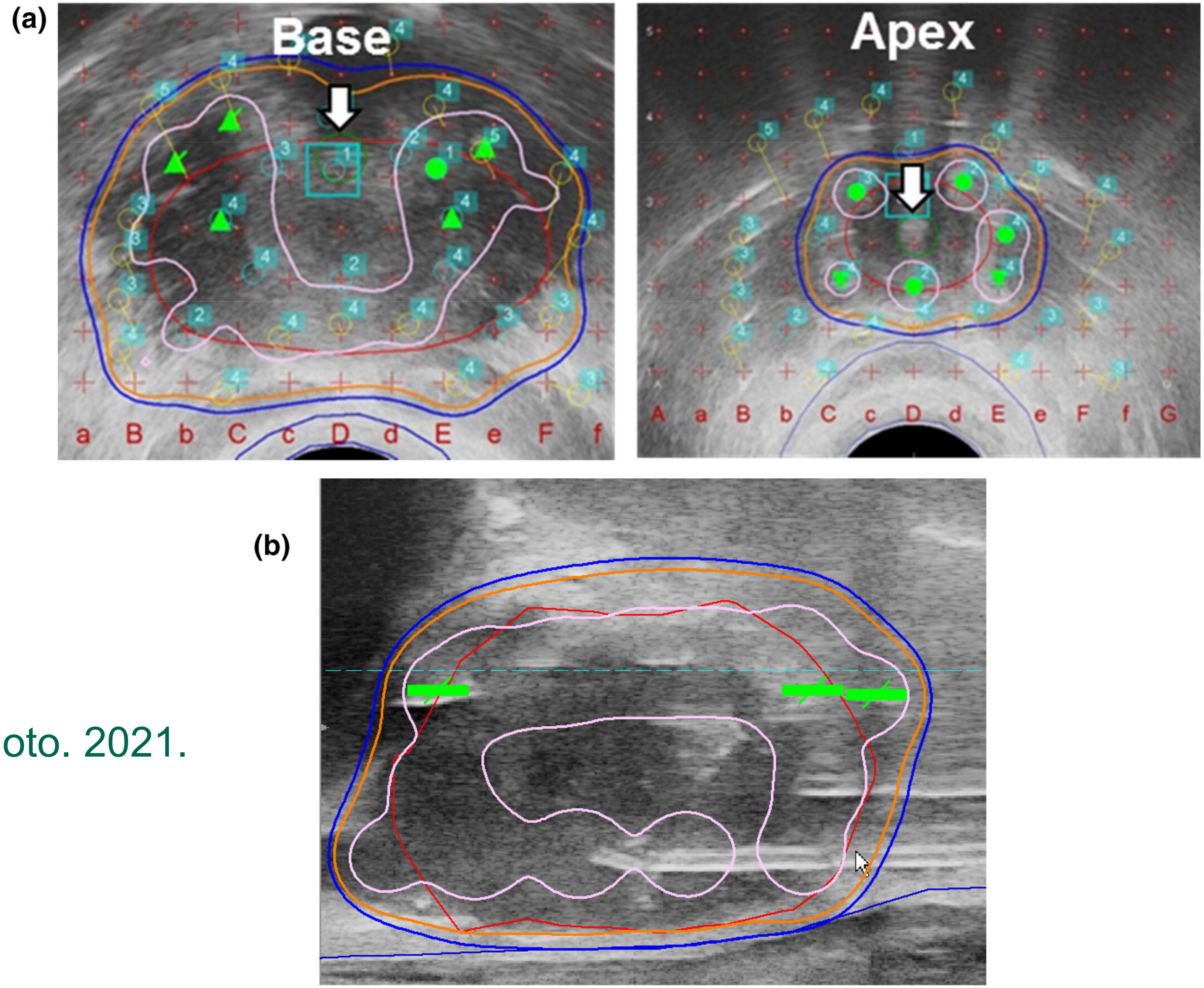

Okamoto. 2021.

Prostate Coils

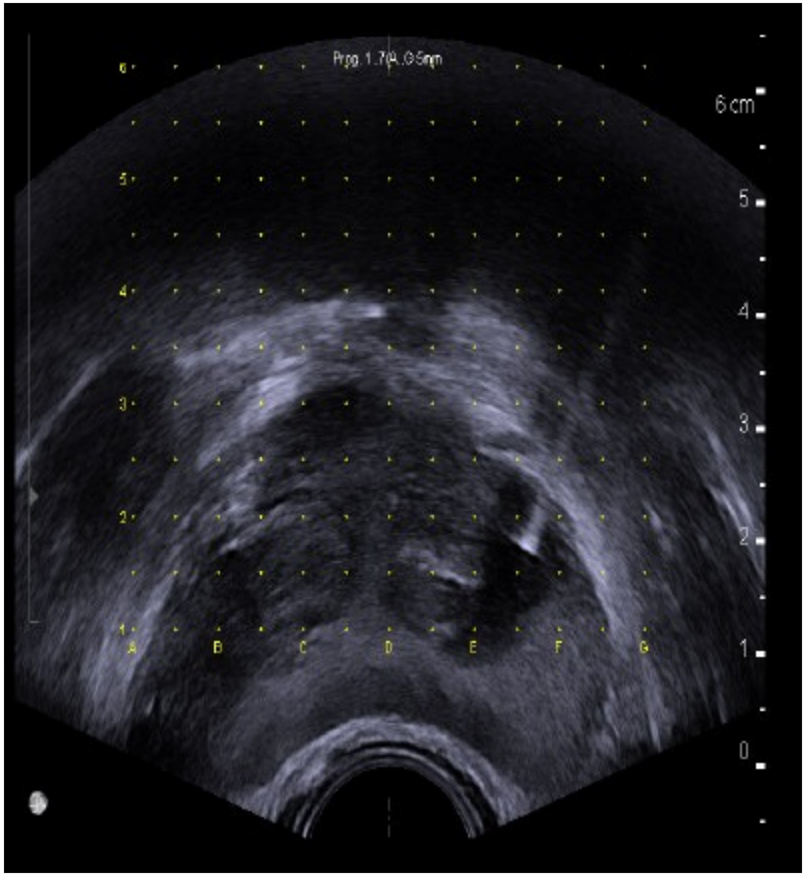

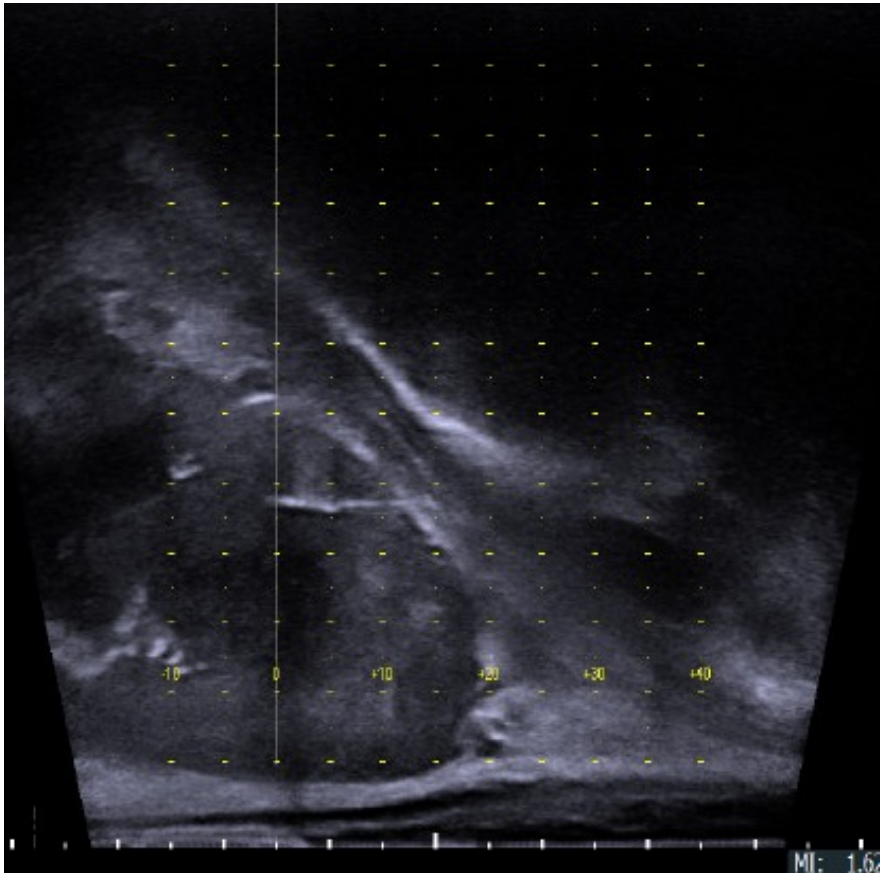

Principles of Ultrasound

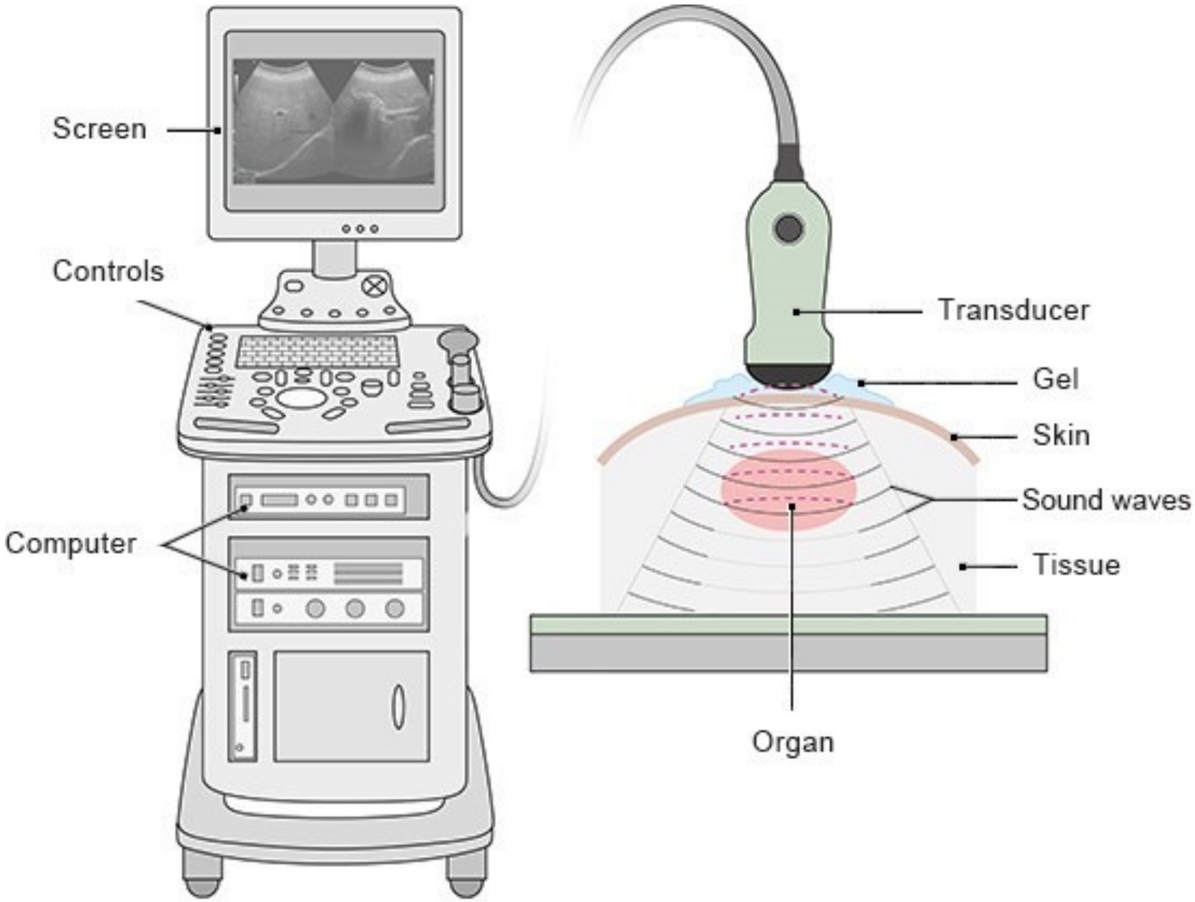

TRUS Transducers

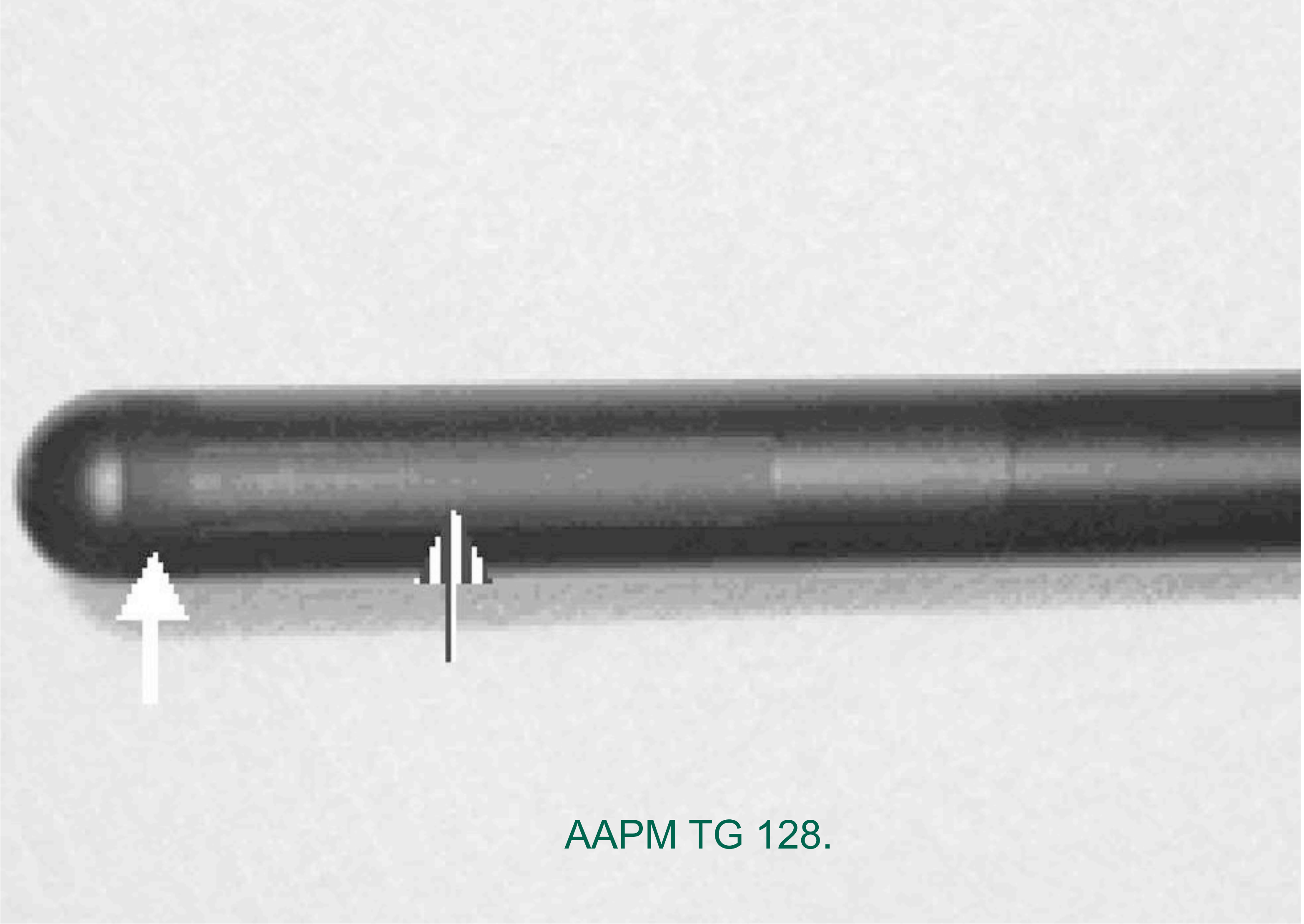

AAPM TG 128.

Ultrasound QA for Brachytherapy

AAPM Task Group 128: Quality assurance tests for prostate brachytherapy ultrasound systems

Douglas Pfeiffer[a)]
Imaging Department, Boulder Community Foothills Hospital, Boulder, Colorado 80301

Steven Sutlief
Radiation Therapy, VA Medical Center, VA Puget Sound Health Care System, Seattle, Washingon 98108

Wenzheng Feng
Cardiology and Interventional Radiology, William Beaumont Hospital, Royal Oak, Michigan 48073

Heather M. Pierce
CIRS, Inc., Norfolk, Virginia 23513

Jim Kofler
Radiology, Mayo Clinic, Rochester, Minnesota 55905

TABLE II. Quality control tests: frequencies and action levels.

Test	Minimum frequency	Action level
Grayscale visibility	Annual	Change >2 steps or 10% from baseline
Depth of penetration	Annual	Change >1 cm from baseline
Axial and lateral resolution	Annual	Change >1 mm from baseline
Axial distance measurement accuracy	Annual	Error >2 mm or 2%
Lateral distance measurement accuracy	Annual	Error >3 mm or 3%
Area measurement accuracy	Annual	Error >5%
Volume measurement accuracy	Annual	Error >5%
Needle template alignment	Annual	Error >3 mm
Treatment planning computer volume accuracy	Acceptance testing	Error >5%

Online Adaptive Radiotherapy

Ethos

- Varian
- CT-based
- AI driven
  - Segmentation
  - Planning
- Must be ran on a Halcyon
  - Originally made for LMIC's

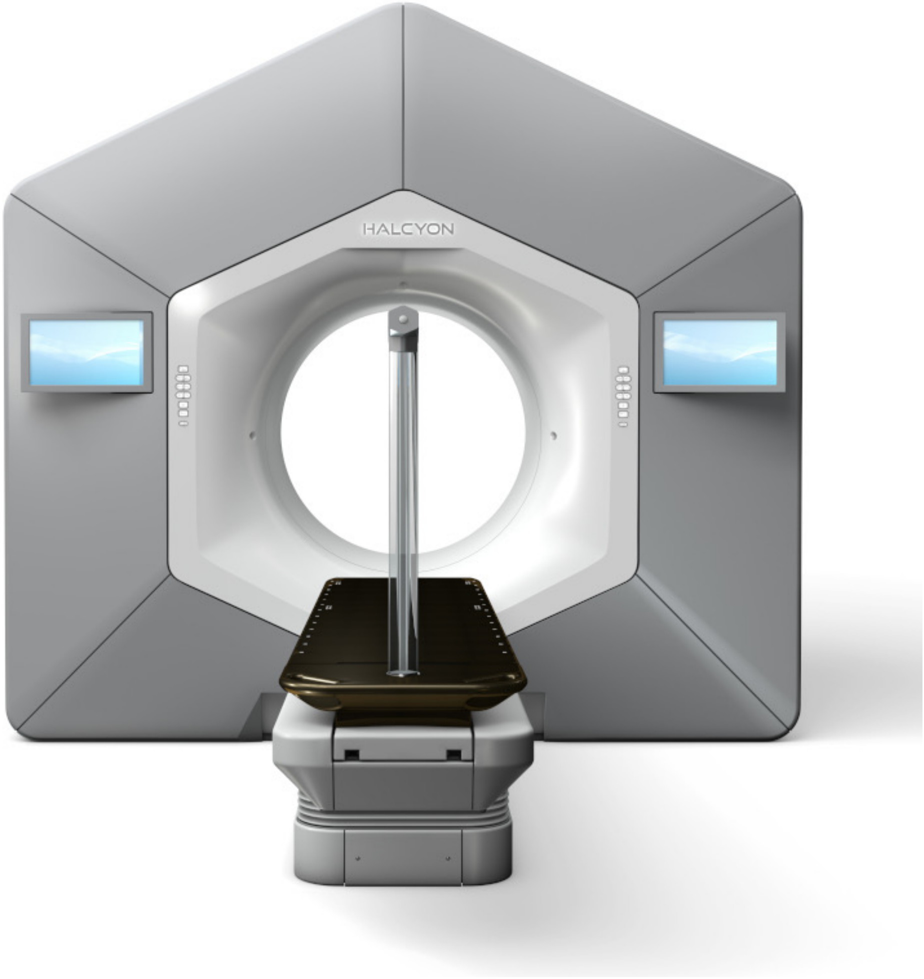

Dartmouth Health

Ethos Adaptive Planning

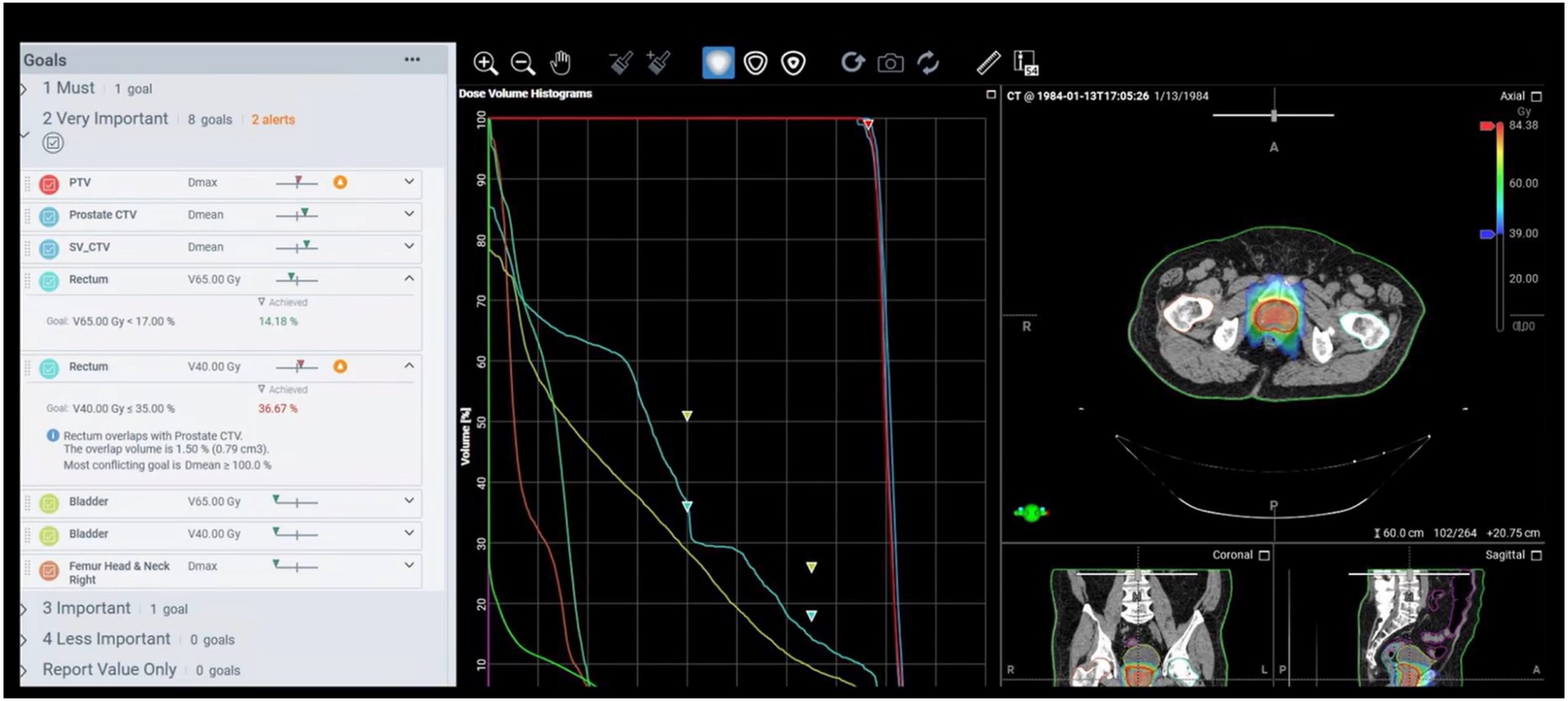

RefleXion

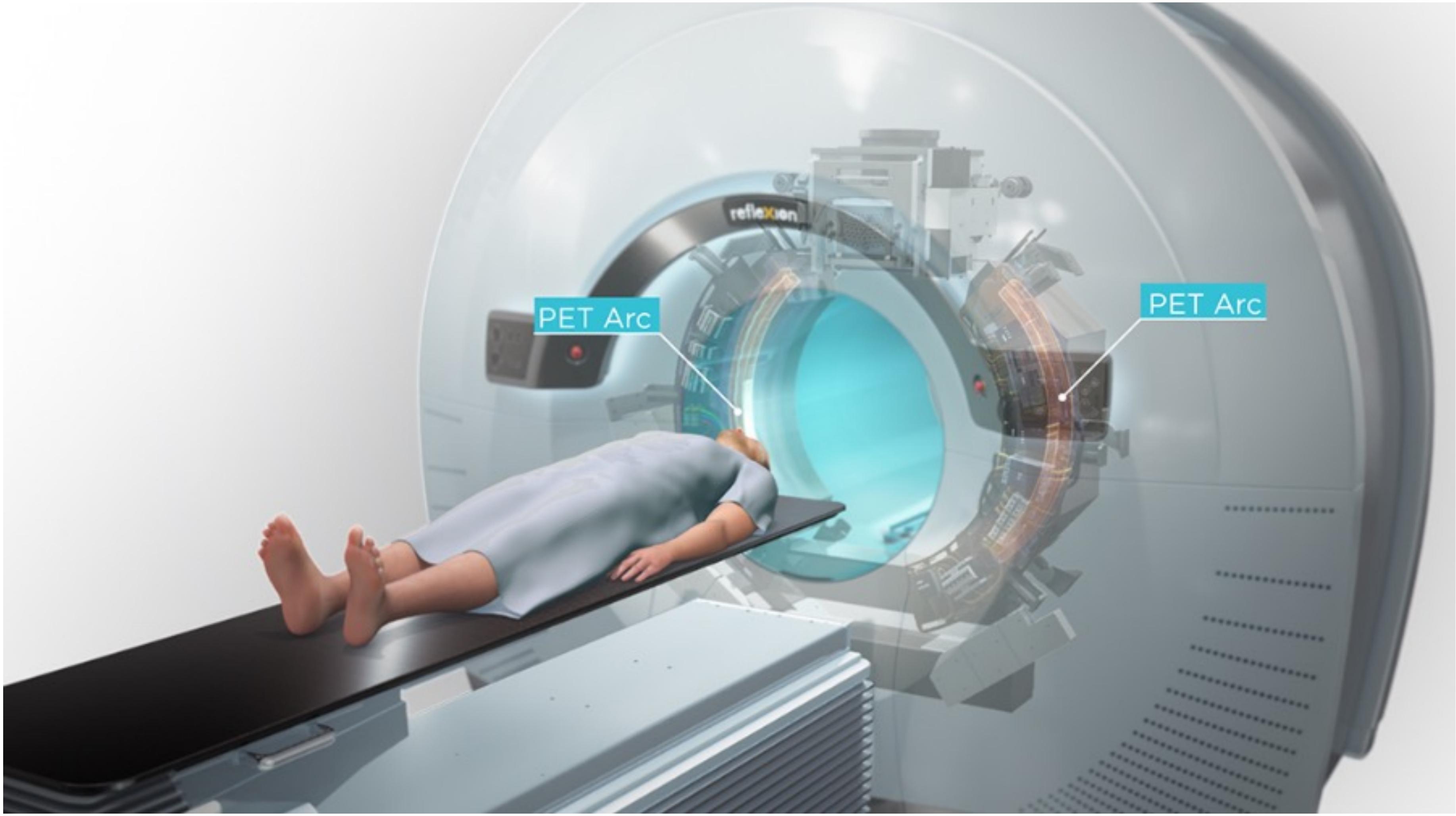

Dartmouth Health

MR-Guided Radiotherapy

- Visualization of inter- and intrafractional changes in tumor and OAR's
  - Superior soft tissue contrast
- Gating
- Possibility for daily adaptation

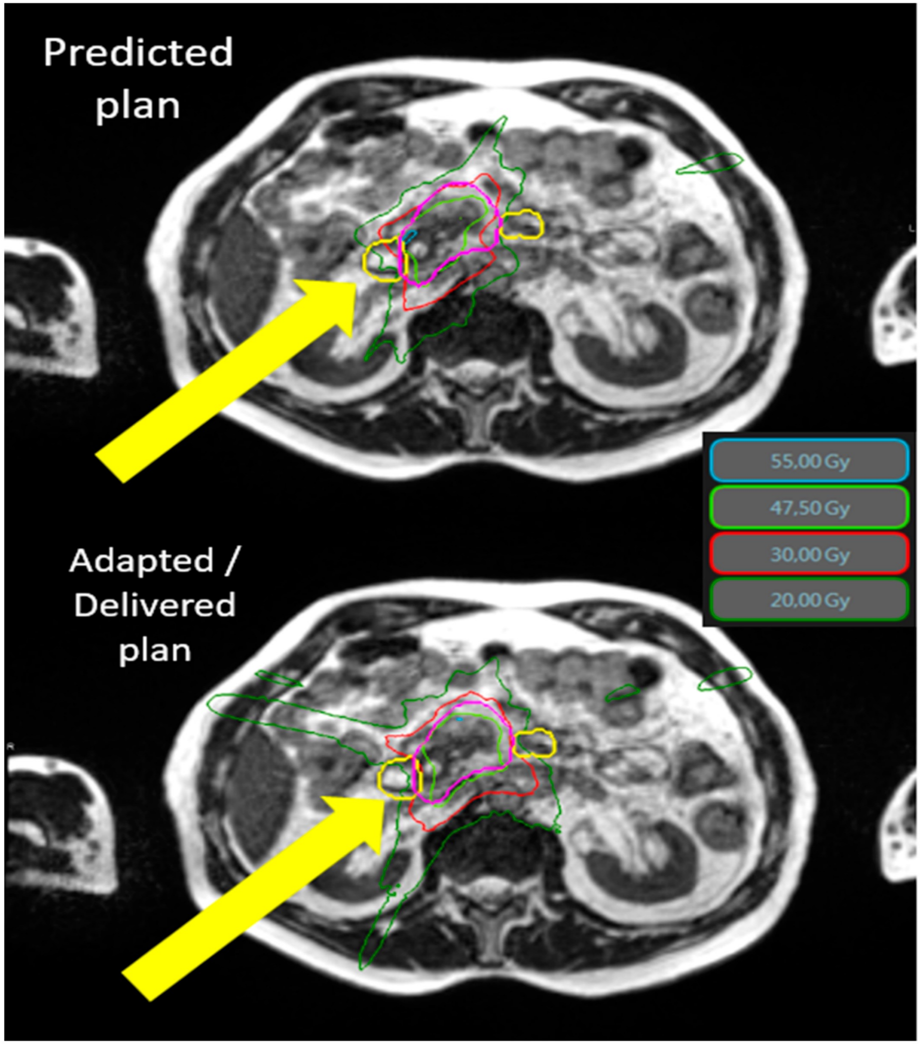

Bordeau et al. 2023.

MRIdian System

Unity System

Dartmouth Health

Emerging Systems

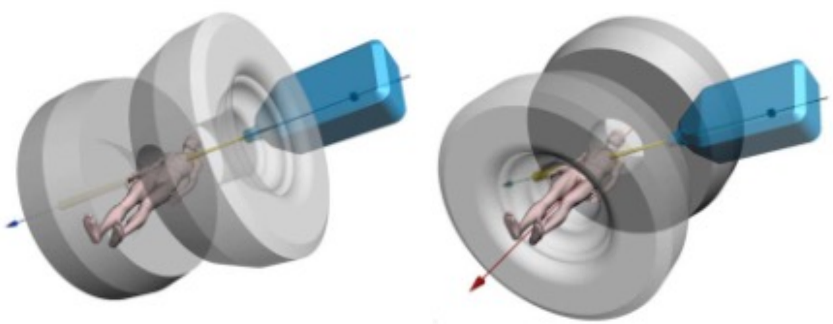

The Australian MRI-Linac program (1.0T)

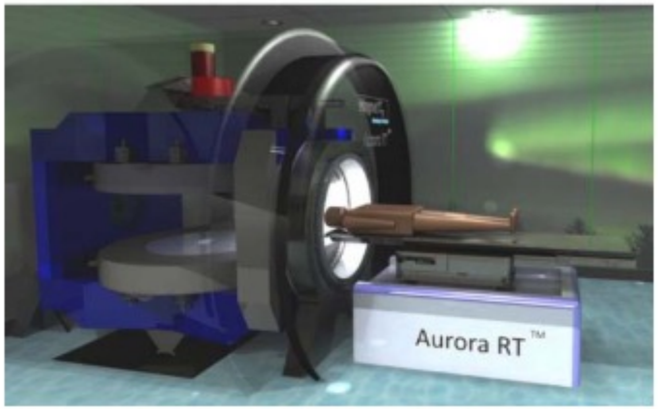

MagentTx Aurora-RT™ (0.5T)

Design Differences

Raaymakers et al. 2009.

Klüter. 2019.

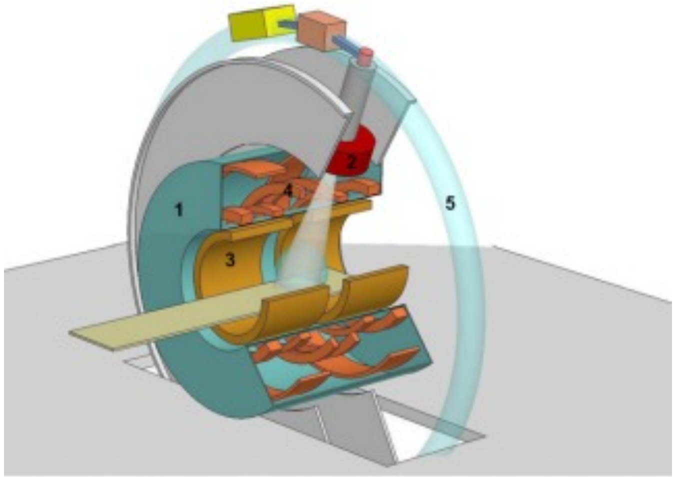

- Field strength
- Magnet design
- Motion management functionality

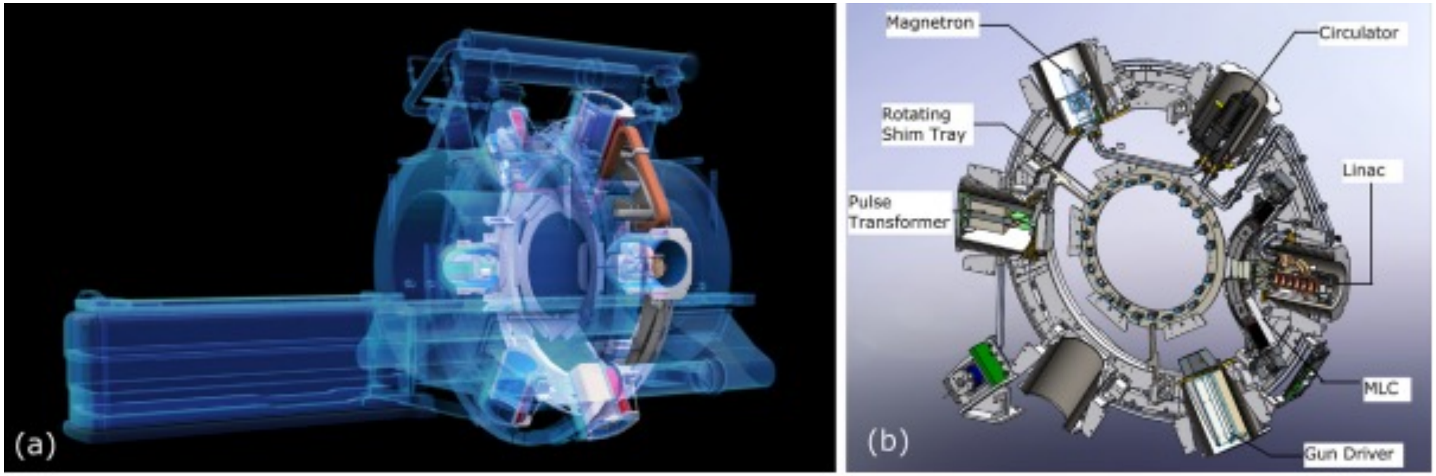

Design Differences

Table 2

Comparison of the MRIdian and Unity MRI-Linac radiotherapy platforms.

Feature	MRIdian	Unity
Construction	Split Magnet Design	Single Magnet Design
Imaging	Trufi Sequence Imaging based	Range of Imaging sequences available
Gating	Real time tracking and automatic gating	Real time tracking without automatic gating
Treatment	Gantry rotation maximum speed of 0.5 rpm	Gantry rotation maximum speed of 6.0 rpm

Ng et al. 2023.

bSSFP

- Called True FISP (Trufi) by Siemens
- Continual RF pulses to achieve steady-state magnetization dynamics
- Most efficient use of magnetization
  - Fast sequences
  - Cine mode up to 8 fps
- T_2/T_1 weighting

$$S_{bal} \approx k \sin\alpha \frac{e^{\frac{-TE}{T_2}}}{1+\cos\alpha+(1-\cos\alpha)\left(\frac{T_1}{T_2}\right)}$$

Tissue	T2/T1
Muscle	0.05
Liver	0.08
Brain	0.11
Fat	0.30
CSF/Fluids	0.70

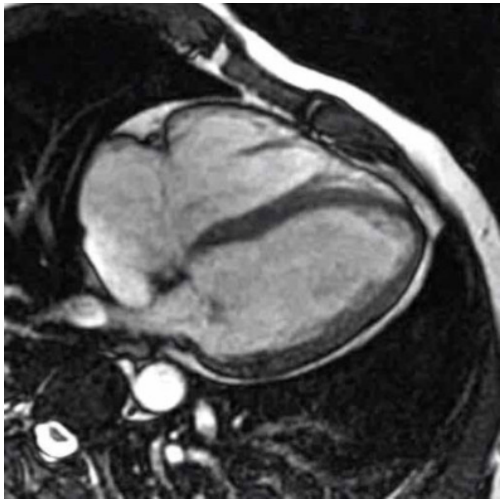

Schleffler

Work Flow

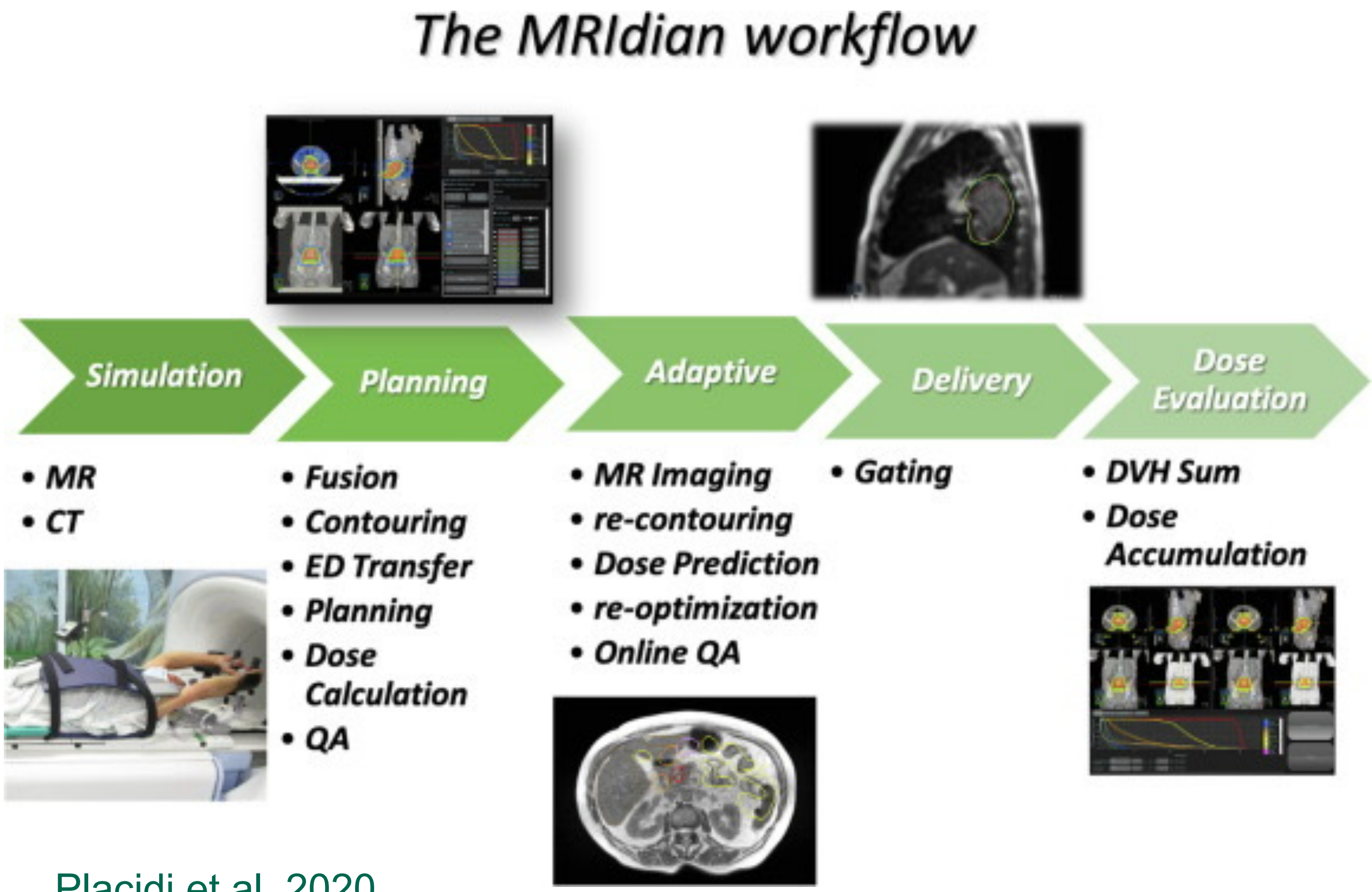

Placidi et al. 2020.

MRIdian Planning

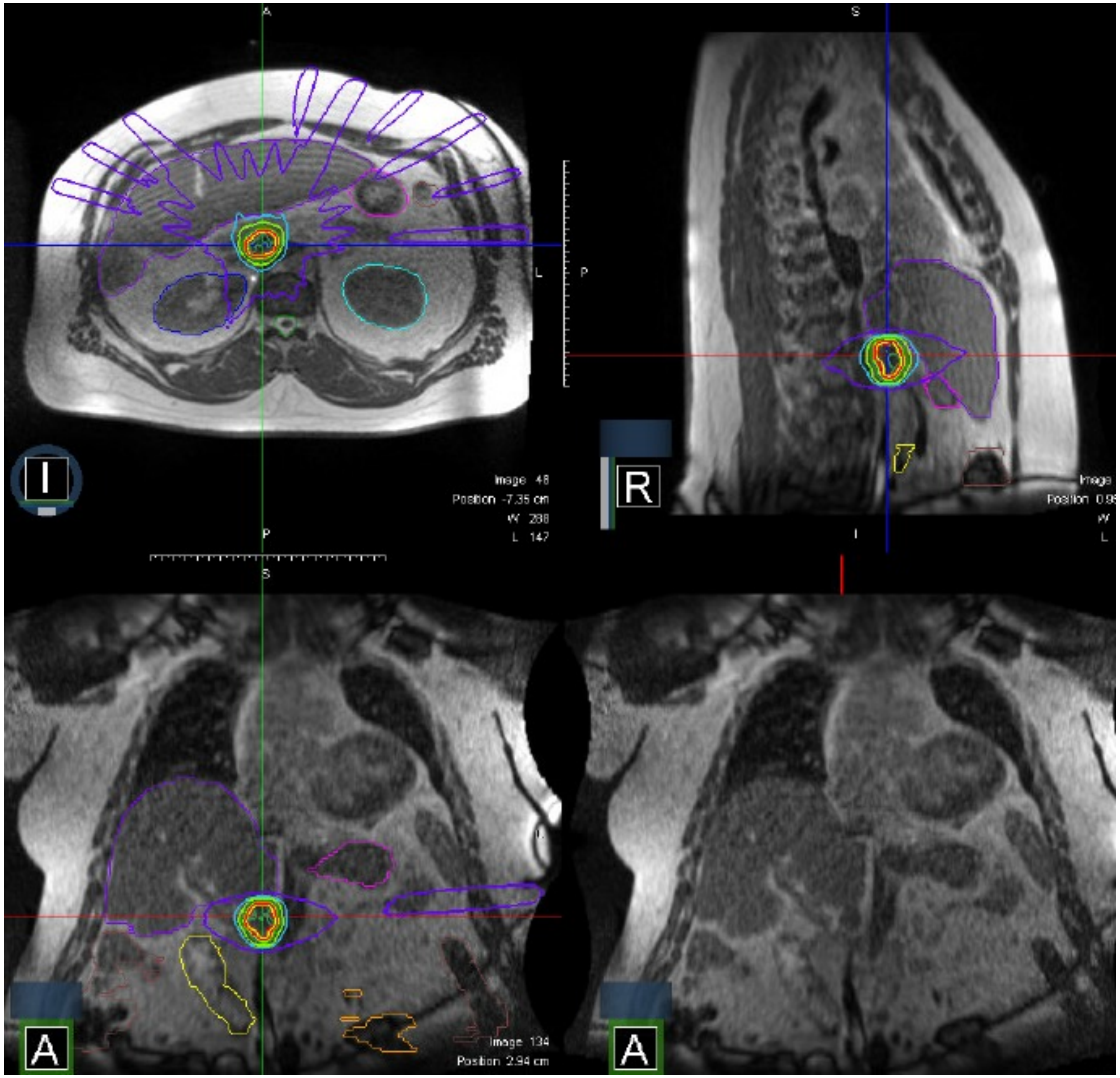

MRIdian Gating

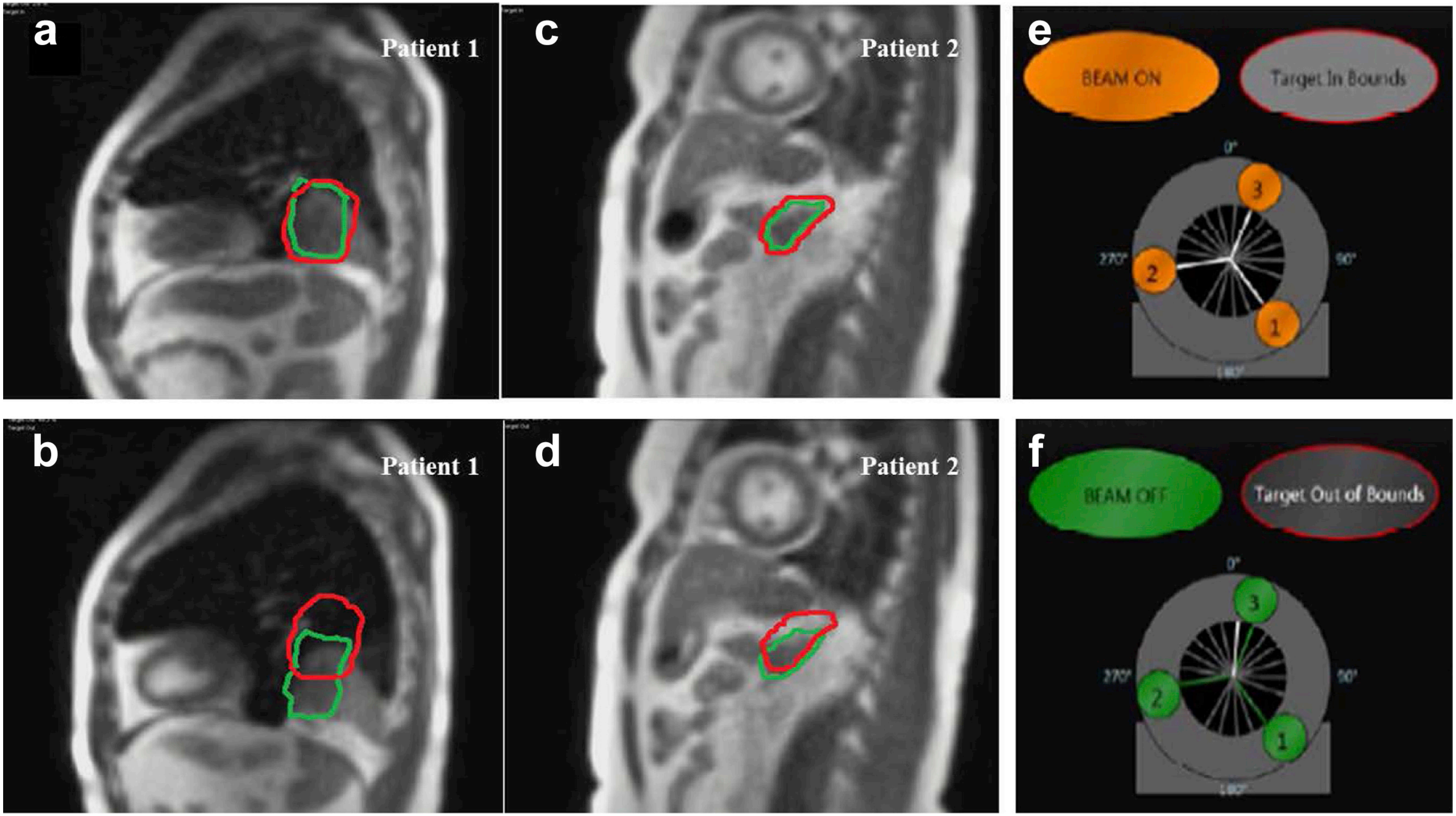

Fischer-Valuck et al. 2017.

Clinical Data

ELSEVIER
Radiotherapy and Oncology
Volume 191, February 2024, 110064

Original Article

Stereotactic MR-guided on-table adaptive radiation therapy (SMART) for borderline resectable and locally advanced pancreatic cancer: A multi-center, open-label phase 2 study

Michael D. Chuong [a], Percy Lee [b], Daniel A. Low [c], Joshua Kim [d], Kathryn E. Mittauer [a], Michael F. Bassetti [e], Carri K. Glide-Hurst [e], Ann C. Raldow [f], Yingli Yang [f], Lorraine Portelance [g], Kyle R. Padgett [g], Bassem Zaki [h], Rongxiao Zhang [h], Hyun Kim [i], Lauren E. Henke [i], Alex T. Price [i], Joseph D. Mancias [j], Christopher L. Williams [j], John Ng [k], Ryan Pennell [k]...Parag Jitendra Parikh [d]

The Future of Radiotherapy?

Can We Move Past Morphology?

- Tumor heterogeneity
  - Not accounted for in RO
- Functional MR
  - Cellularity
  - Perfusion
  - Metabolism
- Dose escalation
- Biologically-guided RT plan adaptation

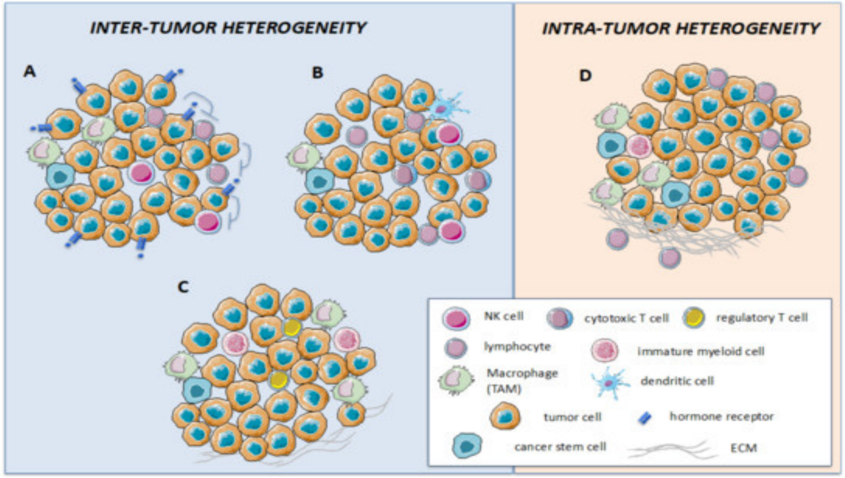

Perrone et al. 2021

Functional Imaging in RT

Naghavi

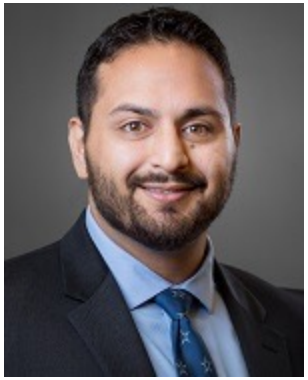

Phase 2 Clinical Trial of Radiomic Habitat–Directed Radiation Dose Escalation for High-Grade Soft Tissue Sarcoma

Protocol Number: 21136

- Dose painting based off MR functional markers
  - High ADC → 50 Gy
  - Low ADC / High DCE → 60 Gy
  - Low ADC / Low DCE → 70 GY

Diffusion Weighted Imaging

- Brownian motion
- Cellularity ~ cell packing density → proliferation
- ADC = apparent diffusion coefficient
- ADC decreases with cellularity
- Edema/necrosis

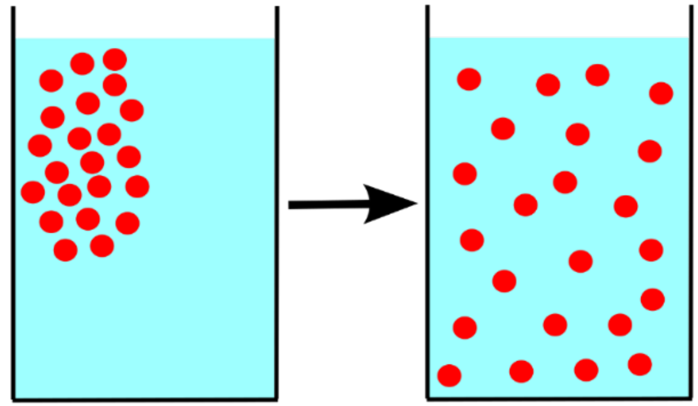

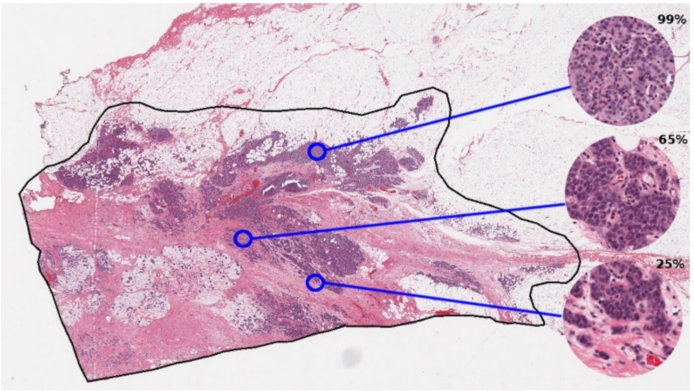

Akbar et al. 2019

Einstein

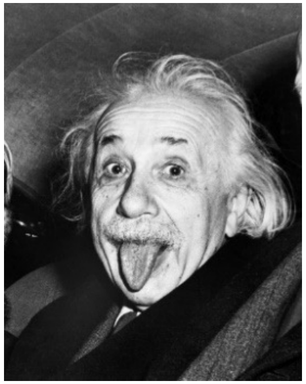

Dartmouth Health

ADC Mapping in Oncology

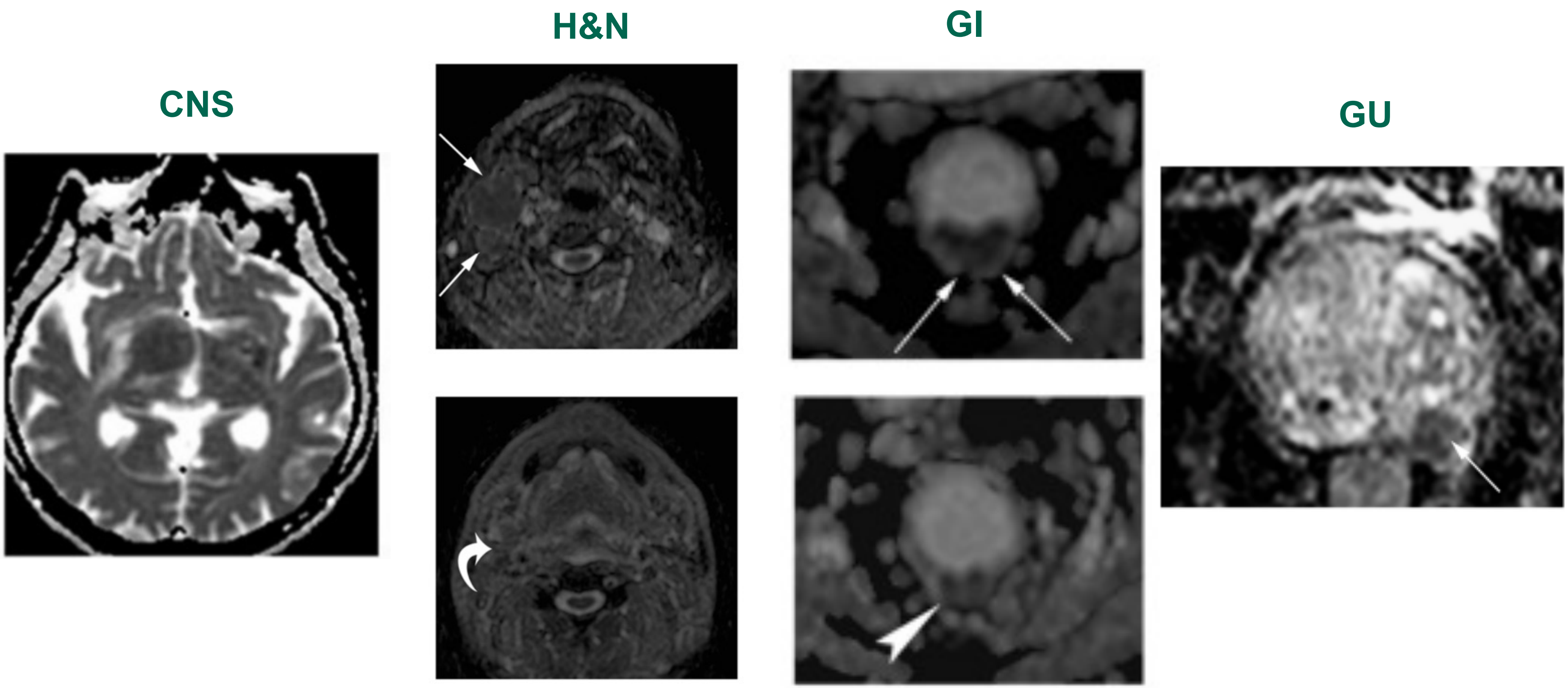

Messina et al. 2020

How Do We Measure Diffusion?

We introduce diffusion-sensitizing gradients!

$$b = \gamma^2 G^2 \delta^2 \left(\Delta - \frac{\delta}{3}\right)$$

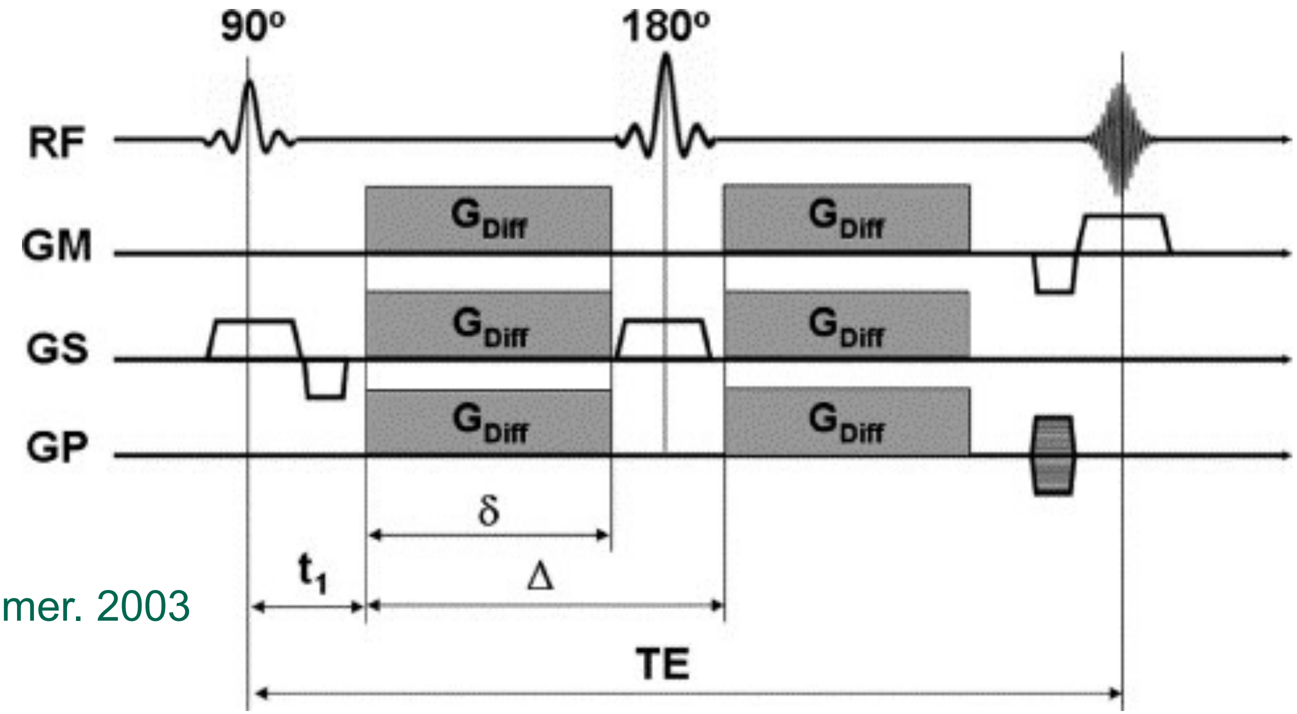

Bammer. 2003

Le Bihan

ADC Mapping

$$S = S_0 e^{-b*ADC}$$

$$D = -\frac{1}{b_1 - b_0} ln\left(\frac{S_1}{S_0}\right)$$

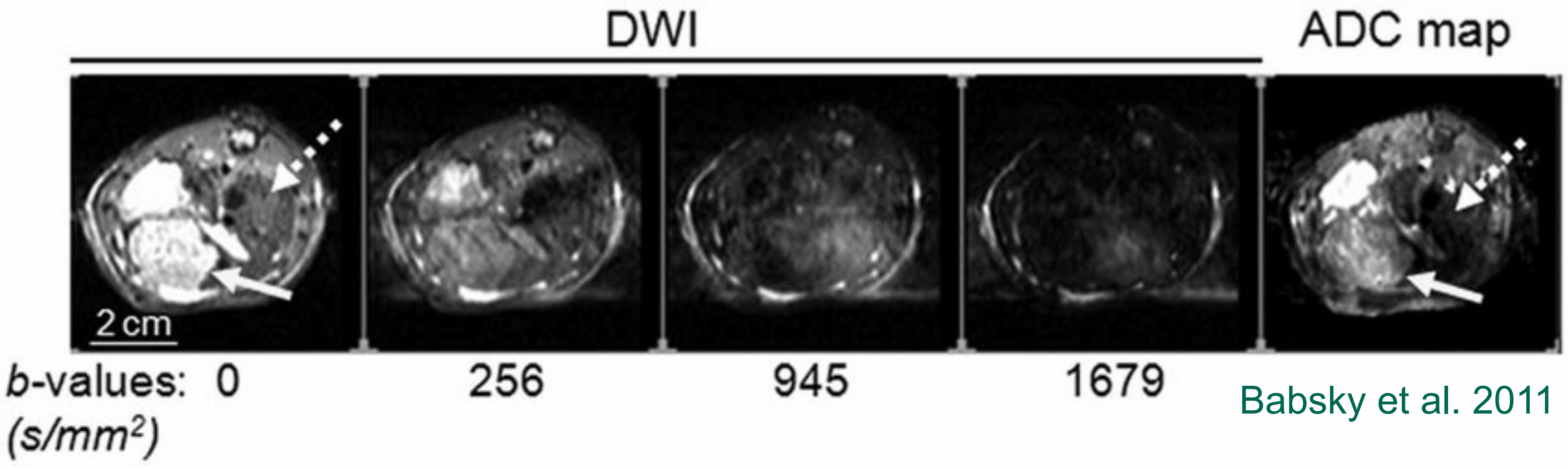

Babsky et al. 2011

Signal decreases with increasing b-value

DWI on a MRIdian

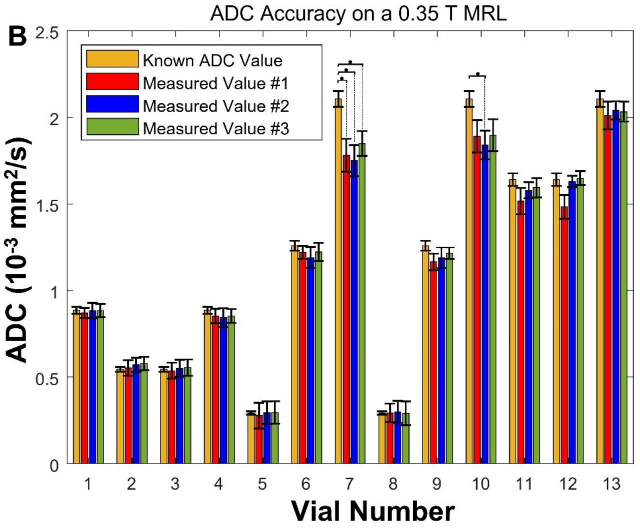

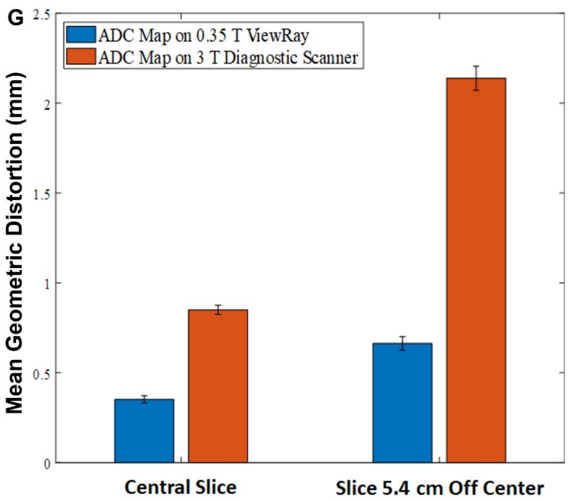

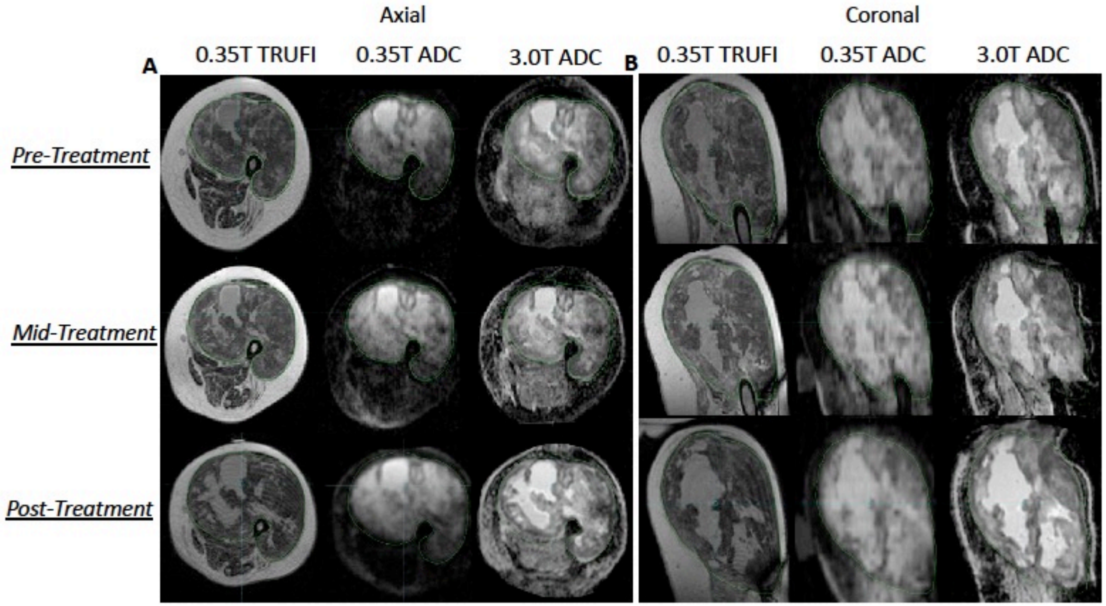

Weygand et al. 2023

ADC Mapping

- Diffusion tensor imaging (DTI) allows 3D mapping of white matter tracts
- Models diffusion coefficient as a tensor
- Fractional anisotropy reflects the directionality of diffusion
- Can potentially assess microscopic extent of GBM within peritumoral edema
- λ's are eigenvalues of diffusion tensor

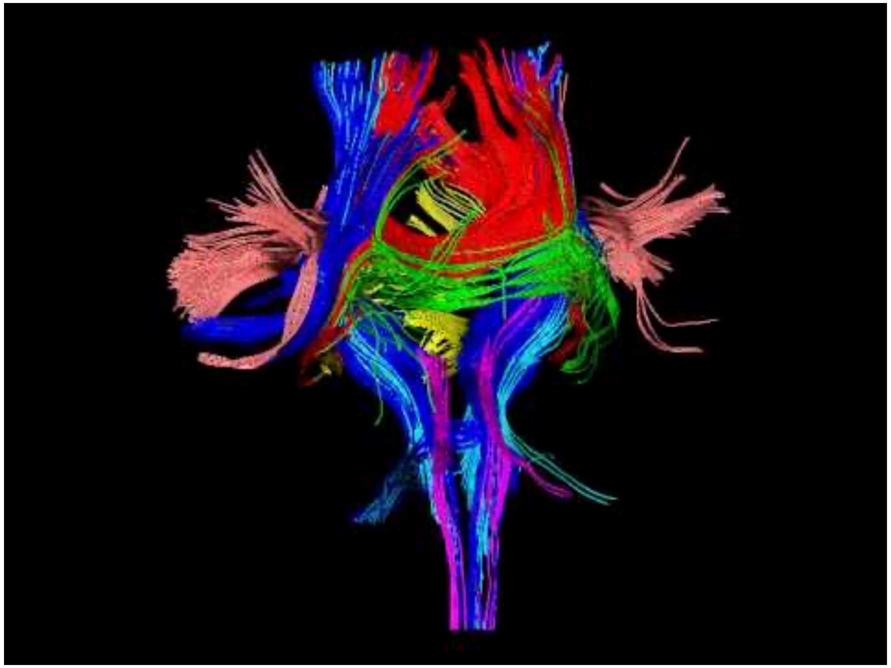

$$FA = \frac{\sqrt{(\lambda_1 - \lambda_2)^2 + (\lambda_2 - \lambda_3)^2 + (\lambda_3 - \lambda_1)^2}}{\sqrt{2}\sqrt{\lambda_1^2 + \lambda_2^2 + \lambda_3^2}}$$

DTI on a MRIdian

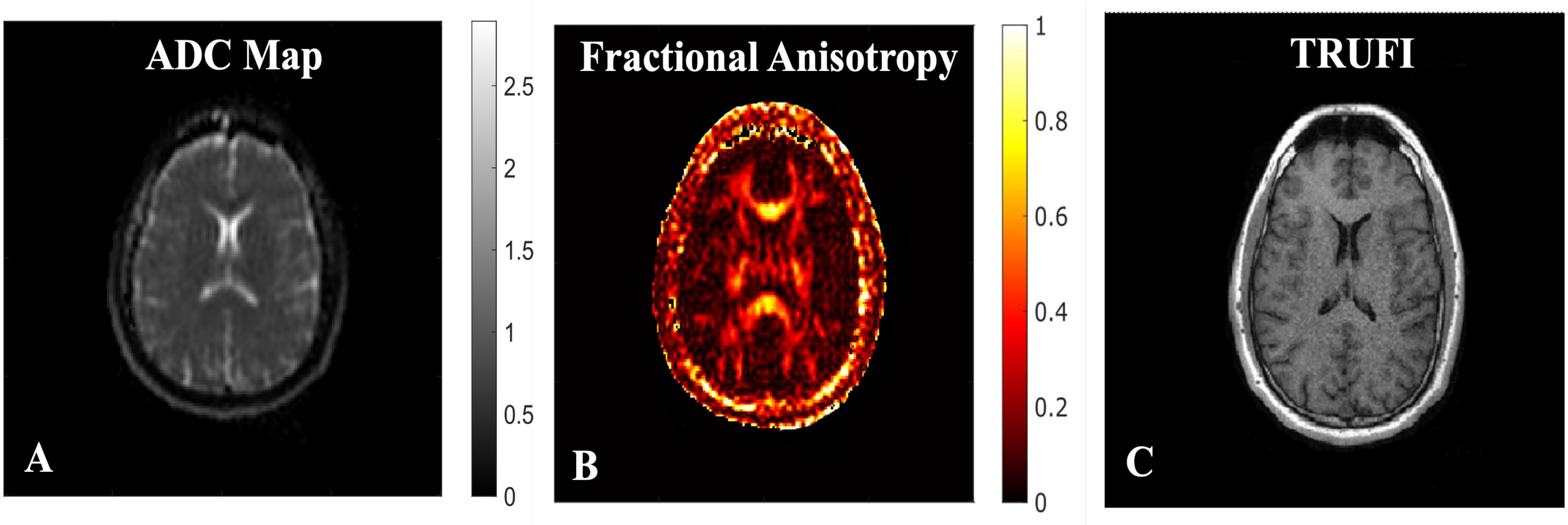

Perfusion Imaging

- Perfusion is the passage of fluid through the circulatory or lymphatic system (usually referring to the delivery of blood to a capillary bed in tissue)
- Helps us identify vascularity characteristics of tumor tissue
- 3 MR-based techniques

T_1-post

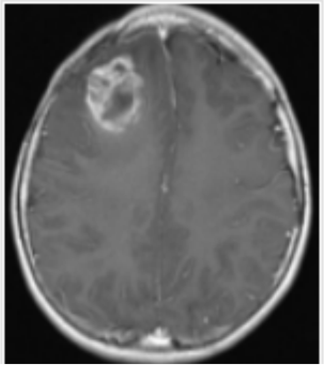

DSC

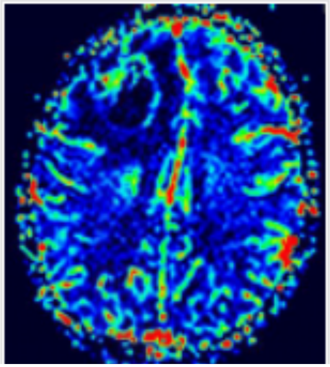

DCE

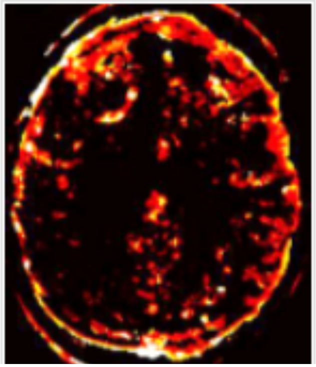

ASL

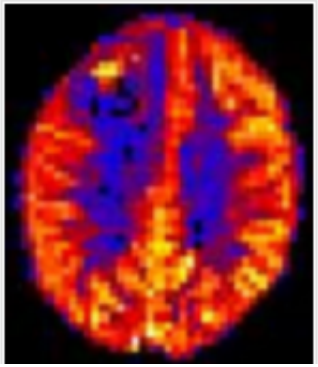

Dartmouth Health

Dynamic Contrast Enhanced

BBB breakdown in glioma

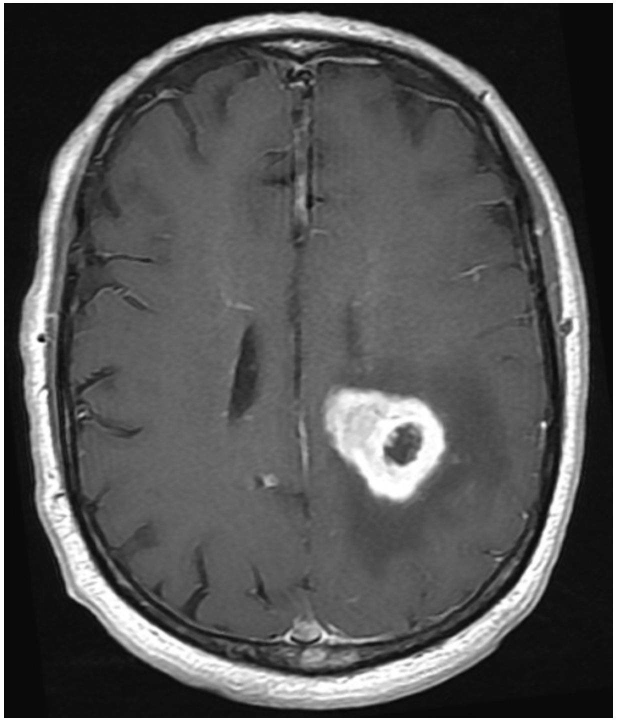

$$\frac{dC_t}{dt} = K^{trans}\left(C_p - \frac{C_t}{v_e}\right)$$

- Gd is administered and T_1 shortening enhancement is quantified
  - T_1w 3D spoiled GRE
- Gd concentration determined
- K^{trans} quantifies capillary permeability which is increased in gliomas, brain mets, and MS

$$\frac{1}{\Delta T_1} \sim [Gd]$$

DCE In Cancer

- Useful in assessing therapeutic response
  - ➢ Progression vs pseudo-progression
  - ➢ Recurrence vs radionecrosis

k^{trans} map

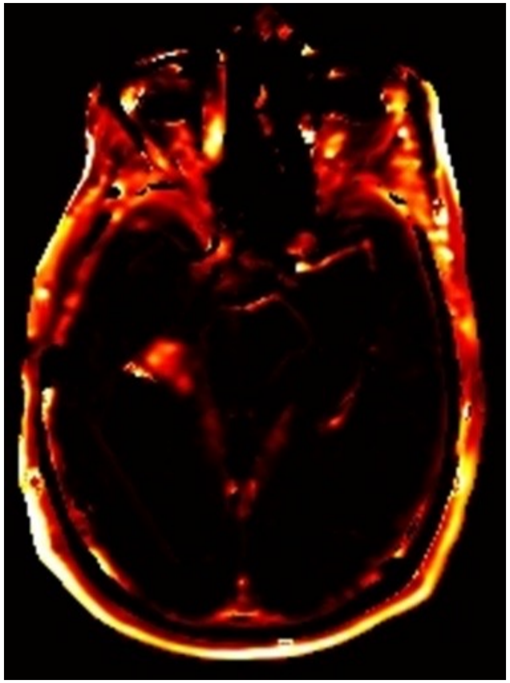

10 months later

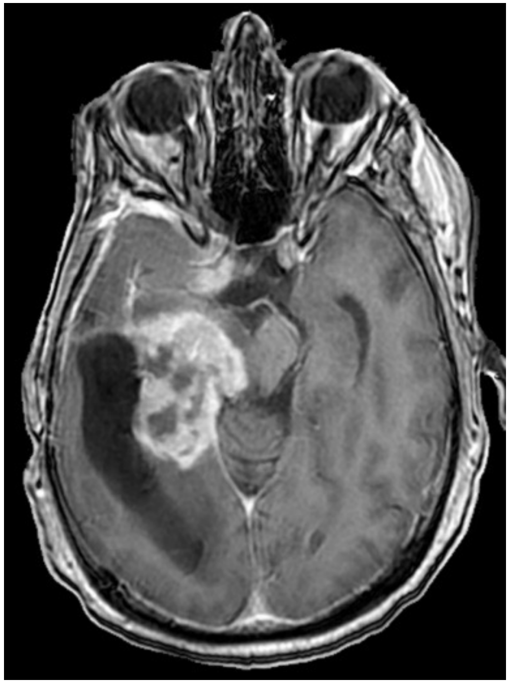

Proton Spectroscopy

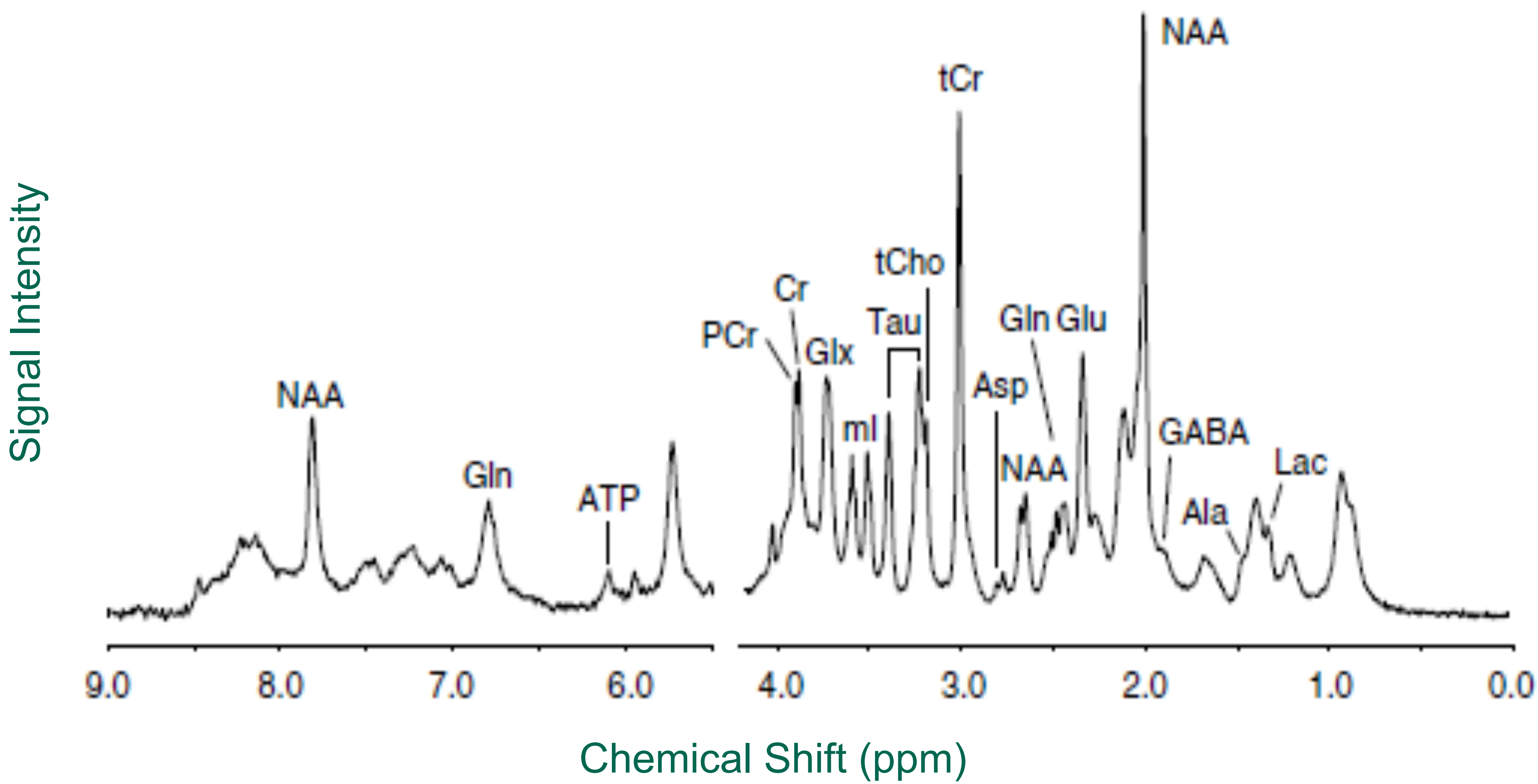

de Graaf. *In vivo NMR Spectroscopy*. 2007.

Metabolite Mapping

Healthy brain

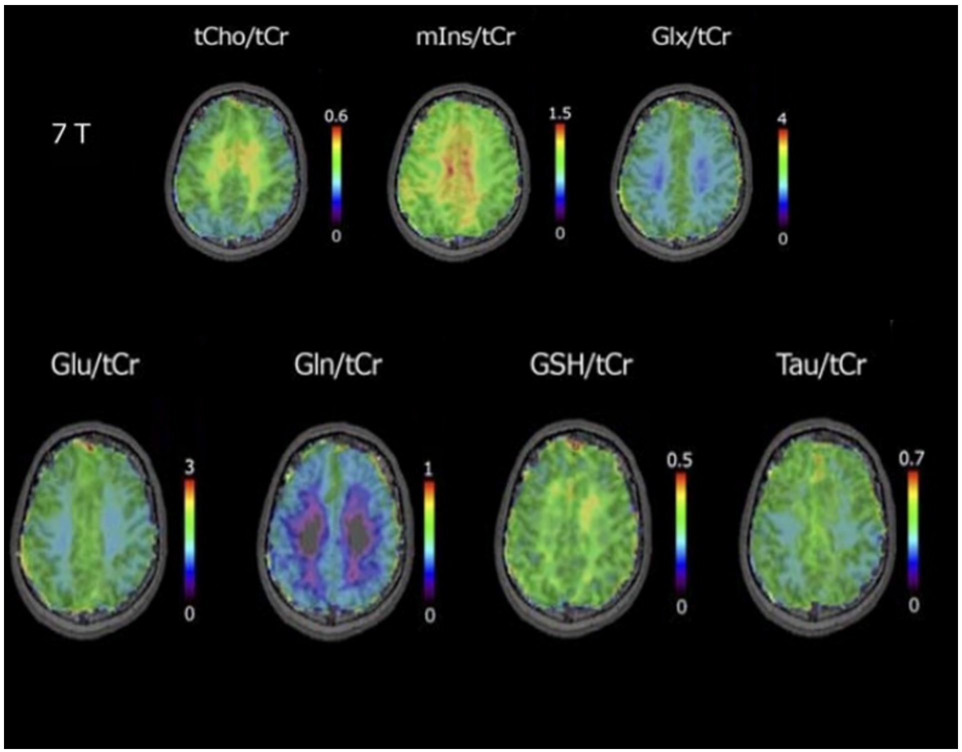

Anaplastic oligoastrocytoma

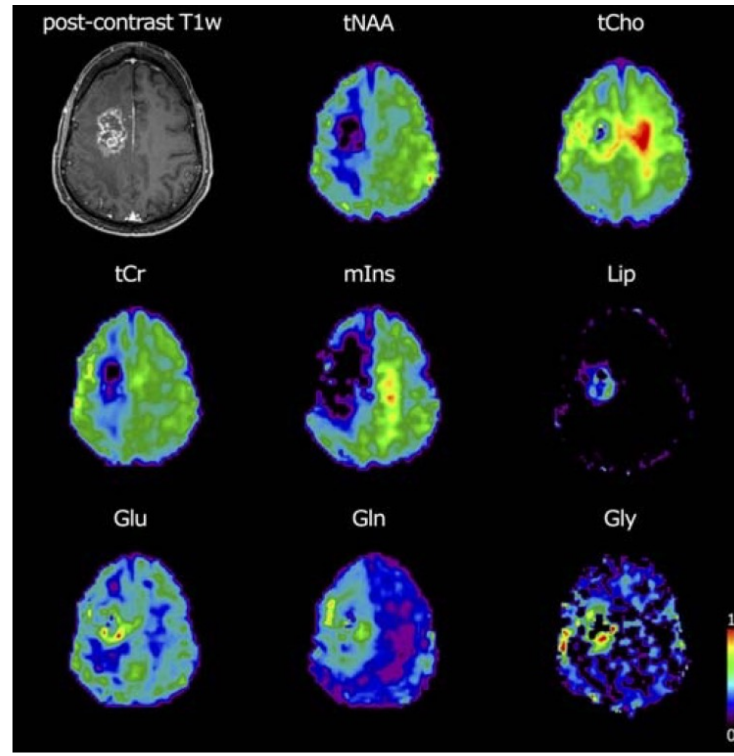

Gruber et al. 2017

^{31}P MRSI

Interrogates cellular energetics

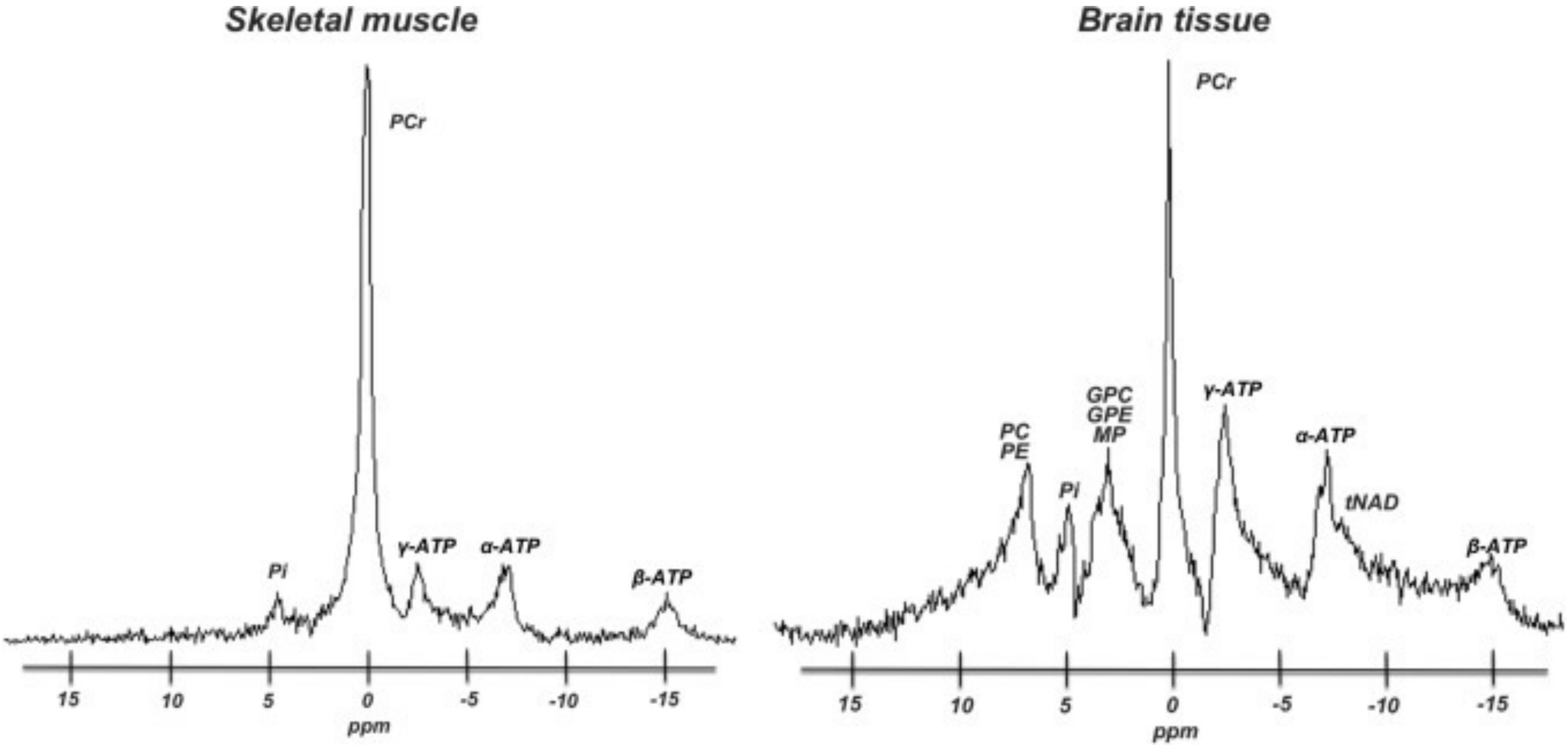

Santos-Díaz et al. 2020

Intracellular pH Mapping

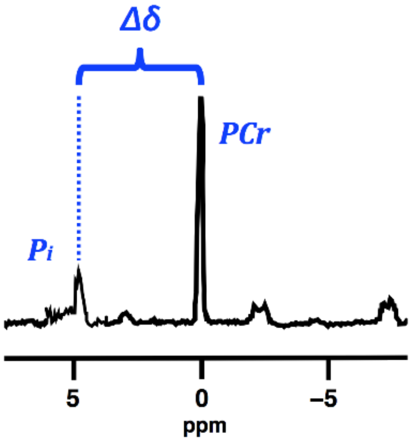

- Intracellular pH can be quantified by measuring the chemical shift between P_i and PCr
- 0.1 ppm → .008 pH units

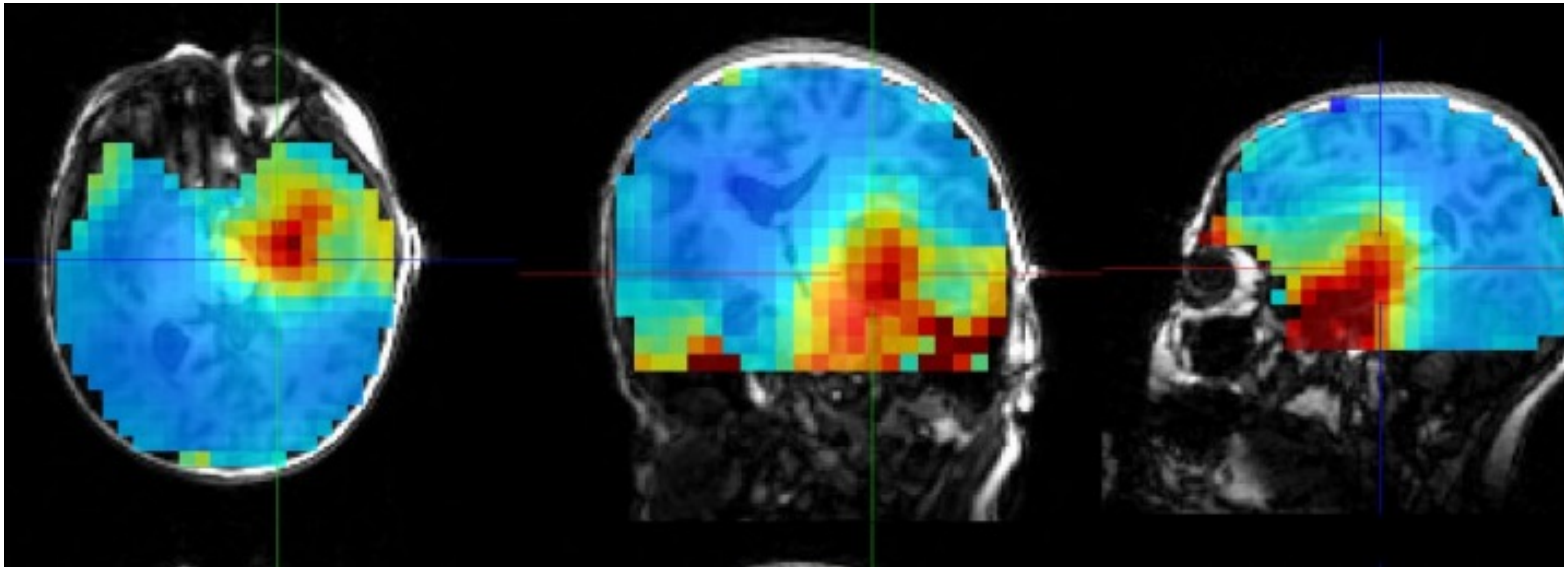

Korzowski et al. 2020

^{2}H MRSI Lactate Imaging

- Patient was orally administered ^{2}H-enriched glucose and ^{2}H MRSI was performed
- Lactate (downstream of glucose) can be imaged

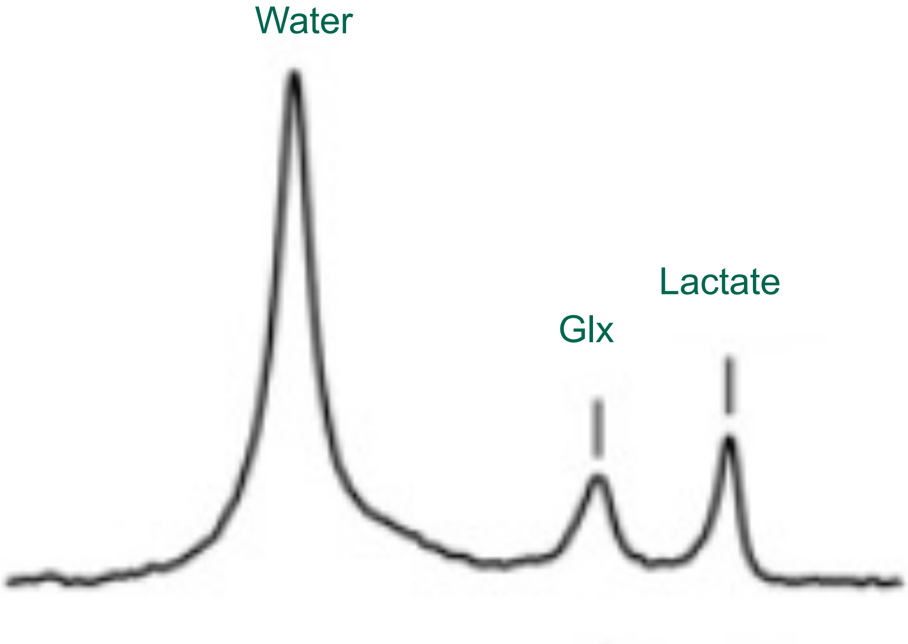

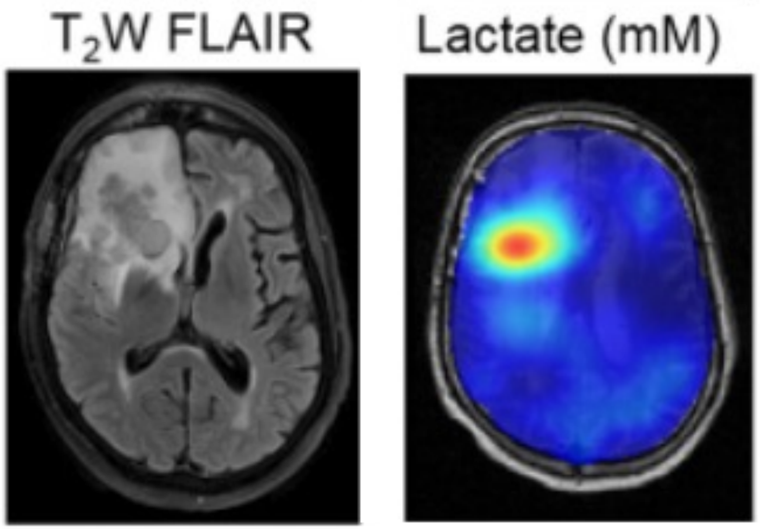

De Feyter et al. 2018

^{13}C Hyperpolarized Imaging

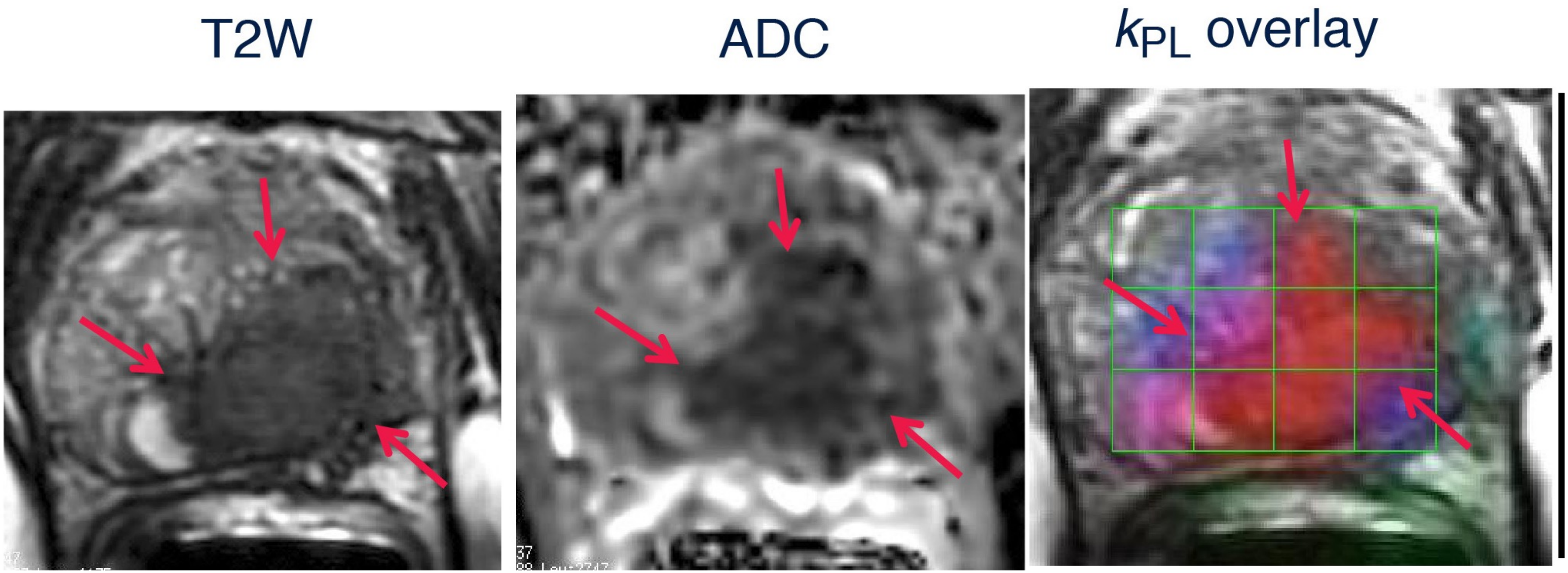

Aggarwal et al. 2017

Conclusion

- Imaging is ubiquitous is radiation oncology
- Every step in the process
- New trend: online adaptive radiotherapy
- Functional imaging may change everything!

References

- Jaffray DA, Siewerdsen JH, Wong JW, Martinez AA. Flat-panel cone-beam computed tomography for image-guided radiation therapy. *International Journal of Radiation Oncology*Biology* Physics*. 2012.
- AAPM TG 66. 2003.
- Pan T, Lee TY, Rietzel E, Chen GTY. 4D-CT imaging of a volume influenced by respiratory motion on multi-slice CT. *Medical Physics*. 2004.
- Wagner TH, Meeks SL, Bova FJ, Friedman WA, Willoughby TR, Kupelian PA, Tome W. Optical tracking technology in stereotactic radiation therapy. *Medical Dosimetry*. 2007.
- AAPM TG 128. 2008.
- AAPM TG 104. 2009.

References

- AAPM TG 135. 2011.
- Weygand J, Fuller CD, Ibbott GS, Mohamed ASR, Ding Y, Hwang KP, Wang J. Spatial precision in magnetic resonance imaging-guided radiation therapy: The role of geometric distortion. *International Journal of Radiation Oncology*Biology*Physics*. 2016.
- AAPM TG 132. 2017.
- AAPM TG 174. 2019.
- Stafford RJ. The physics of magnetic resonance imaging safety. *Magnetic Resonance Imaging Clinics of North America*. 2020.
- AAPM TG 284. 2021.